

UNCLASSIFIED

AD NUMBER
AD453872
NEW LIMITATION CHANGE
TO Approved for public release, distribution unlimited
FROM Distribution authorized to U.S. Gov't. agencies and their contractors; Administrative/Operational Use; OCT 1964. Other requests shall be referred to Air Force Flight Dynamics Laboratory, Attn: Research and Technology Div., Wright-Patterson AFB, OH 45433.
AUTHORITY
AFFDL ltr dtd 13 Oct 1975

THIS PAGE IS UNCLASSIFIED

AD 453 872

ASD-TDR-62-194

A HALF-BRIDGE TYPE STRAIN GAGE FOR USE AT ELEVATED TEMPERATURES

TECHNICAL DOCUMENTARY REPORT No. ASD-TDR-62-194

OCTOBER 1964

AF FLIGHT DYNAMICS LABORATORY
RESEARCH AND TECHNOLOGY DIVISION
AIR FORCE SYSTEMS COMMAND
WRIGHT-PATTERSON AIR FORCE BASE, OHIO

Project No. 1347, Task No. 134702

(Prepared under Contract No. AF 33(616)-7686 by
High Temperature Instruments Corp., Philadelphia 33, Pennsylvania)

20070924049

NOTICES

When Government drawings, specifications, or other data are used for any purpose other than in connection with a definitely related Government procurement operation, the United States Government thereby incurs no responsibility nor any obligation whatsoever; and the fact that the Government may have formulated, furnished, or in any way supplied the said drawings, specifications, or other data, is not to be regarded by implication or otherwise as in any manner licensing the holder or any other person or corporation, or conveying any rights or permission to manufacture, use, or sell any patented invention that may in any way be related thereto.

DDC release to OTS not authorized.

Qualified requesters may obtain copies of this report from the Defense Documentation Center (DDC), (formerly ASTIA), Cameron Station, Bldg. 5, 5010 Duke Street, Alexandria, Virginia, 22314.

Copies of this report should not be returned to the Research and Technology Division, Wright-Patterson Air Force Base, Ohio, unless return is required by security considerations, contractual obligations, or notice on a specific document.

FOREWORD

The original development work upon which this report is based was carried out by the High Temperature Instruments Corporation of Philadelphia, Pa., under Air Force Contract No. 33(616)-7686, Project No. 1347, and Task No. 134702.

Development work under this contract began November 14, 1960, and ceased September 22, 1961. Further development work on the Half-Bridge strain gage, supported by High Temperature Instruments Corporation, is continuing.

This project was initiated by The Strength Branch, Structural Division, Directorate of Engineering Test, Deputy of Test and Support, of the Aeronautical Systems Division. Technical coordination was provided by Mr. James Mullineaux, ASTESS-4.

This report was released by the Experimental Mechanics Branch, Structural Division, Air Force Flight Dynamics Laboratory, Research and Technology Division.

ABSTRACT

Development of the Half-Bridge strain gage previously reported in WADD TR. 60-680 has continued. Gage manufacturing and testing techniques were standardized. A theoretical analysis of gage performance is included.

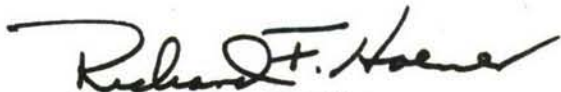
The following tests were made:

- (1) Response of gages to rapid radiant heating.
- (2) Measurement of gage factor at room temperature and as a function of temperature.
- (3) Response of gages to slow (oven) heating.
- (4) Gage drift at constant temperature.

It is shown that:

- (1) Gage performance depends strongly on bridge voltage.
- (2) The gage material selected on the basis of previous tests (Nichrome) is not fully acceptable for gage use, even in the Half-Bridge configuration, because of a metallurgical transition occurring above 1000° F.
- (3) The poorest Nichrome Half-Bridge strain gages tested exhibited a temperature coefficient of less than 3 microohms/ohm/°F to 1000° F, more than an order of magnitude better than currently available uncompensated high temperature gages.
- (4) Gage use above 1500° F is not generally feasible because of a lack of adequate cements and bonding techniques at these temperatures.

Publication of this technical documentary report does not constitute Air Force approval of the reports' findings or conclusions. It is published only for the exchange and stimulation of ideas.

A handwritten signature in black ink, reading "Richard F. Hoener". The signature is written in a cursive style with a prominent horizontal stroke at the beginning.

RICHARD F. HOENER
Actg Chief, Structures Division
AF Flight Dynamics Laboratory

TABLE OF CONTENTS

<u>Section</u>	<u>Page</u>
I. Introduction	1
II. Theoretical Considerations	4
Bridge Circuitry	4
Thermal EMF's	14
III. Steady State Heat Transfer Characteristics	20
IV. Effect of Differential Thermal Expansion	31
V. Gage Manufacturing Procedures	43
VI. Steady State Tests	51
VII. Gage Performance under Transient Heating Conditions	70
VIII. Gage Cements and Gage Bonding Techniques	90
IX. Gage Installation Techniques	98
X. Summary and Conclusions	100
Appendix I	101
Appendix II	103
Appendix III	104
References	105
Addendum - National Bureau of Standards Report 8004	106

LIST OF FIGURES

<u>Figure</u>		<u>Page</u>
1	Sketch of Half-Bridge Strain Gage	2
2	Bridge Circuit with Meter Connected Between Junction of Gage Arms and Junction of Ratio Arms	5
3	Bridge Circuit with Meter Connected to Extremities of Gage Arms	5
4	Basic Wheatstone Bridge Circuit Including Lead-Wire Resistance; Power Supply Across Gage	10
5	Basic Wheatstone Bridge Circuit Including Lead-Wire Resistance; Meter Across Gage	10
6	Half-Bridge Strain Gage Circuit Showing Junctions of Dissimilar Materials	
	6a. Circuit with Power Supply Across Gage	15
	6b. Circuit with Meter Across Gage	15
7	Equivalent Circuits Obtained by Treating Junctions as Batteries	
	7a. Circuit with Power Supply Across Gage	17
	7b. Circuit with Meter Across Gage	17
8	Characteristic Response of a Typical Half-Bridge Strain Gage to Rapid Heating with Various Bridge Voltages	21
9	Cross-section of Gage Installation and Idealized Case for Analysis	
	9a. Cross-section of Gage Installation	22
	9b. Idealized Case for Analysis	22
10	Resistance of Nichrome and Nichrome V as a Function of Temperature	32
11	Calculated Temperature Difference Between Compensating and Strain-sensitive Arms of a 60 ohm, 1 inch Nichrome Half-Bridge Strain Gage	34

<u>Figure</u>		<u>Page</u>
12	Variation of $\frac{\Delta R_a}{R_{a,0}} - \frac{\Delta R_c}{R_{c,0}}$ vs. Temperature for $\beta_{sp} = \beta_a = 0$, 60 ohm Nichrome Half-Bridge Strain Gage	37
13	Calculated Apparent Resistance Change for a 1" 60 ohm Nichrome Half-Bridge Strain Gage	39
14	Calculated Temperature Difference between Arms of a 120 ohm, 1/2" Nichrome V Half-Bridge Strain Gage	40
15	Calculated Temperature Difference between Arms of a 120 ohm, 1/2" Nichrome V Half-Bridge Strain Gage	41
16	Calculated Values of Apparent Strain of a 120 ohm, 1/2" Nichrome V Half-Bridge Strain Gage; $\beta_{sp} = \beta_a$	42
17	Detail Construction Half-Bridge Strain Gage	44
18	Test Fixture	45
19	Half-Bridge Strain Gage Data Sheet	46
20	Details of Half-Bridge Strain Gage Manufacturing	48
21	Teflon Mold	49
22	Apparent Strain on Nimonic-90 of Four Half- Bridge Strain Gages of Final Configuration. Runs 1 - 3.	52
23	Apparent Strain on Nimonic-90 of Four Half- Bridge Strain Gages of Final Configuration. Runs 4 and 5.	53
24	Apparent Strain on 316 Stainless (Steel) of Five Half-Bridge Strain Gages of Final Configuration. Cycles 1 - 3.	57

<u>Figure</u>		<u>Page</u>
26	Apparent Strain on Inconel of a PBX Half-Bridge Strain Gage of Final Configuration	60
27	Apparent Strain on Inconel of an Astroceram Half-Bridge Strain Gage of Final Configuration	61
28	Apparent Strain on Inconel of a Quigley 1925 Half-Bridge Strain Gage of Final Configuration	62
29	Apparent Strain on Inconel of a Half-Bridge Strain Gage made of Heat Treated Nichrome	63
30	Apparent Strain on Inconel of a Half-Bridge Strain Gage of Standard Configuration	64
31	Apparent Strain on Inconel of a Half-Bridge Strain Gage of Standard Configuration	65
32	Apparent Strain on Inconel of a Half-Bridge Strain Gage of Standard Configuration	66
33	Percent Change in Output vs. Temperature of Four Half-Bridge Strain Gages of Final Configuration	69
34	Transient Temperature Apparatus - Diagram	71
35	Temperature - Time Relationship for Radiant Heated Specimen (Typical)	79
36	Apparent Strain Vs. Temperature Gage 61-1	85
37	Apparent Strain Vs. Temperature Gage 61-2	86
38	Apparent Strain Vs. Temperature Gage 61-3	87
39	Apparent Strain Vs. Temperature Gage 61-4	88
40	Apparent Strain Vs. Temperature Gage 61-5	89
41	Half-Bridge Strain Gage Installation	99

LIST OF TABLES

<u>Table</u>	<u>Page</u>
I Values of $\alpha_{\Delta t}$ and K	9
II Bridge Sensitivity Factor, K	14
III Thermal EMF's of Various Materials Versus Platinum	18
IV Temperature Difference Between the Arms of a Platinum-Rhodium Half-Bridge Strain Gage	29
V Resistance Ratio and Slope of Resistance-Temperature Curves for Nichrome and Nichrome V from Room Temperature to 2000° F.	31
VI Drift Rate and Zero Shift Data on Four Half-Bridge Strain Gages of the Final Configuration on Nimonic 90 Test Specimens	54
VII Performance of Five Half-Bridge Strain Gages of the Final Configuration on Type 316 Stainless Steel Test Specimens	56
VIII Drift Rate at Various Temperatures for a Nichrome Half-Bridge Strain Gage	67
IX Gage Factor at Various Temperatures for Four Nichrome Half-Bridge Strain Gages	68
X Half-Bridge Strain Gage Data Sheet, Gage No. 61-1	80
XI Half-Bridge Strain Gage Data Sheet, Gage No. 61-2	81
XII Half-Bridge Strain Gage Data Sheet, Gage No. 61-3	82
XIII Half-Bridge Strain Gage Data Sheet, Gage No. 61-4	83
XIV Half-Bridge Strain Gage Data Sheet, Gage No. 61-5	84
XV Effect of Temperature Cycling on Selected Ceramic Cements and Flame-Sprayed Coatings	92

I. INTRODUCTION

The need for a strain gage whose output is insensitive to changes in ambient temperature is well known to those concerned with the measurement of strain at elevated temperatures. Equally well known is the fact that the temperature range and heating rate, to which aircraft and missile structures in particular are being subjected, are increasing. The Half-Bridge Strain Gage was invented and patented by High Temperature Instruments Corporation to provide a gage which would operate effectively independent of the temperature and heating rate of the structure to which it was attached.

The Half-Bridge Strain Gage is shown in Figure 1. It consists of the following components:

(1) A strain sensitive wire which forms one arm of a Wheatstone Bridge and is bonded to the surface of the specimen whose strain is to be measured. This wire is strained as the specimen is strained and is referred to as the strain-sensing arm or the active arm.

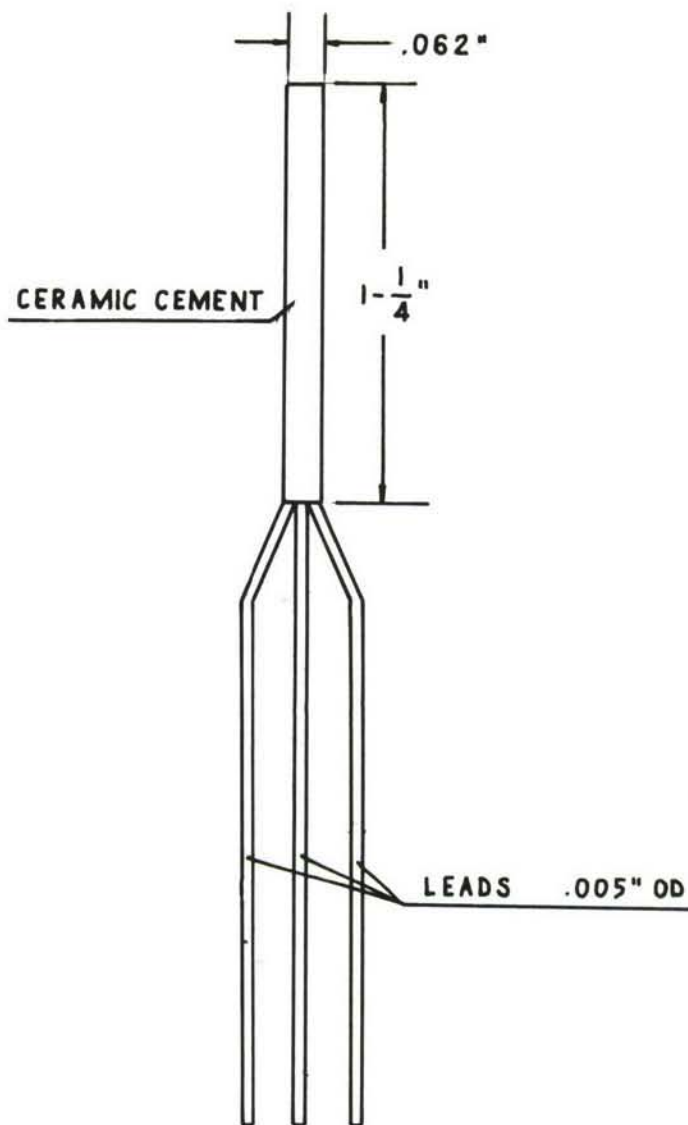
(2) A slack wire which forms an adjacent arm of the Wheatstone Bridge and is enclosed within a fine silica tube of extreme purity which is bonded in proximity to the strain sensing arm so that both wires experience identical ambient temperature variations. This wire does not feel the surface strain and is referred to as the temperature-compensating arm or just the compensating arm. It is electrically connected at one end to the strain-sensing arm.

(3) Electrical lead-out wires, ribbons, or tubes from the junction of the strain-sensing and temperature compensating arms and from their free extremities.

(4) A cement binder for bonding the above components into an integral unit and for providing electrical isolation from the structure whose strain is to be measured.

The original work of High Temperature Instruments Corp., was extended by Air Force sponsorship under Contract No. AF 33(616)-6897.

Manuscript released by authors 6/20/62 for publication as an
RTD Technical Documentary Report.



RESISTANCE : 120 OR 60 Ω ACTIVE } MATCHED TO 1%
 120 OR 60 Ω COMPENSATING }

FIGURE 1. SKETCH OF HALF-BRIDGE STRAIN GAGE.

The results of this contract are given in Reference 1, WADD Technical Report 60-680. This report showed the following:

1. The basic concept of the Half-Bridge Strain Gage was sound and the feasibility of the device was demonstrated.

2. Up to 900° F. Half-Bridge Strain Gages fabricated of Nichrome gave low and repeatable values of apparent strain versus temperature, low drift rates, and small gage factor variation with temperature.

3. As a consequence of the difference in heat loss characteristics of the two wires, the apparent strain of the Half-Bridge Strain Gage is affected by the bridge voltage.

The results of this Air Force contract were very encouraging and a second contract was entered into for further research and development on the Half-Bridge Strain Gage. The results of this second contract are given in the present report.

II. THEORETICAL CONSIDERATIONS

The Half-Bridge Strain Gage may very easily be used with the usual A-C powered strain indicator by following the directions supplied by the indicator's manufacturer for use of the indicator with two external arms. However, when it is desired to use the bridge in D-C circuits, certain precautions must be observed and care must be employed in the design of the measuring circuit. Since the transient heating tests were performed with D-C powered Wheatstone bridges, it is felt that a brief review of the theory concerning these bridges is pertinent. Also, since gages have been made with lead wires which were not of the same material as the sensing elements, thermal emf's can be generated in a Half-Bridge Strain Gage so the effects of these emf's are discussed. Finally, an investigation is made into the steady-state heat transfer characteristics of the two arms and the effects these have on the gage performance.

Bridge Circuitry

Two basic Wheatstone bridge circuit configurations are shown in Figures 2 and 3. In the arrangement shown in Fig. 2, the voltage is applied across the bridge and the center-tap is connected to the meter; in Fig. 3, the power supply and the meter are reversed.

In order to simplify the analysis, the meter impedance is assumed to be infinite, while that of the power supply is zero (i.e., a constant voltage power supply is assumed). Further, the gages are assumed to be pure resistive impedances, and the lead wire resistances are neglected. Resistance changes are assumed to be sufficiently small to permit the use of linear theory. Thus differences may be replaced by differentials and the effects of strain and of temperature may be directly added.

In the bridge configuration shown in Fig. 2, the voltage indicated by the meter is given by

$$\frac{E_o}{E} = \frac{R_a}{R_a + R_c} - \frac{R_1}{R_1 + R_2} \quad (1)$$

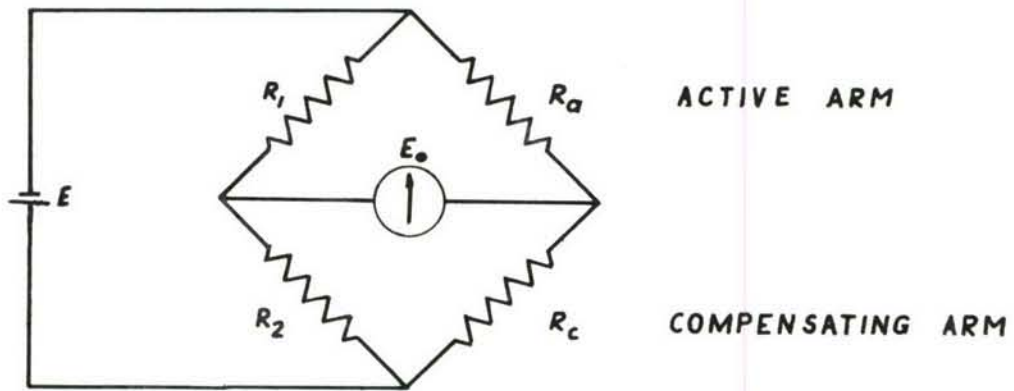


FIGURE 2. BRIDGE CIRCUIT WITH METER CONNECTED BETWEEN JUNCTION OF GAGE ARMS AND JUNCTION OF RATIO ARMS.

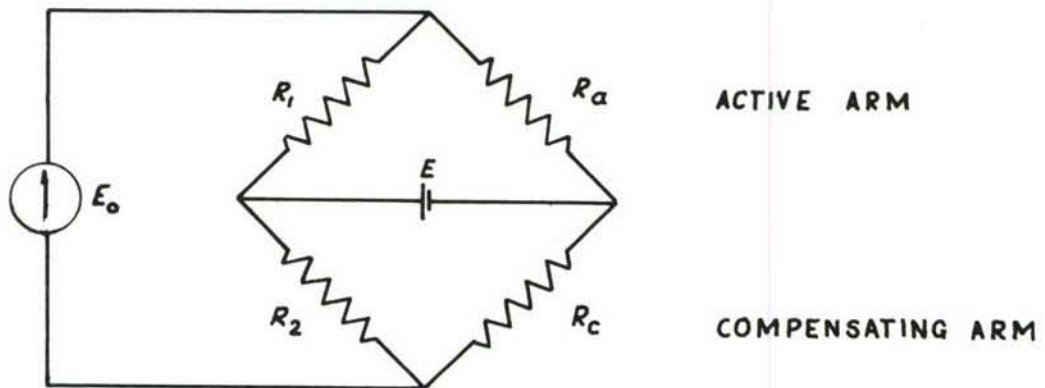


FIGURE 3. BRIDGE CIRCUIT WITH METER CONNECTED TO EXTREMITIES OF GAGE ARMS.

Any change in the resistance of the active and/or compensating arms will cause a change in the bridge output of

$$\begin{aligned} \frac{\Delta E_o}{E} &= \frac{R_c \Delta R_a}{(R_a + R_c)^2} - \frac{R_a \Delta R_c}{(R_a + R_c)^2} \\ &= \frac{R_a \cdot R_c}{(R_a + R_c)^2} \left[\frac{\Delta R_a}{R_a} - \frac{\Delta R_c}{R_c} \right] \end{aligned} \quad (2)$$

For a well-constructed bridge, $R_a \cong R_c$ and, since R_a and R_c remain at substantially the same temperature, R_a stays approximately equal to R_c . We can therefore write

$$\frac{\Delta E_o}{E} = \frac{1}{4} \left[\frac{\Delta R_a}{R_a} - \frac{\Delta R_c}{R_c} \right] \quad (3)$$

For the configuration in Fig. 3, on the other hand, we have

$$\frac{E_o}{E} = \frac{R_a}{R_a + R_1} - \frac{R_c}{R_c + R_2} \quad (4)$$

and

$$\frac{\Delta E_o}{E} = \frac{R_1 \Delta R_a}{(R_a + R_1)^2} - \frac{R_2 \Delta R_c}{(R_c + R_2)^2}$$

or

$$\frac{\Delta E_o}{E} = \frac{R_a R_1}{(R_a + R_1)^2} \left[\frac{\Delta R_a}{R_a} - \left(\frac{R_a + R_1}{R_c + R_2} \right)^2 \left(\frac{R_c \cdot R_2}{R_a \cdot R_1} \right) \frac{\Delta R_c}{R_c} \right] \quad (5)$$

Again, for a properly constructed bridge $R_a \cong R_c$ and $R_1 = R_2$.
Then

$$\frac{\Delta E_o}{E} = \frac{R_a R_1}{(R_a + R_1)^2} \left[\frac{\Delta R_a}{R_a} - \frac{\Delta R_c}{R_c} \right] \quad (6)$$

If K, the sensitivity of the circuit, is defined as

$$K = \frac{\Delta E_o}{E} \left/ \left[\frac{\Delta R_a}{R_a} - \frac{\Delta R_c}{R_c} \right] \right. \quad (7)$$

Then, by comparison with Equation (6)

$$K = \frac{R_a \cdot R_1}{(R_a + R_1)^2} \quad (8)$$

For a Half-Bridge Strain Gage constructed with $R_a = R_c = 120$ ohms, connected to a strain indicator in which the reference arms $R_1 = R_2 = 120$ ohms, the sensitivity of the circuit at the reference temperature will be

$$K = \frac{120 \cdot (120)}{(120 + 120)^2} = \frac{1}{4} = 0.25$$

Equation (6) is identical with Equation (3), and the circuit configurations of Figs. 2 and 3 give the same output.

If, however, a Half-Bridge Strain Gage is constructed so that the resistance in each arm is 60 ohms, and such a bridge is connected to an indicator having $R_1 = R_2 = 120$ ohms, then

$$K = \frac{60 \cdot (120)}{(60 + 120)^2} = \frac{2}{9} = 0.22$$

Thus, when connected to an indicator having 120 ohm reference arms, a Half-Bridge Strain Gage having 60 ohm resistance arms will develop an output 11% less than that of a gage with 120 ohm arms.

For the circuit configuration of Fig. 3 temperature changes must be taken into account, since R_a will vary when the gage is heated while R_i remains unchanged. The resistance of the active arm at the operating temperature may be expressed as:

$$R_{a,t} = R_{a,o} \left[1 + \alpha (t - t_o) \right] \quad (9)$$

where $R_{a,t}$ = resistance of the active arm at temperature t
 $R_{a,o}$ = resistance of the active arm at the reference temperature, t_o
 α = the average temperature coefficient of resistance of the active arm between t_o and t
 t = the operating temperature
 t_o = the reference temperature, usually room temperature.

If we write $\Delta t = t - t_o$, and substitute $R_{a,t}$ for R_a in equation (8), we have

$$K = \frac{R_{a,t} \cdot R_i}{(R_{a,t} + R_i)^2} = \frac{R_{a,o} (1 + \alpha \Delta t) \cdot R_i}{\left[R_{a,o} (1 + \alpha \Delta t) + R_i \right]^2}$$

$$K = \frac{\frac{R_{a,o}}{R_i} (1 + \alpha \Delta t)}{\left[1 + \frac{R_{a,o}}{R_i} (1 + \alpha \Delta t) \right]^2} \quad (10)$$

Table I gives some values of $\alpha \Delta t$ and K for various strain sensing materials.

TABLE I

Values of $\alpha \Delta t$ and K

<u>Material</u>	<u>Operating Temperature, deg. F.</u>	<u>$\alpha \Delta t$</u>	<u>K (a)</u>	<u>K (b)</u>
Nichrome V	2000	.075	.2285	.2497
Nichrome	2000	.15	.2317	.2488
Platinum	1040	2.00	.2400	.1875
Nickel	932	3.20	.2175	.1553

(a) $R_{a,o} / R_i = 1/2$

(b) $R_{a,o} / R_i = 1$

Thus, when the power supply is connected to the center-tap of the Half-Bridge Strain Gage, the resistance of the various bridge arms as well as the temperature coefficient of resistance of the gage arms must be considered for accurate work.

In the above analysis, the lead wire resistances were neglected; to examine the effect of the leads on the sensitivity of the two basic Wheatstone bridge circuits, consider Figures 4 and 5, which show circuit configurations comparable to those in Figures 2 and 3, but with the lead-wire resistance included.

Figure 4 is a bridge circuit arrangement in which the voltage is applied across the gage and the meter connected to the center-tap.

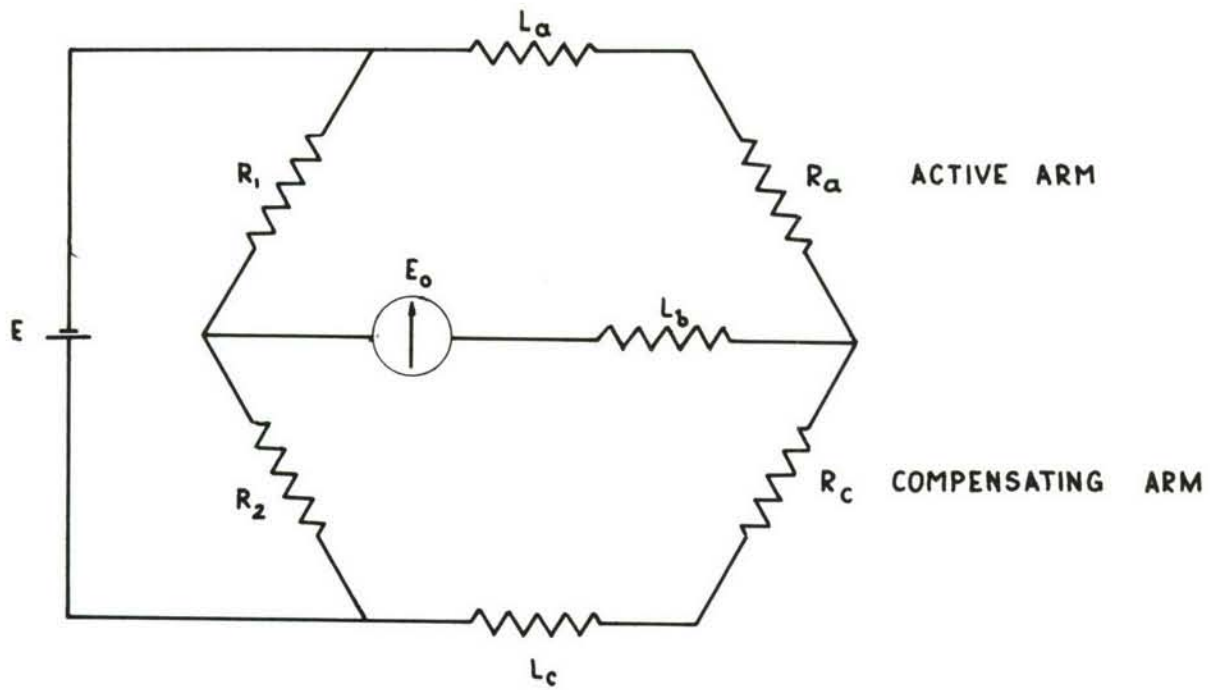


FIGURE 4. POWER SUPPLY ACROSS GAGE.

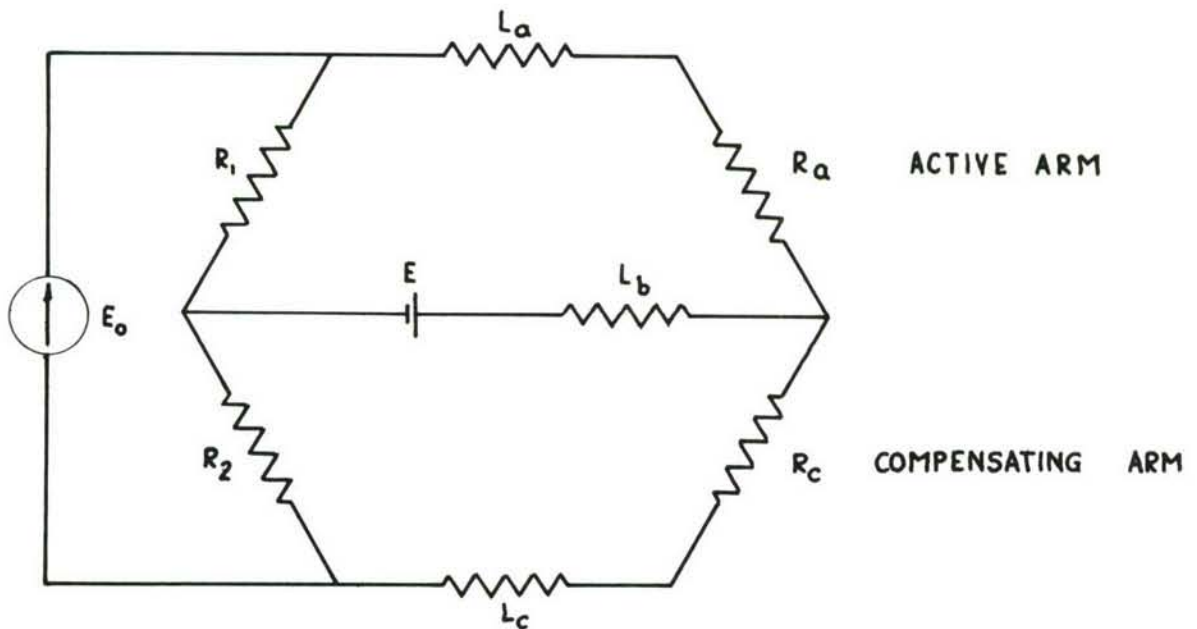


FIGURE 5. METER ACROSS GAGE.

BASIC WHEATSTONE BRIDGE CIRCUIT INCLUDING LEAD-WIRE RESISTANCE.

We make the same assumptions for this case as for the comparable circuit configuration, Fig. 2, except that we now consider the leads to have resistances L_a , L_b and L_c , as shown in Fig. 4. We now have

$$\frac{E_o}{E} = \frac{R_a + L_a}{R_a + L_a + R_c + L_c} - \frac{R_1}{R_1 + R_2} \quad (11)$$

and

$$\begin{aligned} \frac{\Delta E_o}{E} &= \frac{(R_c + L_c) \Delta R_a}{(R_a + L_a + R_c + L_c)^2} - \frac{(R_a + L_a) \Delta R_c}{(R_a + L_a + R_c + L_c)^2} \\ &= \frac{(R_a + L_a)(R_c + L_c)}{(R_a + L_a + R_c + L_c)^2} \left[\frac{\Delta R_a}{R_a + L_a} - \frac{\Delta R_c}{R_c + L_c} \right] \end{aligned} \quad (12)$$

We again assume $R_a = R_c$, and also assume $L_a = L_c$. Then the first term on the right in equation (12) reduces to $1/4$ [Cf. Eq.(3)] . and the second term may be written

$$k \left[\frac{\Delta R_a}{R_a} - \frac{\Delta R_c}{R_c} \right]$$

$$\text{where } k = \frac{R_a}{R_a + L_a} = \frac{R_c}{R_c + L_c} \quad (13)$$

The effect of the lead wire resistance in this configuration is to reduce the sensitivity of the circuit by the factor k .

In the circuit arrangement shown in Figure 5, where the power supply is in series with the center-tap lead, L_b , the effective voltage to the bridge is reduced by $R_t / R_t + L_b$, where R_t is the total equivalent bridge resistance

$$R_t = \frac{(R_a + L_a + R_1)(R_c + L_c + R_2)}{R_a + L_a + R_c + L_c + R_1 + R_2} \quad (14)$$

We thus have

$$\frac{E_o}{E} = \frac{R_t}{R_t + L_b} \left[\frac{R_a + L_a}{R_a + L_a + R_1} - \frac{R_c + L_c}{R_c + L_c + R_2} \right] \quad (15)$$

Determination of the effects of changes in R_a , R_c and L_b on E_o/E by a rigorous solution of Equation (15) requires much tedious algebraic manipulation. Despite the effort required, the results thus obtained do not provide a simple, straight-forward picture of the consequences of changing R_a , R_c and L_b for the practical case. If, however, we assume that the ratio

$R_t / R_t + L_b$ does not change when the resistance of the gage arms and of the gage leads changes, the algebra is considerably simplified. We then have (Appendix I):

$$\frac{\Delta E_o}{E} = \frac{R_t}{R_t + L_b} \left[\frac{R_1 \Delta R_a}{(R_a + L_a + R_1)^2} - \frac{R_2 \Delta R_c}{(R_c + L_c + R_2)^2} \right] \quad (16)$$

or

$$\frac{\Delta E_o}{E} = \frac{R_t}{R_t + L_b} \cdot \frac{R_a R_1}{(R_a + L_a + R_1)^2} \left[\frac{\Delta R_a}{R_a} - \left(\frac{R_a + L_a + R_1}{R_c + L_c + R_2} \right)^2 \frac{R_c R_2}{R_a R_1} \cdot \frac{\Delta R_c}{R_c} \right] \quad (17)$$

If we assume $R_a = R_c$, $R_1 = R_2$ and $L_a = L_c$, we first obtain, from Equation (14)

$$R_t = \frac{(R_a + L_a + R_1)^2}{2 (R_a + L_a + R_1)} = \frac{1}{2} (R_a + L_a + R_1) \quad (18)$$

We now substitute R_a for R_c , R_1 for R_2 , L_a for L_c and $1/2 (R_a + L_a + R_1)$ for R_t in Eq. (17). After simplification, we obtain

$$\frac{\Delta E_o}{E} = \frac{R_a R_1}{(R_a + L_a + R_1) (R_a + L_a + R_1 + 2L_b)} \left[\frac{\Delta R_a}{R_a} - \frac{\Delta R_c}{R_c} \right] \quad (19)$$

The sensitivity of this circuit configuration, as defined by Eq. (7) is

$$K = \frac{R_a \cdot R_1}{(R_a + L_a + R_1) (R_a + L_a + R_1 + 2L_b)}$$

which may be written

$$K = \frac{(R_a + R_1)^2}{(R_a + L_a + R_1) (R_a + L_a + R_1 + 2L_b)} \cdot \frac{R_a \cdot R_1}{(R_a + R_1)^2} \quad (20)$$

Thus, in the bridge arrangement in which the meter is in series with the center-tap gage lead, changes in the resistance of the leads reduce the sensitivity of the circuit by a factor

$$\frac{(R_a + R_1)^2}{(R_a + L_a + R_1) (R_a + L_a + R_1 + 2L_b)}$$

as compared to the case in which lead resistance changes are ignored, Equation (8).

Table II gives values of K for several typical values of gage arm and lead wire resistance.

TABLE II

BRIDGE SENSITIVITY FACTOR, K

Resistance of arms, ohms		Resistance of Leads, Ohms			
		$L_a = 0$ $L_b = 0$	$L_a = 0$ $L_b = 5$	$L_a = 5$ $L_b = 0$	$L_a = 5$ $L_b = 5$
R_a	R_b				
60	60	.2500	.2308	.2304	.2133
60	120	.2222	.2105	.2104	.1995
120	120	.2500	.2400	.2399	.2305

Thermal EMF's

Any junction of two dissimilar metals may give rise to a thermal emf. Figure 6 shows the possible sources of thermal emf's in Half-Bridge Strain Gage measuring circuits. As before, two circuit configurations require consideration: that shown in Figure 6a, in which the power supply is connected across the gage, and the arrangement shown in Figure 6b, where the meter is connected across the gage.

It can be seen that thermal emf's in the circuits shown may have their origin in the junctions between the gage arms and the gage leads (junctions 2, 4 and 6) and at the junctions between the gage leads and the external leads to the meter and power supply (junctions 1, 3 and 5). Junctions are denoted by solid circles, and are numbered for reference.

Analysis of the effect of thermal emf's is simplified when the following assumptions are made:

1. No thermal emf's are generated in the external circuitry.
2. The meter resistance is infinite.
3. The power supply voltage is zero.
4. The temperature gradient across the width of the gage is zero.

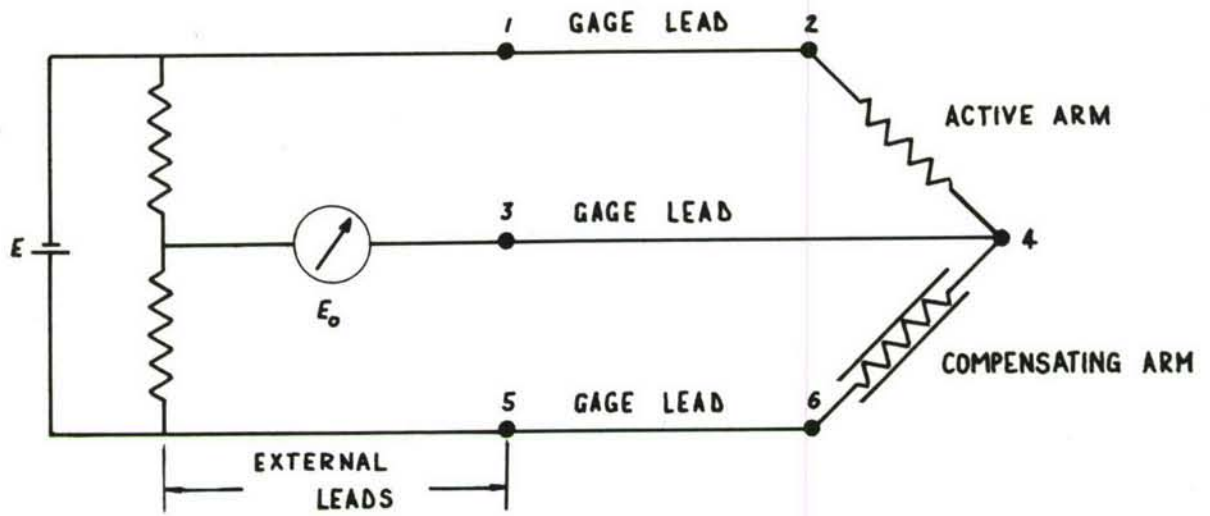


FIGURE 6/a. CIRCUIT WITH POWER SUPPLY ACROSS GAGE.

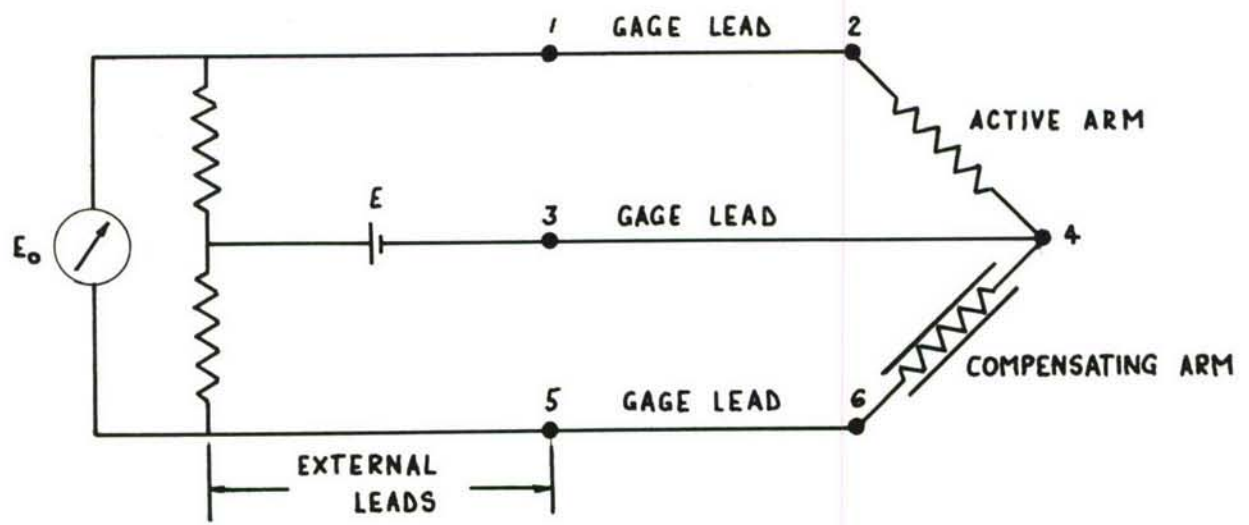


FIGURE 6/b. CIRCUIT WITH METER ACROSS GAGE.

FIGURE 6. HALF-BRIDGE STRAIN GAGE CIRCUIT SHOWING JUNCTIONS OF DISSIMILAR MATERIALS.

Each of the junctions shown in Fig. 6 may be represented as a battery. The equivalent circuits are shown in Fig. 7. The potential developed at each junction, ϵ_i , is determined by the materials forming the junction and by the temperature of the junction.

The same material is used in both arms of the gage. All three gage leads are made from a second material, while the external leads are all made of a third material. Because of this, junctions 1, 3 and 5 are identical, and junctions 2, 4 and 6 are likewise identical.

Since we have assumed that there is no temperature gradient across the gage, the temperatures of junctions 1, 3 and 5 must be the same. Furthermore, junctions 2 and 6 must also all be at one temperature. From this, it follows that $\epsilon_1 = \epsilon_3 = \epsilon_5$ and $\epsilon_2 = \epsilon_6$. Furthermore, the polarity of the potentials ϵ_1 , ϵ_3 and ϵ_5 must be the same; the polarities of the potentials ϵ_2 , ϵ_4 and ϵ_6 must also be the same.

For the configuration shown in Fig. 6a and Fig. 7a, therefore, the resultant thermal emf will be

$$E_o = \epsilon_1 + \epsilon_2 - \epsilon_4 - \epsilon_3 = \epsilon_5 + \epsilon_6 - \epsilon_4 - \epsilon_3 \quad (21)$$

If there is no temperature gradient along the length of the gage, $\epsilon_1 = \epsilon_3 = \epsilon_5$ and $\epsilon_2 = \epsilon_4 = \epsilon_6$, so that $E_o = 0$, and there is no resultant thermal emf. If, however, there is a thermal gradient along the gage, then $E_o \neq 0$, and the meter will indicate a voltage output even though the power supply voltage is zero. When the power supply is turned on the meter indication will be the algebraic sum of the net thermal emf and the output of the bridge due to strain and temperature effects. Thermal emf's generated by various materials against platinum are shown in Table III.

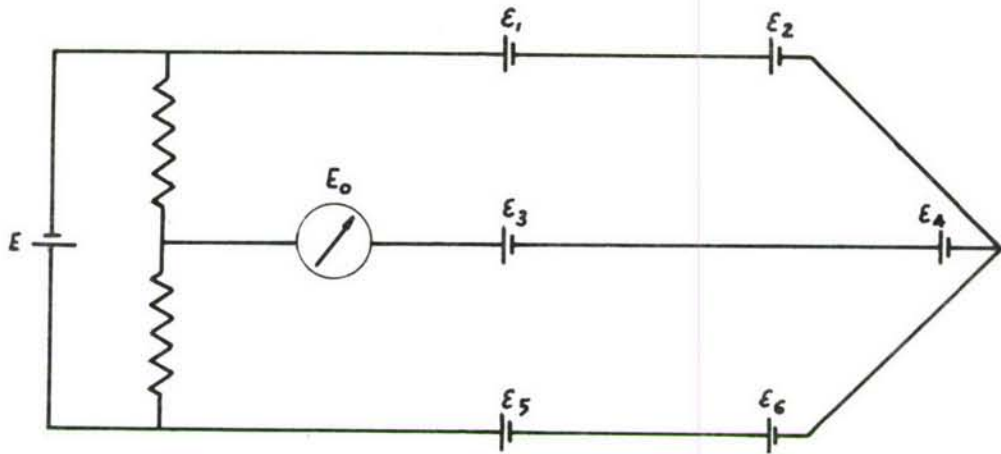


FIGURE 7a. CIRCUIT WITH POWER SUPPLY ACROSS GAGE.

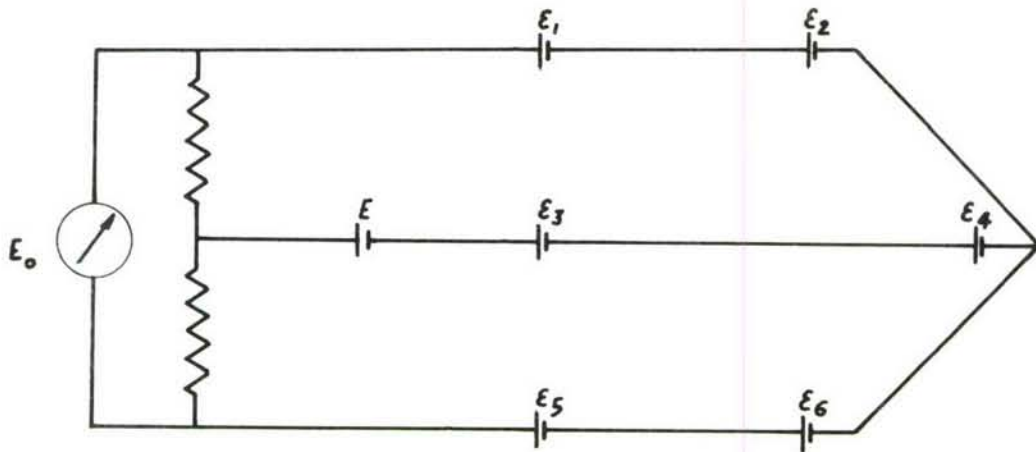


FIGURE 7b. CIRCUIT WITH METER ACROSS GAGE.

FIGURE 7. EQUIVALENT CIRCUITS OBTAINED BY TREATING JUNCTIONS AS BATTERIES.

TABLE III

THERMAL EMFS OF VARIOUS MATERIALS VERSUS PLATINUM *

<u>Temperature</u> <u>Degrees C.</u>	<u>Emf - Millivolts</u>		
	<u>Nichrome</u>	<u>Nickel</u>	<u>Silver</u>
100	.85	- 1.48	.74
200	2.01	- 3.10	1.77
300	3.41	- 4.59	3.05
400	5.00	- 5.45	4.57
500	6.76	- 6.16	6.36
600	8.68	- 7.04	8.41
700	10.78	- 8.10	10.75
800	13.08	- 9.35	13.36

* Source - American Institute of Physics Handbook, McGraw-Hill, 1957, p. 4-7 - 4-9.

This table shows that the thermal emfs may be of an order of magnitude comparable to the signal generated by the strain itself, or to the signal generated by the lack of perfect temperature compensation, and may easily be confused with the desired signal unless proper precautions are observed. Precautions used in testing Half-Bridge Strain Gages at High Temperature Instruments Corp., include the use of A-C instruments for static testing, the measurement of bridge output with zero applied bridge voltage for dynamic testing, and the use of the circuit shown in Figure 6b when possible.

Fig. 6b shows the bridge arranged with the power supply connected to the center tap and the meter across the gage. This arrangement is shown in Fig. 7b as an equivalent battery circuit. Here again, both with respect to polarity and magnitude,

$\epsilon_1 = \epsilon_3 = \epsilon_5$ and $\epsilon_2 = \epsilon_6$. For this configuration, the effective bridge voltage, ϵ_{eff} is the sum of the power supply voltage and the net thermal emf.

$$\epsilon_{eff} = E + \sum \epsilon_i \quad (22)$$

$$\sum \epsilon_i = \epsilon_3 + \epsilon_4 - \epsilon_2 - \epsilon_1 = \epsilon_3 + \epsilon_4 - \epsilon_6 - \epsilon_5 \quad (23)$$

But since $\epsilon_1 = \epsilon_3$ and $\epsilon_3 = \epsilon_5$, Equation (22) becomes

$$\epsilon_{eff} = E + (\epsilon_4 - \epsilon_2) = E + (\epsilon_4 - \epsilon_6) \quad (24)$$

For the materials considered, the value of the net thermal emf, $(\epsilon_4 - \epsilon_2)$, is under 1% of E when the lengthwise temperature gradient is not extremely high, and may therefore be neglected.

One way of completely eliminating the problem of thermal emf's is to make the sensing wires, the internal leads, and the external lead all of the same material. This procedure is not practicable until a suitable strain sensitive wire has been selected for detailed study because of the high cost and time delay in procuring such materials. However, since very good results were obtained with Nichrome V wire, Nichrome V tubing has been obtained and gages made with Nichrome V sensing wire and Nichrome V leads. These gages should exhibit no thermal emfs in transient tests and will be checked further. Complete performance data on these gages are not available since the materials for their construction were obtained too late in the contract to permit adequate testing.

III. STEADY STATE HEAT TRANSFER CHARACTERISTICS

Figure 8 shows the response of a typical Half-Bridge Strain Gage to variations in the input voltage level, while the temperature of the installation was being raised at 60 degrees F. per second. The ordinate is bridge output divided by input voltage, $\Delta E_o / E$, converted to apparent strain using a nominal gage factor of 2.000. The effect of the input voltage level is apparent from the fact that curves for the various levels are not superimposed on one another.

The major effect of changes in the input voltage level is to alter the current through the gage arms. The power dissipated as heat in the gage arms changes as the square of the current. A study was therefore undertaken to determine the effect of this "self-heating" on the performance of the Half-Bridge Strain Gage under steady state conditions.

A cross-section through a typical Half-Bridge Strain Gage installation is shown in Figure 9a. This figure shows the strain sensing wire, the center-tap lead wire, and the silica tube with the compensating wire all in the cement. For the purposes of analysis the following assumptions were made:

1. Steady state conditions prevail.
2. End effects may be neglected and the problem treated in two dimensions.
3. The temperatures of the specimen, the ambient air, the cement, the outer wall of the silica tube, and the strain sensitive wire are uniform and the same.
4. The presence of the center-tap lead wire may be neglected.
5. The temperature drop through the silica tubing is negligible.
6. The temperature of the compensating wire is uniform.
7. The compensating wire is centrally located in the silica tube.
8. The voltage drops in both arms of the Half-Bridge Strain Gage are of the same order of magnitude.

With these assumptions the situation reduces to that shown in Figure 9b. For this idealized case we have two concentric cylinders separated by an air gap. The inner cylinder is at a temperature t_c and the outer cylinder a temperature t_s .

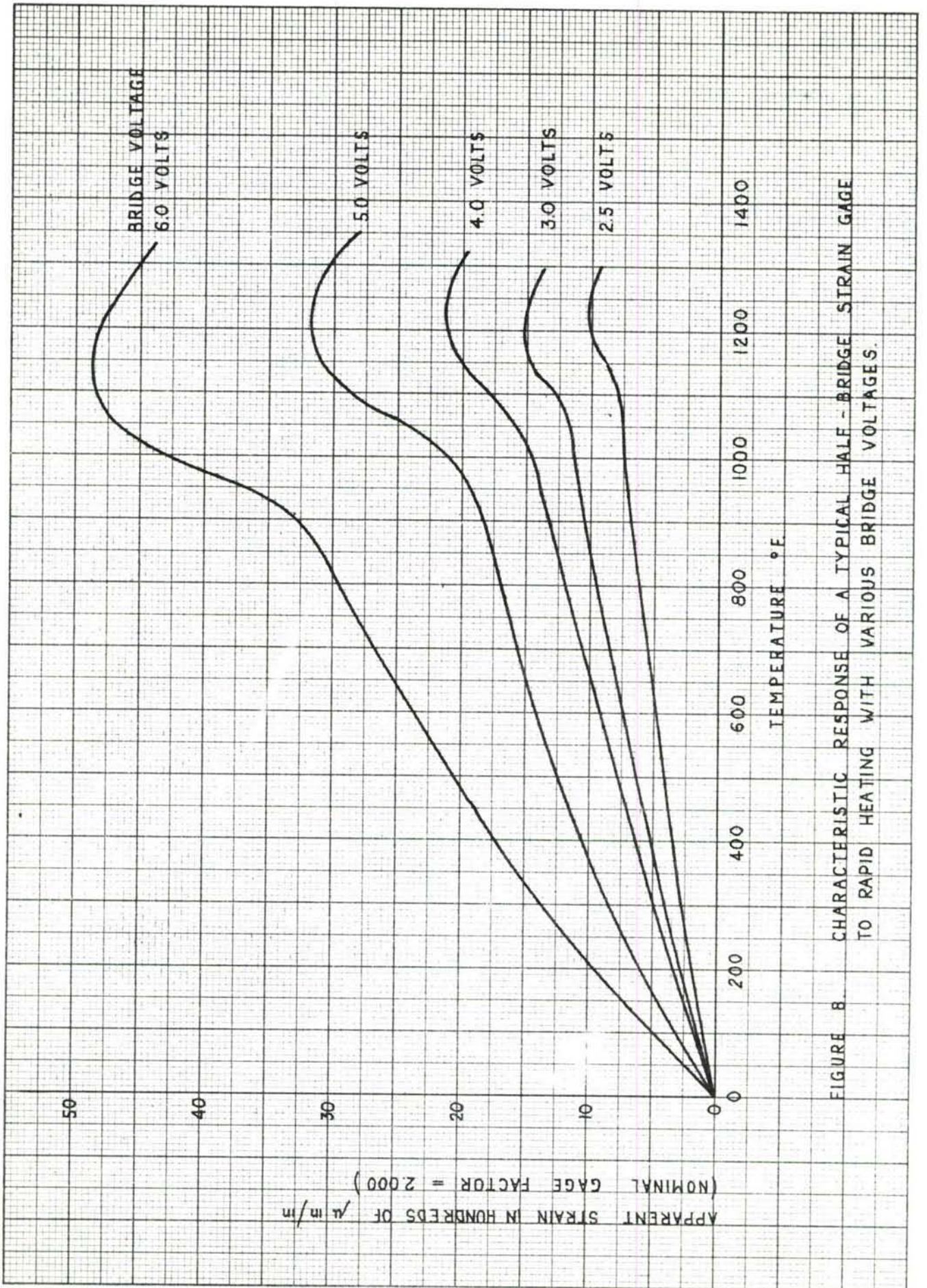


FIGURE 8. CHARACTERISTIC RESPONSE OF A TYPICAL HALF-BRIDGE STRAIN GAGE TO RAPID HEATING WITH VARIOUS BRIDGE VOLTAGES.

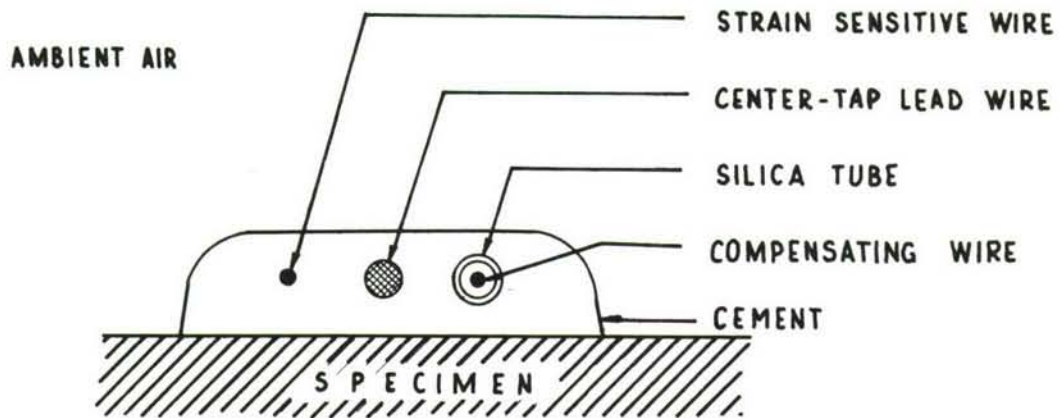


FIGURE 9a. CROSS-SECTION OF GAGE INSTALLATION.

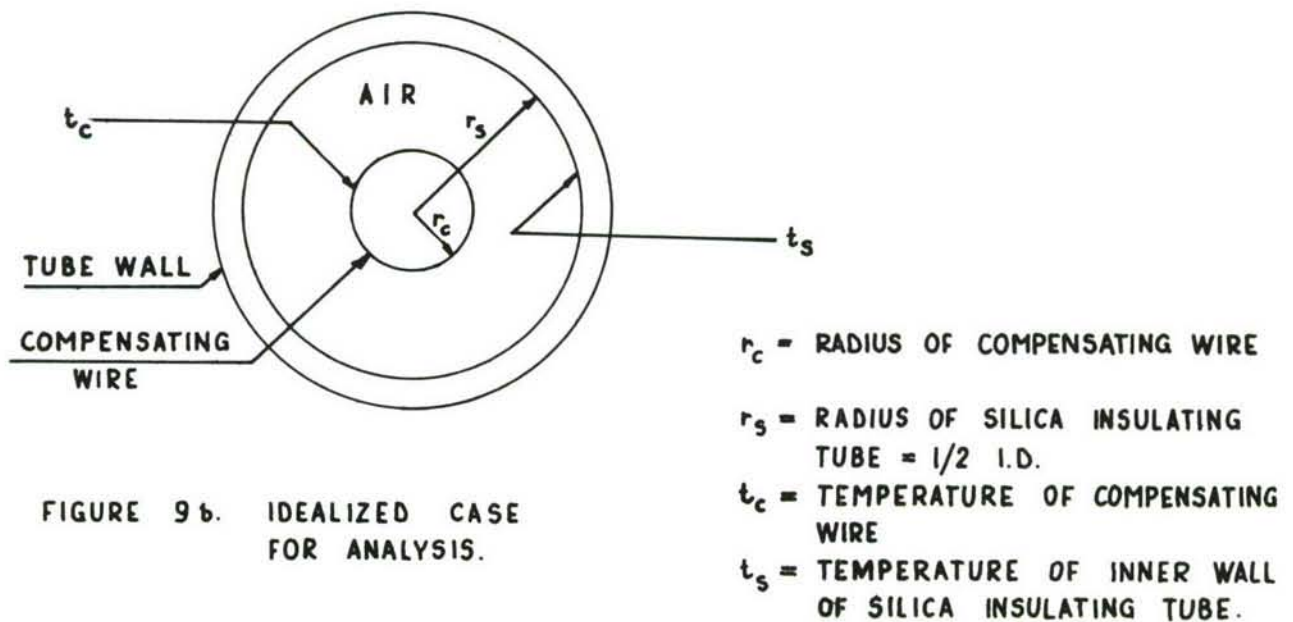


FIGURE 9b. IDEALIZED CASE FOR ANALYSIS.

FIGURE 9. CROSS-SECTION OF GAGE INSTALLATION AND IDEALIZED CASE FOR ANALYSIS.

Heat may be transferred from the compensating wire to the inner wall of the silica insulating tube by one or more of the following means: by radiation, by conduction and by convection. If q is the rate of heat loss of the wire, then

$$q = q_{\text{rad}} + q_{\text{cond}} + q_{\text{conv}} \quad (25)$$

where the rate of heat loss by each mechanism is indicated by the symbol q with the appropriate subscript.

For horizontal annuli, Liu has shown (11) that the ratio of heat transfer by conduction and convection combined to transfer by conduction alone,

$$\frac{q_{\text{cond}} + q_{\text{conv}}}{q_{\text{cond}}}$$

is determined by the dimensionless parameter.

$$\left(\frac{Pr^2 \cdot Gr}{1.36 + Gr} \right), \text{ where } Pr \text{ the Prandtl}$$

$$\text{number} = \frac{C_p \mu}{k}, \quad Gr \text{ is the}$$

$$\text{Grashoff number} = \frac{\rho^2 g \beta (t_c - t_s) (r_c - r_s)^3}{\mu^2}$$

and C_p is the specific heat at constant pressure, μ is the coefficient of viscosity, k is the thermal conductivity, ρ is the density, g is the gravitational acceleration, β is the coefficient of thermal expansion, t_c and t_s are the temperatures of the compensating wire and the inner wall of the silica insulating tube, respectively, and r_c and r_s are the radii of the compensating wire and of the inner wall of the silica tube. When this parameter has a value less than 10^3 , then

$$\frac{q_{\text{cond}} + q_{\text{conv}}}{q_{\text{cond}}} = 1 \quad (26)$$

When appropriate values, expressed in consistent units, are substituted, the parameter has a calculated value of about 1.5×10^{-8} for a temperature of 0°F. , and about 2.4×10^{-5} for 1000°F. Consequently, Equation (26) holds for the temperature range 0° to 1000°F. , and heat transfer by convection may be neglected. Under steady state conditions, we may then write for the compensating wire:

$$q = q_r + q_c \quad (27)$$

where q = rate at which heat is generated in the wire

q_r = rate at which heat is lost by radiation

q_c = rate at which heat is lost by conduction.

Now, $q = E^2 / R_{c,2}$, where E is the voltage drop across the compensating arm, and $R_{c,2}$ is the resistance of the compensating arm at the operating temperature, t_2 .

In Appendix II, it is shown that the resistance of the compensating arm at t_2 may be expressed as its resistance at the reference temperature multiplied by one or more factors involving temperature intervals and temperature coefficients of resistance for those intervals. Then

$$R_{c,2} = R_{c,0} \left[1 + \alpha_1 (t_1 - t_0) \right] \left[1 + \alpha_2 (t_2 - t_1) \right] \quad (28)$$

where $R_{c,0}$ = resistance of compensating arm at the reference temperature, t_0
 α_1 = average temperature coefficient of resistance of the compensating arm between t_0 and t_1
 α_2 = average temperature coefficient of resistance between t_1 and t_2
 t_0 = reference temperature, usually room temperature
 t_1 = ambient temperature of the gage
 $t_2 = t_{c,2}$ = temperature of the compensating arm under steady state conditions.

The resistance of the compensating arm at the reference temperature may also be expressed as

$$R_{c,0} = \frac{\rho L}{\pi r_c^2} \quad (29)$$

where ρ is the resistivity of the compensating wire at room temperature, and L and r_c are the length and radius of the wire.

By combining Equations (28) and (29), we obtain for the rate of heat generation in the compensating arm

$$q = \frac{\pi r_c^2 \epsilon^2}{\rho L \left[1 + \alpha_1 (t_1 - t_0) \right] \left[1 + \alpha_2 (t_2 - t_1) \right]} \quad (30)$$

The rate of heat loss of the wire by conduction is given by

$$q_{tc} = \frac{2 \pi k L (t_c - t_s)}{\ln \left(\frac{r_s}{r_c} \right)} \quad (31)$$

where k = thermal conductivity of air
 L = length of the compensating wire
 t_c = temperature of the compensating wire
 t_s = temperature of the inner wall of the silica insulating tube
 r_s = radius of silica insulating tube
 r_c = radius of compensating wire.

The rate of loss of heat from the wire by radiation is

$$q_r = 2 \pi r_c L \delta \bar{F} (T_c^4 - T_s^4) \quad (32)$$

where r_c and L are the radius and length of the compensating arm,

δ = Stefan-Boltzman constant
 \bar{F} = shape-emissivity factor
 T_c = absolute temperature of compensating wire
 T_s = absolute temperature of inner wall of silica insulating tube.

For the geometry considered, $\bar{F} = \epsilon$, the emissivity of the inner wall of the silica tube. Since $T_c - T_s$ will be small compared to T_c or T_s , it is permissible to make the following approximation (for derivation, see Appendix III):

$$T_c^4 - T_s^4 \cong 4 T_s^3 (T_c - T_s) = 4 T_s^3 (t_c - t_s) \quad (33)$$

Substitution into Equation (32) gives for the rate of heat loss by radiation

$$q_r = 8 \pi r_c L \delta \epsilon T_s^3 (t_c - t_s) \quad (34)$$

By comparison of Equation (27) with Equations (30), (31) and (34), and after eliminating π , we obtain

$$\frac{r_c^2 E^2}{\rho L [1 + \alpha_1 (t_1 - t_0)] [1 + \alpha_2 (t_2 - t_1)]} = \frac{2 k L (t_c - t_s)}{\ln\left(\frac{r_s}{r_c}\right)} + 8 r_c L \delta \epsilon T_s^3 (t_c - t_s) \quad (35)$$

If we let

$$C_1 = \frac{r_c^2 E^2}{\rho L [1 + \alpha_1 (t_1 - t_0)]}$$

and

$$C_2 = \frac{2 k L}{\ln\left(\frac{r_s}{r_c}\right)} + 8 r_c L \delta \epsilon T_s^3$$

we may write Equation (35) as

$$\frac{C_1}{1 + \alpha_2 (t_2 - t_1)} = C_2 (t_c - t_s) \quad (36)$$

The ambient temperature, t_1 , is the temperature of the outer wall of the silica tube (Assumption 3, page 14). Since a negligible temperature drop across the wall of the insulating tube was also assumed, the ambient temperature must be the same as the temperature of the inner wall of the silica tube, or $t_1 = t_s$. Furthermore, when the compensating wire is at the operating temperature $t_c = t_2$.

If the temperature change of the compensating arm due to Joule heating is designated by Δt_c , then

$$\Delta t_c = t_2 - t_1 = t_c - t_s \quad (37)$$

and Equation (36) may be rewritten as

$$\frac{c_1}{1 + \alpha_2 \Delta t_c} = c_2 \Delta t_c$$

$$\alpha_2 (\Delta t_c)^2 + \Delta t_c - \frac{c_1}{c_2} = 0 \quad (38)$$

The quadratic equation gives

$$\Delta t_c = \frac{-1 \pm \sqrt{1 + 4\alpha_2 \frac{c_1}{c_2}}}{2\alpha_2} \quad (39)$$

The negative sign in front of the radical has no physical significance in the situation under consideration and may be dropped. Rearrangement gives

$$\Delta t_c = \frac{1}{2\alpha_2} \left(\sqrt{1 + 4\alpha_2 \frac{c_1}{c_2}} - 1 \right) \quad (40)$$

From the fact that for $a \ll 1$

$$\sqrt{1+a} \approx 1 + \frac{a}{2}$$

we have, if we temporarily assume

$$4\alpha_2 \frac{c_1}{c_2} \ll 1$$

$$\Delta t_c = \frac{c_1}{c_2} \quad (41)$$

$$\Delta t_c = \frac{r_c^2 E^2}{2 \rho L^2 [1 + \alpha_1 (t_1 - t_0)] \left[\frac{k}{L_n (r_s / r_c)} + 4 r_c \epsilon \epsilon T_s^3 \right]} \quad (42)$$

Equation (42) predicts that the difference in temperature between the compensating and active arms of the Half-Bridge Strain Gage will increase as the square of the radius of the compensating wire and with the square of the bridge voltage. It will decrease as the resistivity, length, temperature coefficient of resistance, temperature and emissivity of the compensating wire increase. The temperature difference is also reduced the higher the ambient temperature, and the closer the ratio r_s / r_c approaches unity.

The temperature differences developed between the arms of Half-Bridge Strain Gages made from various materials were determined experimentally as a function of the ambient temperature of the gage and of the bridge voltage.

The data tabulated in Table IV is typical of that obtained in the experimental studies. The data resulted from measurements of a platinum-rhodium alloy gage, for which $\alpha_1 = \alpha_2 = 1000 \mu \text{ ohm/ohm/deg. F.}$, $E = 2.5$ volts, $L = 0.98$ inches and r_c and r_s were 0.00023 and 0.003 inches respectively.

TABLE IV

TEMPERATURE DIFFERENCE BETWEEN THE ARMS OF A PLATINUM - RHODIUM HALF-BRIDGE STRAIN GAGE

<u>Ambient Temperature, Degrees F.</u>	<u>Temperature of Compensating Arm, Degrees F.</u>	<u>Temperature Difference Degrees F.</u>
70	215	145
170	304	134
270	393	123
370	485	115
470	577	107

For a temperature change of Δt degrees, where $\Delta t = t_1 - t_0$, and t_1 and t_0 are the ambient and reference temperatures, there is a corresponding resistance change which is given by

$$\frac{\Delta R}{R_0} = \alpha_1 \Delta t, \quad (43)$$

where R_0 is the resistance at temperature t_0 and α_1 is the average temperature coefficient of resistance in the temperature range from t_0 to t_1 .

Thus, for the 100-degree rise in ambient temperature from 70° to 170° F, the fractional resistance change in the active arm of the gage will be

$$\begin{aligned} \frac{\Delta R_a}{R_a} &= \alpha_1 \Delta t_a = 10^3 \mu \Omega / \Omega / ^\circ F \times 10^2 ^\circ F = \\ &= 100,000 \mu \Omega / \Omega \end{aligned}$$

At the same time, the temperature of the compensating arm changes from 215° to 304° F., so that

$$\begin{aligned} \frac{\Delta R_c}{R_c} &= \alpha_1 \Delta t_c = 10^3 \mu \Omega / \Omega / ^\circ F \times 89 ^\circ F = \\ &= 89,000 \mu \Omega / \Omega \end{aligned}$$

The bridge unbalance will be

$$\frac{\Delta R_a}{R_a} - \frac{\Delta R_c}{R_c} = 100,000 - 89,000 = 11,000 \mu \Omega / \Omega$$

The measured apparent strain of this gage was 8000 $\mu \Omega / \Omega$, in reasonably good agreement with the calculated value.

IV. EFFECT OF DIFFERENTIAL THERMAL EXPANSION

For typical specimens of Nichrome and Nichrome V, the manufacturer has published data (2) on the electrical resistance at a series of temperatures up to 2000° F. The resistance ratio

R_t / R_o , has been calculated and the values tabulated in Table V. Figure 10 is the plot of the ratio. The slope of the curve at any point is the temperature coefficient of resistance for the given material. Values of the slope at various temperatures have been read from the curve and entered in Table V.

TABLE V

RESISTANCE RATIO AND SLOPE OF RESISTANCE-TEMPERATURE
CURVES FOR NICHROME AND NICHROME V FROM ROOM TEMPERATURE
TO 2000° F.

Ambient Temperature Degrees F.	<u>Nichrome V</u>		<u>Nichrome</u>	
	Resistance Ratio R_t / R_o	Temperature Coefficient $\mu \Omega / \Omega / ^\circ F$	Resistance Ratio R_t / R_o	Temperature Coefficient $\mu \Omega / \Omega / ^\circ F$
68	1.000	137	1.000	144
200	1.016	122	1.019	128
400	1.037	97	1.044	128
600	1.054	70	1.070	128
800	1.066	39	1.092	96
1000	1.070	-11	1.108	56
1200	1.064	-27	1.112	0
1400	1.062	12	1.118	51
1600	1.066	30	1.130	68
1800	1.072	30	--	--
2000	1.078	30	--	--

Using values of α from Table V, the difference in temperature between the compensating and the strain-sensitive arms of a Nichrome Half-Bridge Gage were computed from Equation (42), for ambient temperatures from room to 1600° F. The gage under consideration had a resistance of 60 ohms at 68° F. It was 1.0 inch long, with $r_c = 0.00045$ and $r_s = 0.003$ inches. In the computations, ζ was assumed to be unity and the values of the thermal conductivity of air as a function of temperature are taken from Kreith (2).

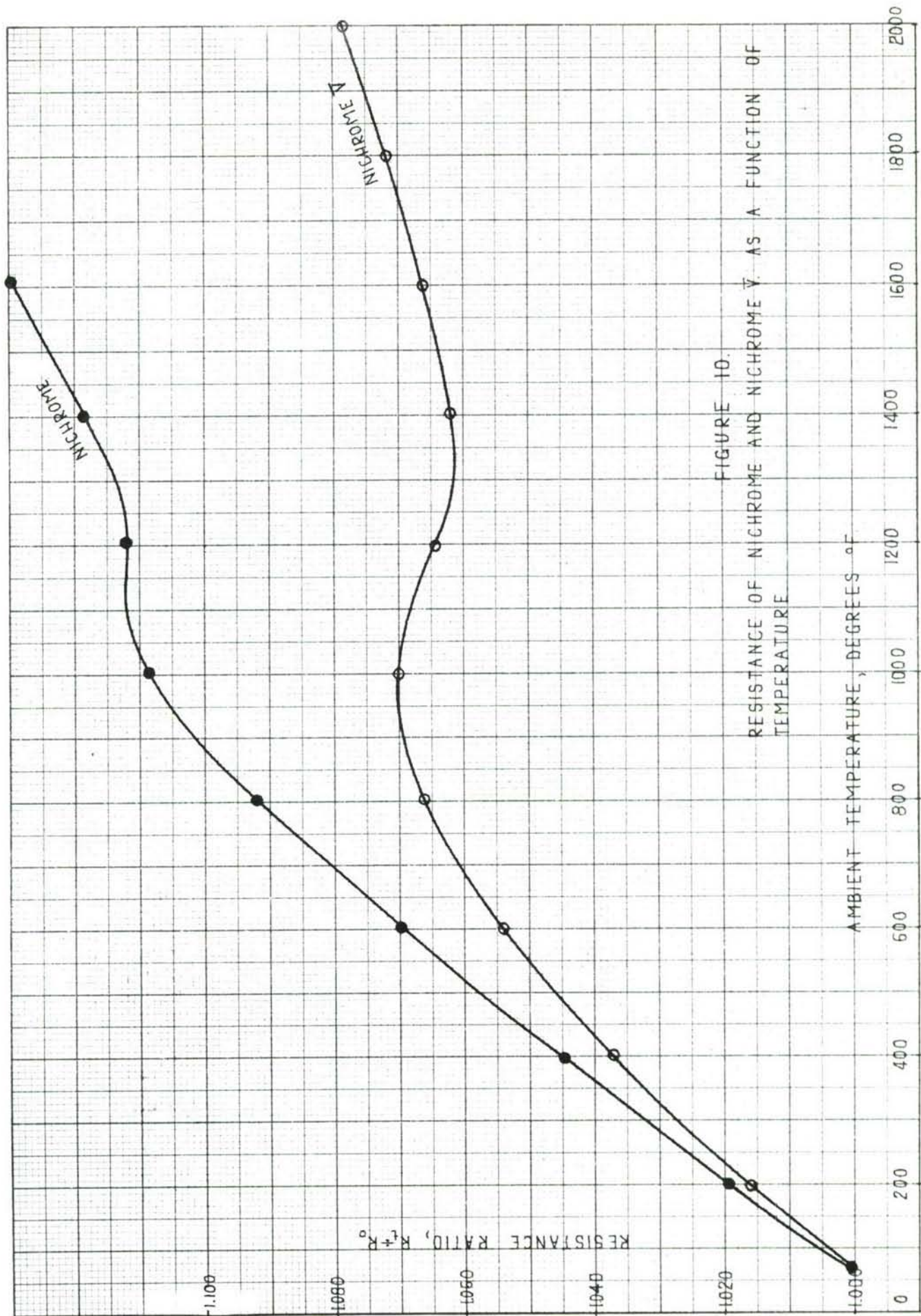


FIGURE 10.
RESISTANCE OF NICHROME AND NICHROME V AS A FUNCTION OF TEMPERATURE

The calculated temperature difference, Δt_c , is plotted in Figure 11 for two values of bridge voltage. The decrease in the temperature difference as the temperature increases is largely a result of the increase in the thermal conductivity of air. Radiation plays a small part, accounting for only 8.9% of the total heat transfer at 1600° F.

From the temperature difference and the slope of the resistance-temperature curve it is now possible to calculate the apparent strain of the gage. To do this properly it is first necessary to make an assumption as to the specimen material to which the gage is bonded. As the gage and specimen are heated they expand. The expansion is given by

$$\Delta L = L_o \beta (t_1 - t_o) \quad (44)$$

where ΔL = the change in length

L_o = the length at the reference temperature

β = the linear coefficient of thermal expansion

t_1 = ambient temperature

t_o = the reference temperature

If β of the specimen does not equal β of the active wire, then a strain is induced in the strain sensitive arm. The magnitude of this strain will be equal to the difference between the coefficient of thermal expansion of the specimen and the strain sensitive wire. This strain will then cause a change in the resistance of the strain sensitive wire of magnitude.

$$\frac{\Delta R_\alpha}{R_\alpha} = (\beta_{sp} - \beta_\alpha) (t_1 - t_o) G_\alpha \quad (45)$$

where R_α is the resistance of the active arm, β_{sp} and β_α are the linear coefficients of thermal expansion of the specimen and of the active arm of the gage, and G_α is the strain sensitivity of the active arm at the ambient temperature, t_1 .

TEMPERATURE DIFFERENCE AT t_c DEGREES °F

40
35
30
25
20
15
10
5
0

ARM VOLTAGE 1.5 VOLTS (BRIDGE VOLTAGE 3.0 VOLTS)

ARM VOLTAGE 1.0 VOLT
(BRIDGE VOLTAGE 2.0 VOLTS)

200 400 600 800 1000 1200 1400 1600

AMBIENT TEMPERATURE in °F

FIGURE 11. CALCULATED TEMPERATURE DIFFERENCE BETWEEN COMPENSATING AND STRAIN-SENSITIVE ARMS OF A 60 Ω , 1", NICHROME HALF BRIDGE STRAIN GAUGE $r_1 = 0.00045$, $r_0 = 0.003$.

The total change in the resistance of the strain-sensitive arm of the gage due to thermal effects is thus

$$\frac{\Delta R_a}{R_{a,0}} = \alpha (t_1 - t_0) + (\beta_{sp} - \beta_a) (t_1 - t_0) G_a + \alpha (\beta_{sp} - \beta_a) (t_1 - t_0)^2 G_a \quad (46)$$

where $R_{a,0}$ is the resistance of the strain-sensitive or active arm of the gage at the reference temperature, and the other terms have been defined previously. The resistance of the compensating arm at the operating temperature has been shown (Appendix II and Equation 28) to be

$$R_{c,2} = R_{c,0} \left[1 + \alpha_1 (t_1 - t_0) \right] \left[1 + \alpha_2 (t_2 - t_1) \right]$$

The total change in the Half-Bridge Strain Gage in terms of the parameters used in Wheatstone bridge analysis is then given by

$$\begin{aligned} \frac{\Delta R_a}{R_{a,0}} - \frac{\Delta R_c}{R_{c,0}} = & (\beta_{sp} - \beta_a) (t_1 - t_0) G_a + \\ & + \alpha_1 (\beta_{sp} - \beta_a) (t_1 - t_0)^2 G_a - \alpha_2 (t_2 - t_1) \left[1 + \alpha_1 (t_1 - t_0) \right] \end{aligned} \quad (47)$$

or

$$\frac{\Delta R_a}{R_{a,0}} - \frac{\Delta R_c}{R_{c,0}} = \left[1 + \alpha_1 (t_1 - t_0) \right] \left[(\beta_{sp} - \beta_a) (t_1 - t_0) G_a - \alpha_2 (t_2 - t_1) \right] \quad (48)$$

It will become apparent that the term $(\beta_{sp} - \beta_a)(t_i - t_o)G_a$ is of extreme importance in the determination of a Half-Bridge Strain Gage output. Changes in the value of any one of the factors in this term will change the amount of compensation obtained with the gage. At present, the gage under study has experimentally shown that it can be compensated on Inconel to within 1/10 to 2/10 of a micro-inch per inch per degree Fahrenheit. This value falls inside the error in the quoted values for thermal expansion coefficients and, indeed, within the lot-to-lot variation of thermal expansion coefficient. The capabilities of the Half-Bridge Strain Gage are such that one must know the coefficient of thermal expansion to a higher degree of accuracy than heretofore to obtain the maximum compensation. It should also be pointed out that the effects of heating rate, cold work, and previous thermal history on the specimen's thermal expansion is another area that should be investigated.

To illustrate the effect of $(\beta_{sp} - \beta_a)(t_i - t_o)G_a$, values of

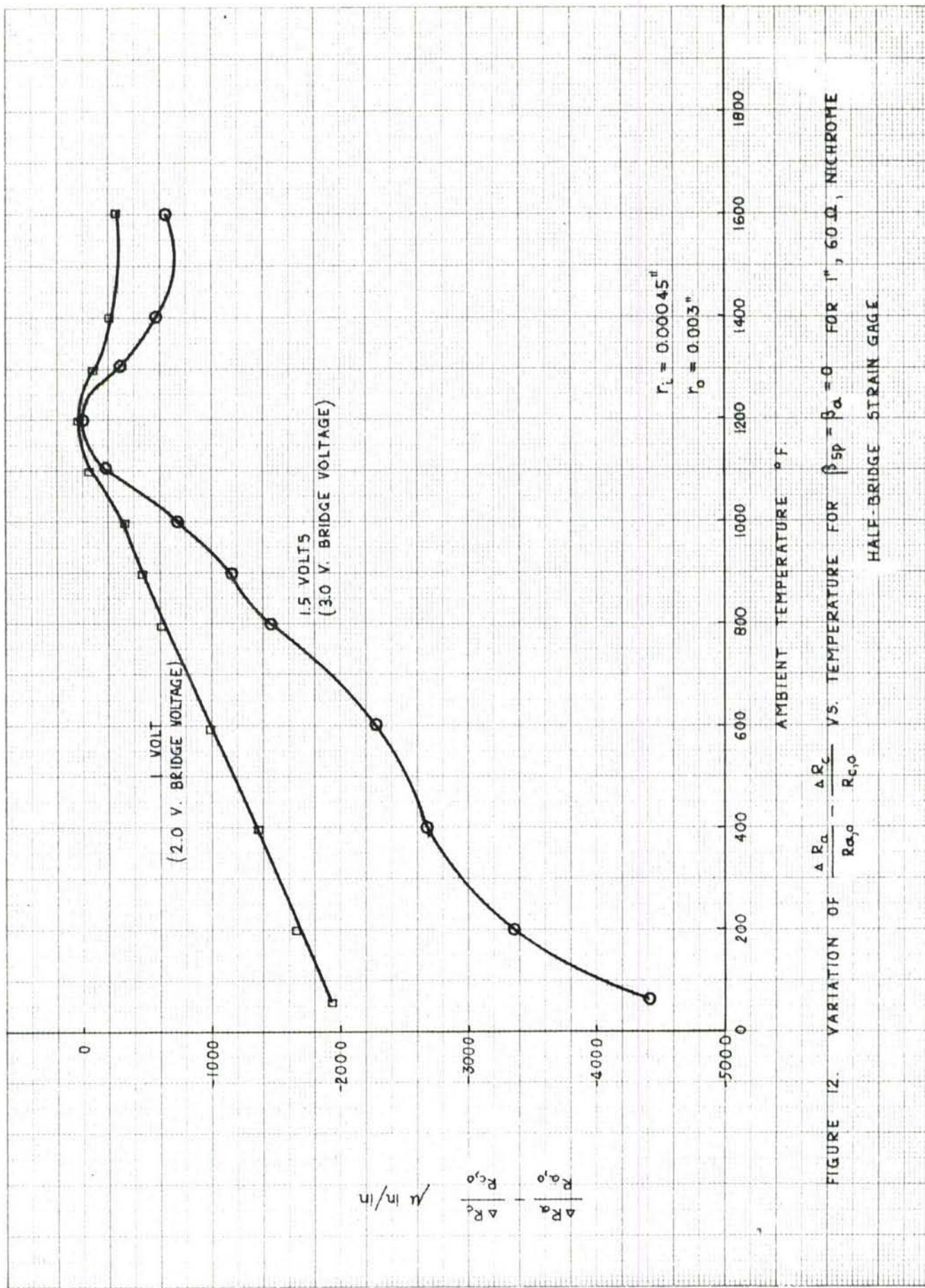
$$\frac{\Delta R_a}{R_{a,0}} - \frac{\Delta R_c}{R_{c,0}}$$

were calculated for the case where $\beta_{sp} - \beta_a = 0$ and plotted in Figure 12. The curves in Figure 12 should be proportional to the apparent strain of a Half-Bridge Strain Gage.

Note that while negative values of apparent strain are given for room temperature, it is common practice to balance the bridge with the appropriate bridge voltage applied. The room temperature values would then be zero and the apparent strain would be the change in

$$\frac{\Delta R_a}{R_{a,0}} - \frac{\Delta R_c}{R_{c,0}}$$

The effect of thermal expansion was investigated by taking the average value of the thermal expansion coefficient for Nichrome between 68 and 1800° F., from reference (3) and the average value of thermal expansion for Inconel between 70° and 1400° F. from reference (4). The values are 9.4 and 7.0 parts per million per degree Fahrenheit, respectively. A nominal strain sensitivity of



2.2 was assumed for room temperature and it was assumed that the decrease in strain sensitivity with temperature would balance out the increase in $[1 + \alpha_1 (t_1 - t_0)]$. The results are shown in Figure 13 in terms of apparent resistance change or the change in the value of $\Delta R_a / R_{a0} - \Delta R_c / R_{c0}$ from the room temperature value. Figure 13 contains the curve of the apparent resistance change versus the temperature for the same gage but with $\beta_{sp} - \beta_a = -1.8 \mu \text{ in/in/}^\circ\text{F}$. The difference between the curves for different values of $\beta_{sp} - \beta_a$ illustrate the importance of a precise knowledge of the values of both β_{sp} and β_a . A comparison with the experimental data for this gage, which is discussed in Chapter 4, indicates a very good correlation between the theoretical calculations and the experimental results.

A final study using equation (42) was made on a prototype model of a Nichrome V gage with Nichrome V leads. This gage was designed to be constructed of only one material so as to completely eliminate any thermal emfs. Testing of the gage had not been carried out at the end of the contract period so no experimental data is available for comparison. The study was made for the following conditions:

- $E = 1/2, 1, 2, 3, 4$ and 5 volts
- $R_0 = 120$ ohms
- $t_0 = 68^\circ \text{F}$.
- $\zeta = 1.0$
- $r_c = .000225$ inches
- $r_s = .003$ inches
- $L = .45$ inches

The calculated values of temperature difference between the two arms are shown in Figure 14 as a function of ambient temperature for various bridge voltages and in Figure 15 as a function of bridge voltages for various ambient temperatures. From this data, values of apparent strain (for a gage factor setting of 2.000) were calculated and plotted in Figure 16 for the case where $\beta_{sp} = \beta_a$. The response of the gage when bonded to a material for which β_{sp} does not equal β_a can be calculated from this figure.

Figure 16 illustrates a factor of Half-Bridge Strain Gage performance that had been difficult to explain, namely, the anomolous behavior of the gage in the temperature range of $900^\circ\text{-}1100^\circ \text{F}$., reference 1. In this range a "hump" appeared in the apparent strain curve of the Half-Bridge Strain Gages made from Nichrome and Nichrome V. This behavior may be explained by the change in slope of the resistance-temperature curve of the wire comprising the gage.

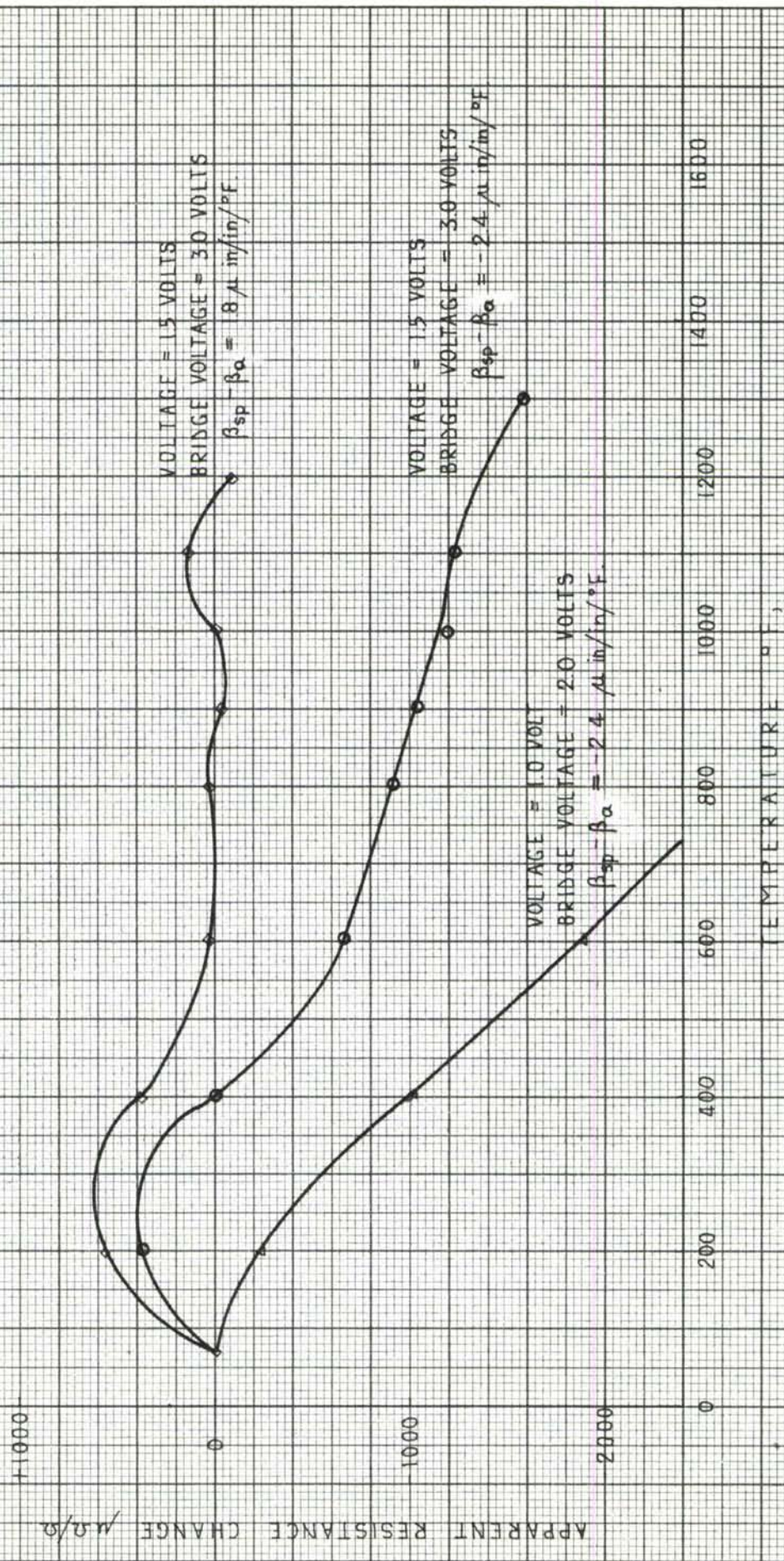


FIGURE 13. CALCULATED APPARENT RESISTANCE CHANGE FOR A 1", 60 Ω , NICHROME HALF-BRIDGE STRAIN GAGE $r_1 = 0.00045''$ $r_0 = 0.003''$

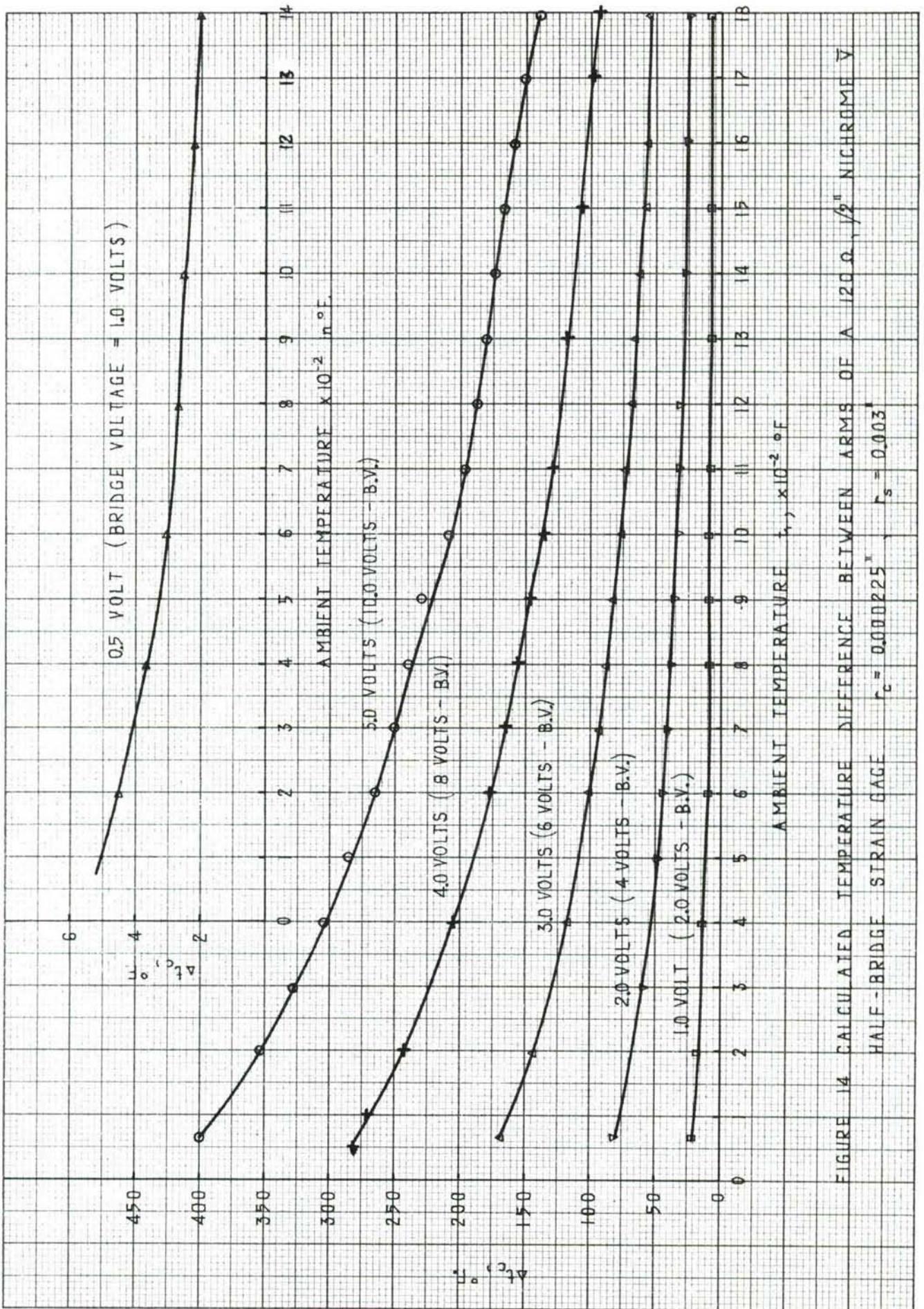


FIGURE 14 CALCULATED TEMPERATURE DIFFERENCE BETWEEN ARMS OF A 120 Ω, 1/2" NICHROME V
 HALF-BRIDGE STRAIN GAGE $r_c = 0.000225$, $r_s = 0.003$

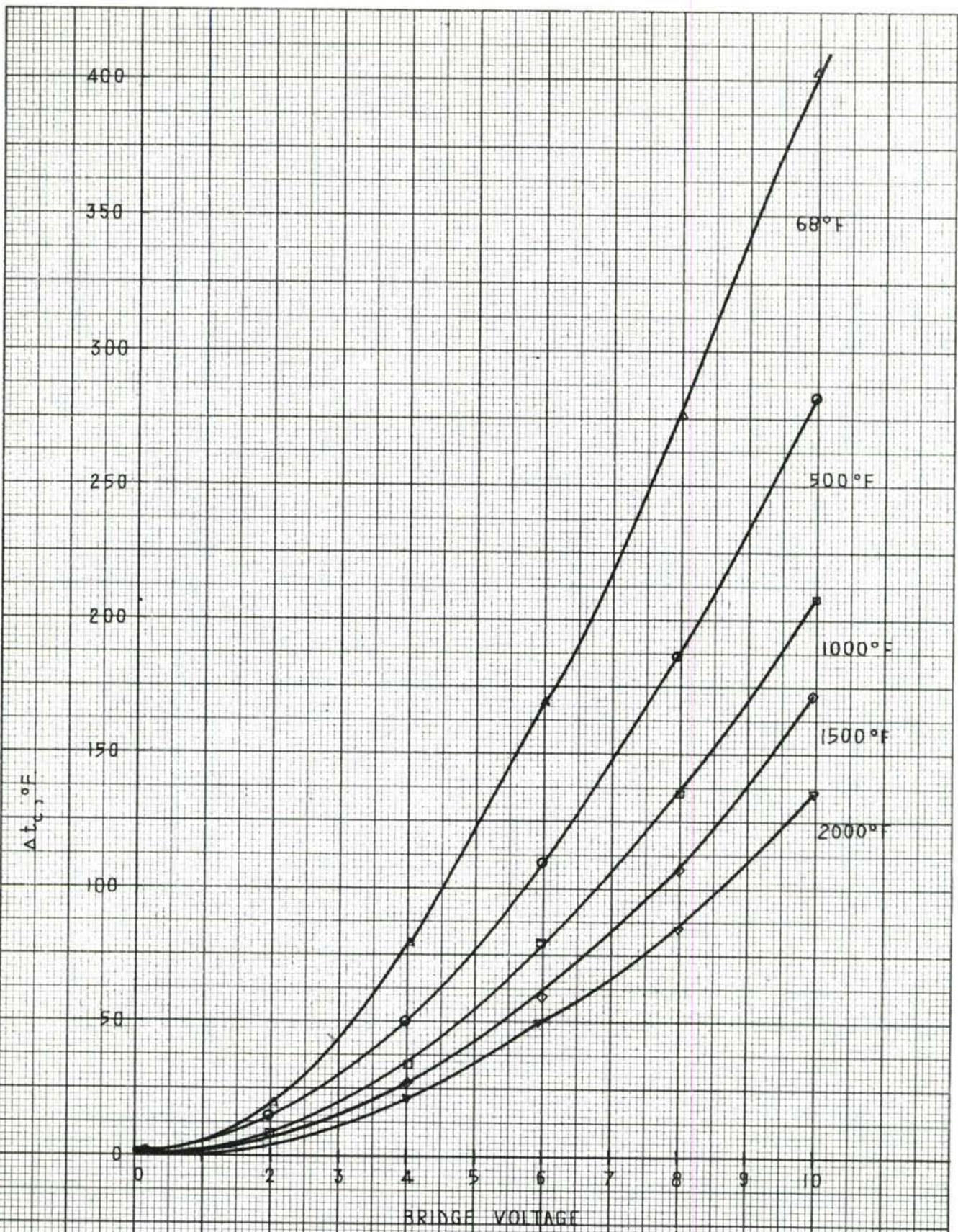
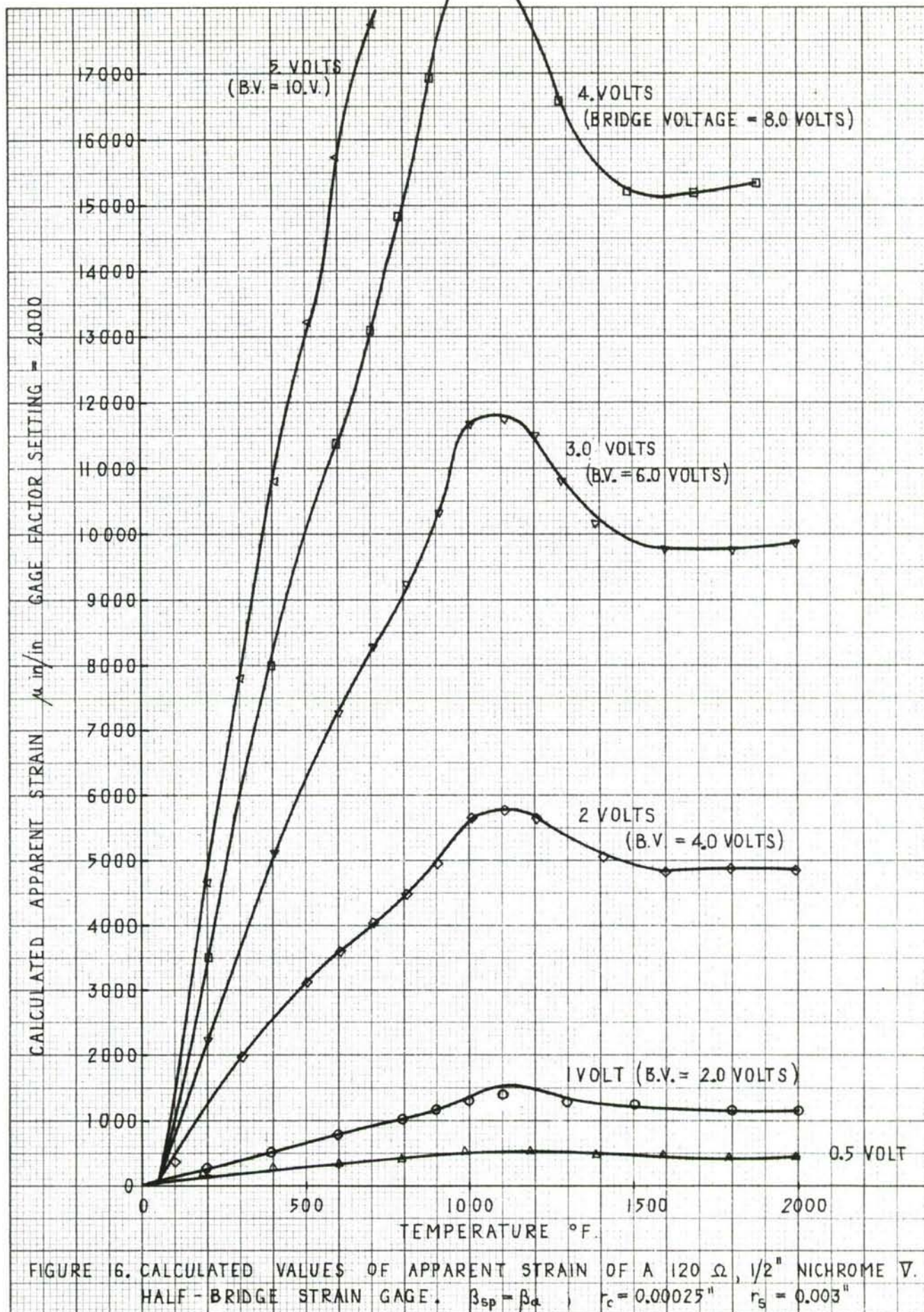


FIGURE 12 CALCULATED TEMPERATURE DIFFERENCE BETWEEN ARMS OF
 A 120 Ω, 1/2" NICHROME \bar{V} HALF-BRIDGE STRAIN GAGE $r_c = 0.000225''$
 $r_s = 0.003''$



V. GAGE MANUFACTURING PROCEDURES

Half-Bridge strain gages were manufactured and tested from November 1960 to September 1961. A number of alloys were screened during this program and many gage configurations were studied. At least three hundred finished gages were fabricated. From this intensive search and procedure it became increasingly apparent that "Nichrome V" (Driver-Harris Co.) was as good or better than materials currently available. A list of these materials follows:

1. Platinum
2. Platinum - 30% Iridium
3. Baker Alloy 1729
4. 40% Silver, 60% Palladium
5. Inconel X
6. 302 Stainless Steel
7. H. T. 600
8. H. T. 600A
9. H. T. 700
10. Ni 35% - Cr 20% - Balance Fe.

A final gage design, Figure 17, was frozen for prototype production, having the following specifications:

1. Overall gage length nominally 1"
2. Gage width .062"
3. Active grid resistance 60 ohms plus or minus .5 ohms
4. Inactive grid resistance 60 ohms plus or minus .5 ohms
5. Grid wire diameter (active and inactive) .0008"
6. Gage leads .005" o.d. grade A nickel
7. Gage encapsulation material, PBX ceramic cement.

Throughout the course of the prototype production, jigs and fixtures were designed for speed and simplicity while still retaining high quality standards. The length of time required to set up and test a single Half-Bridge strain gage made it desirable to develop a method of screening so that completed gages could be either accepted or rejected for test. A simple fixture for mounting a gage on a test specimen was built, Figure 18, and a data chart was developed, as illustrated in Figure 19.

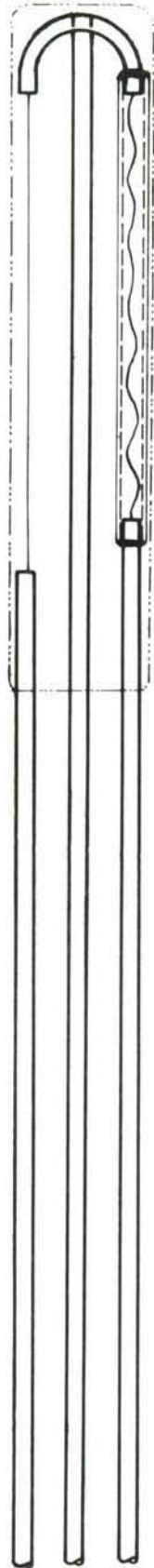


FIGURE 17. DETAIL CONSTRUCTION HALF-BRIDGE STRAIN GAGE.

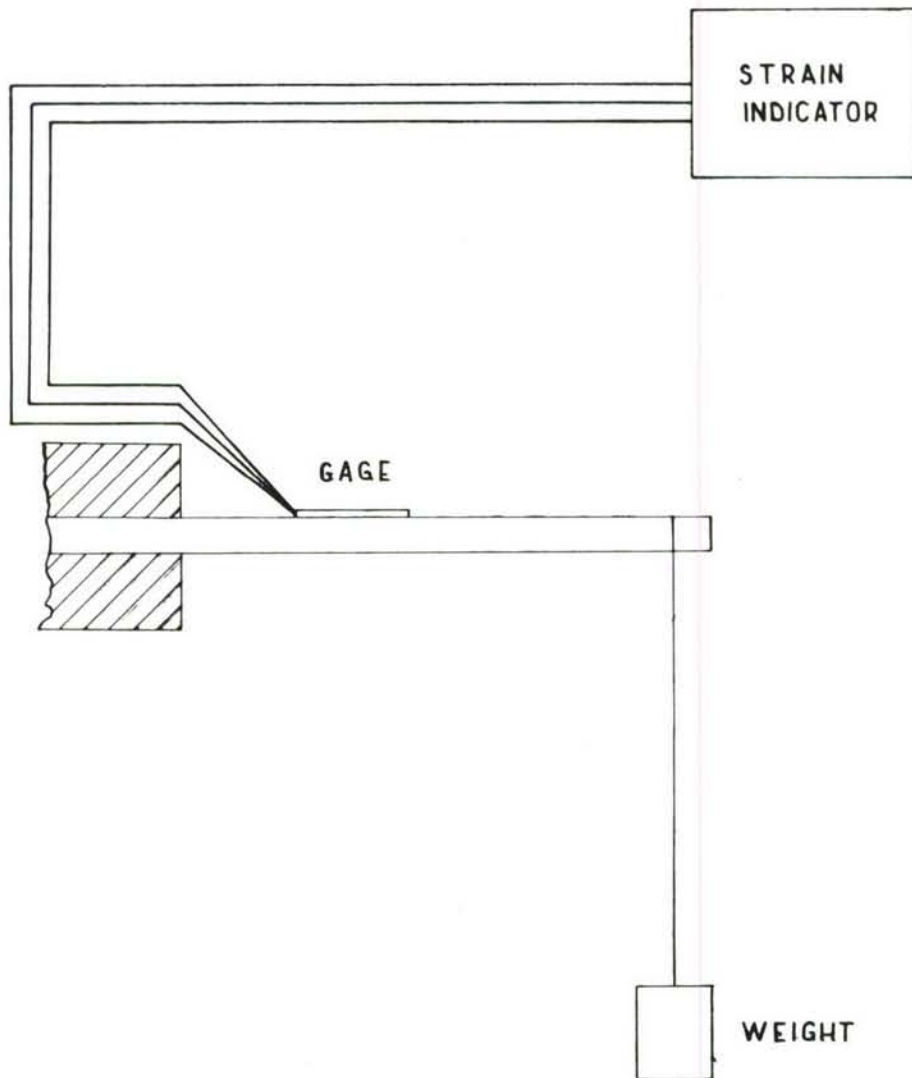


FIGURE 18. TEST FIXTURE.

HALF-BRIDGE STRAIN GAGE
Data Sheet

Gage Number:
 Gage Wire: Wire Size:
 Lead Material: Lead Size:
 Silicon Tubing Size: Cement:
 Specimen Material: Specimen Size:
 Gage Length:
 Configuration:
 Heat Treatment:
 Cure:
 Resistance: $R_a =$
 $R_c =$

Load Check

Load	Arm 1	Δ 1	Arm 2	Δ 2	Total	Gage	Δ t	
0 gms								
100 "								Accepted
200 "								Rejected
300 "								
500 "								

Cycle	Voltage	Max.	Temp.	Heating Time	Fan	Notes
1						
2						
3						
4						
5						
6						
7						
8						
9						
10						
11						
12						
13						
14						
15						
16						
17						
18						
19						
20						
21						
22						
23						
24						
25						

FIGURE 19. HALF-BRIDGE STRAIN GAGE DATA SHEET

1. Manufacturing Procedures

The Half-Bridge high temperature strain gage departs radically from simple grid construction in wire or foil and becomes quite complex to fabricate, therefore extreme care and quality control must be exercised during all phases of assembly. The various steps in assembling Half-Bridge strain gages are illustrated in Figure 20, and are as follows:

(A) shows a micro-bore metallic tube cut to proper size.

(B) is a strain sensitive filament threaded through the metallic tube prior to cold swaging.

(C - D) illustrate the strain sensitive filament cut to size after the cold swaging process.

(E) shows the metallic tube formed into a cross bar with the strain sensitive filaments in position.

(F) illustrates the two filaments with one convoluted so as to render it slack and strain inactive when in proper position.

(G) shows two metallic lead tubes attached and cold-swaged to the active and inactive strain sensitive filaments.

(H) shows a metallic lead tube welded to the center of the cross bar and functioning as a common center tap.

(I) shows the completed skeletal framework of the Half-Bridge high temperature strain gage.

(J) shows the skeletal framework of the gage mounted in the special Teflon fixture prior to ceramic encapsulation. This special Teflon fixture for mounting and curing the gages is illustrated in Figure 21.

2. Curing Procedures

The Half-Bridge high temperature strain gage was designed to operate at temperatures above 600° F., therefore a ceramic type cement must be used in lieu of organic compounds and adhesives. A number of ceramic compounds and cements have been tried as strain gage adhesives during our investigation. Allen PBX ceramic cement (Robert G. Allen Co., Mechanicville, N. Y.) was found to have the following desirable characteristics:

1. High electrical resistivity over a range of temperatures to 1500° F and the ability to adhere to a wide variety of substrates.

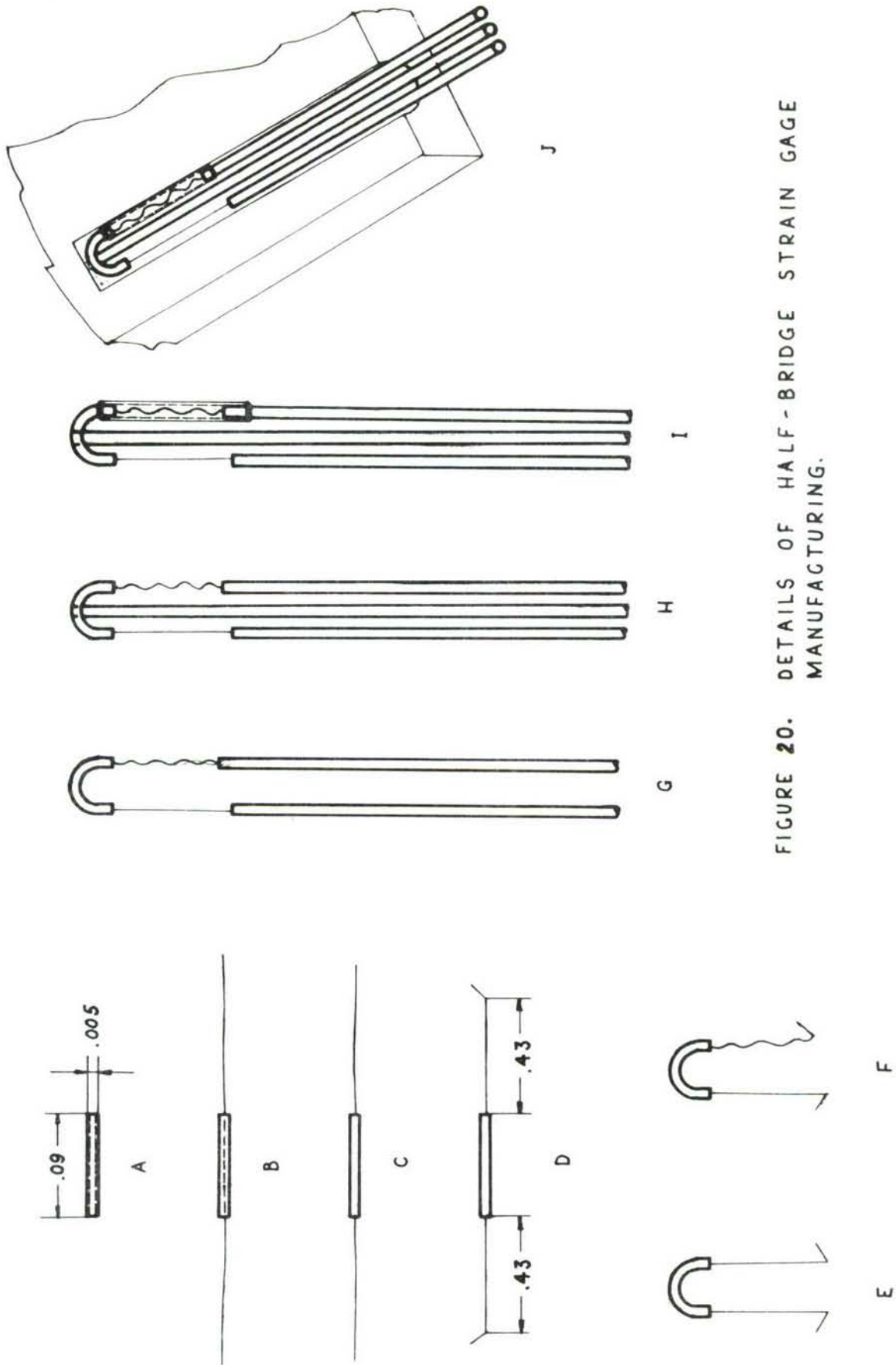


FIGURE 20. DETAILS OF HALF-BRIDGE STRAIN GAGE MANUFACTURING.

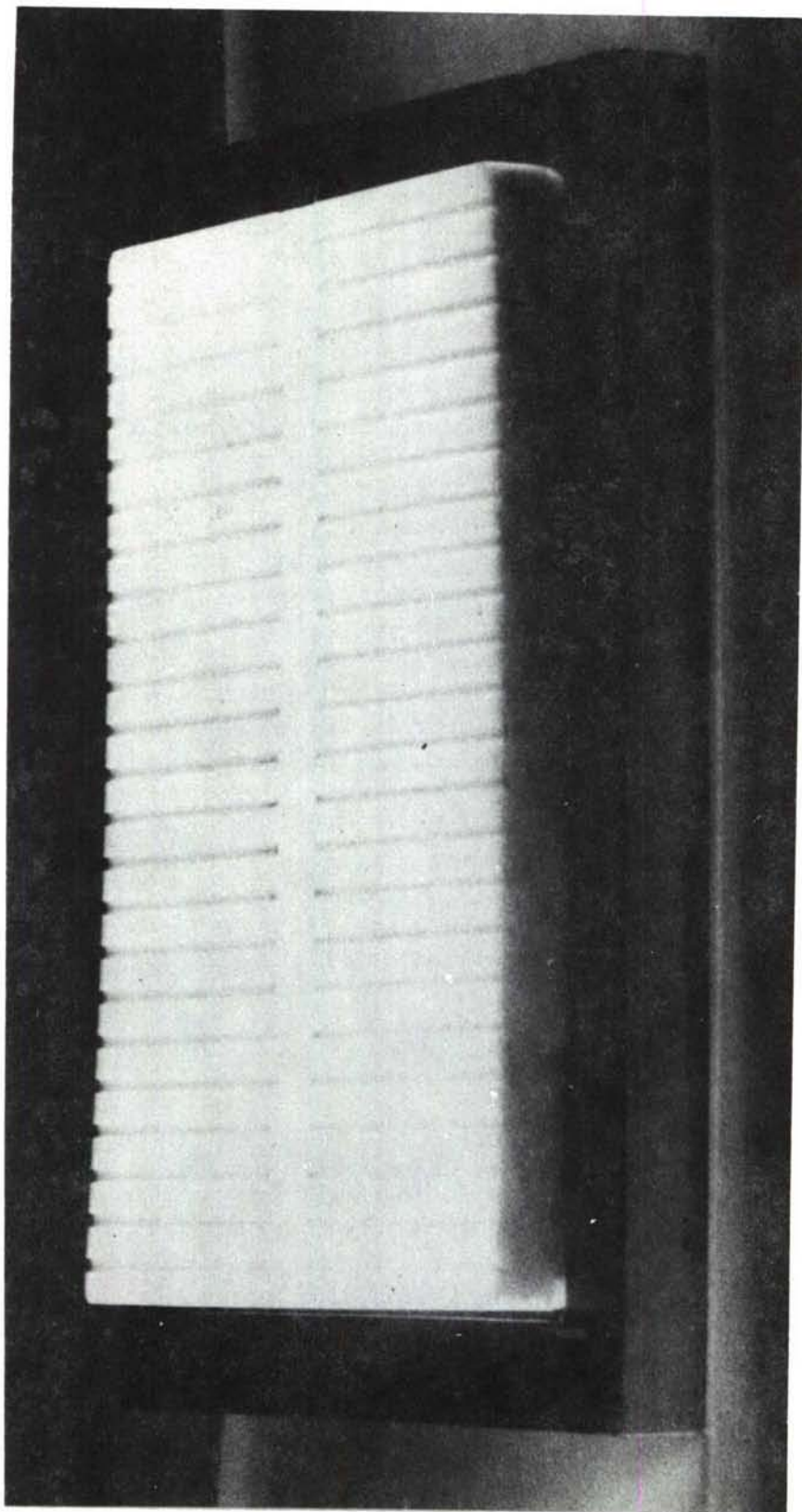


FIGURE 21. TEFLON MOLD

2. Good thermal shock properties. Since this particular contract stressed extremely high heating rates, the ability to transmit strains accurately without spalling was of prime importance.

The best encapsulating material for the Half-Bridge high temperature strain gage would be, if possible, the adhesive that normally binds a gage to a substrate. One of the problems encountered was the selection of a fixture material that would serve as a mold and still not adhere to the PBX ceramic cement. In this connection, "Teflon" was selected as the fixture material. This fixture is illustrated in Figure 21.

PBX ceramic cement is commercially available as a two-component system. One component is a powder which is comprised of high purity aluminum oxide and high purity fused quartz, ground to a very fine particle size. The other component, which functions as the binder, is a complex phosphate chromate. When these two components are mixed in the proportions of approximately two parts of powder to one part of the binder, the cement becomes quite practical to use as a strain gage cement and also as an encapsulent material.

As illustrated in Figure 21, the cement is poured into the mold of the fixture. The gages are all encapsulated in the fixture and allowed to air-dry for two hours in a dry atmosphere. This air-drying procedure is best carried out with infra-red lamps in the immediate vicinity. After this air-drying period, the fixture is placed in a drying oven and held at 300° F for approximately one hour, then allowed to cool normally to room temperature. The cement will not adhere to the Teflon mold providing that the molds are highly polished and maintained in this polished condition at all times. The gages generally pop out of the molds of the fixture during the cooling cycle.

3. Final Inspection

When the fixture, Fig. 21, has cooled to room temperature, the gages are removed and visually inspected for warping and cracks in the semi-cured ceramic. This inspection is accomplished under ten-power magnification. The finished gages are then checked for electrical resistance and must conform to the specifications outlined on page 43. The gages are then placed in appropriate containers containing silica gel so that the semi-cured gages are not subjected to moisture. In effect, these gages are complete in this semi-cured condition and will be further cured when installed for actual test subject to final curing at 600° F for one hour. PBX ceramic cement becomes water-insoluble after this last cure.

VI. STEADY STATE TESTS

During the course of the program a large number of gages were tested. These gages were made of several different materials and were manufactured in different configurations. Very often the changes between prototypes were of a very minor nature. For this reason, and because the primary purpose of the testing was to guide the development of the Half-Bridge strain gage, the majority of the data that will be presented here is data on the final gage configuration. This final configuration consisted of a .0009" diameter Nichrome wire and a .006" inside diameter silica tube. The leads were nickel tubes with a .005" outside diameter. The gages were all made in the standard fixture described in section V.

The first experimental data presented, Figs. 22 and 23, shows the apparent strain as a function of temperature for a set of four Half-Bridge strain gages of the final configuration. These gages were mounted onto Nimonic 90 specimens with PBX ceramic cement and cured for one hour at 600° F. A standard Baldwin-Lima-Hamilton Type N Strain Indicator with a bridge voltage of 3.5 volts was used to record the resistance change of the gages. The temperature was measured by means of thermocouples whose output was read on a Leeds and Northrup Millivolt Potentiometer. Switching and initial balancing were obtained with a Baldwin Type 525 Switching and Balancing Unit.

The specimens were inserted into the oven and heated to the test temperature. At the test temperature, readings were taken over a period of two hours. The oven was then turned off and the installation allowed to cool to room temperature. During cooling, the apparent strain was recorded at intervals of approximately 100° F.

Figures 22 and 23 show data for five cycles on the first four gages. In Run No. 1 (Figure 22) the first heating cycle after the cure is shown. The maximum temperature of this cycle was 600° F. At this temperature there was no drift in the output of any of the gages in a period of two hours. The apparent strain data was taken on cooling and the curves plotted so that all the gages read zero at room temperature. The time (in minutes) required to cool to various temperatures is given by the numbers in large circles over the top curve. The data for Runs 2 through 5 is summarized in Table VI.

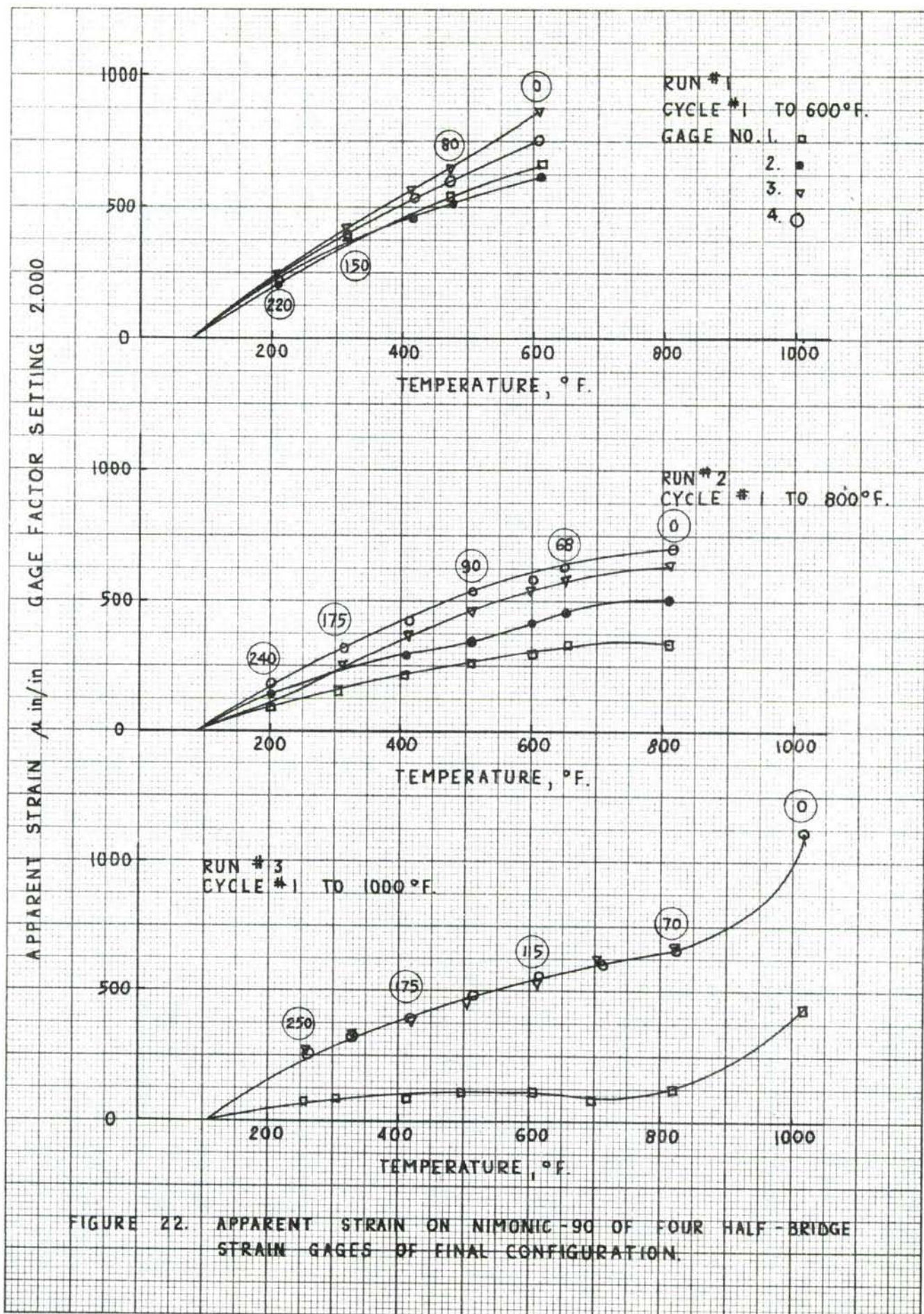


FIGURE 22. APPARENT STRAIN ON NIMONIC-90 OF FOUR HALF-BRIDGE STRAIN GAGES OF FINAL CONFIGURATION.

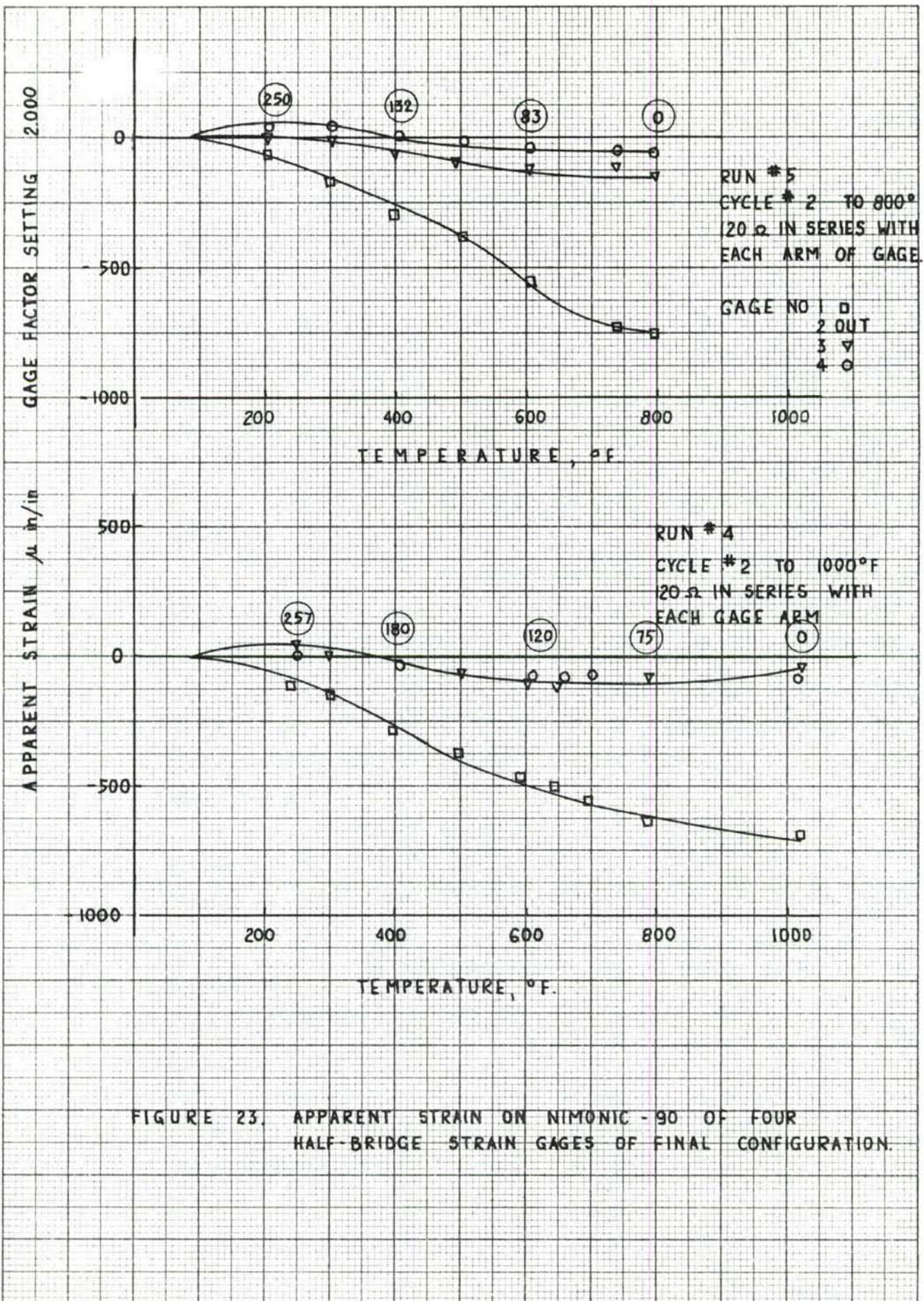


FIGURE 23. APPARENT STRAIN ON NIMONIC - 90 OF FOUR HALF-BRIDGE STRAIN GAGES OF FINAL CONFIGURATION.

TABLE VI

DRIFT RATE AND ZERO SHIFT DATA ON FOUR HALF-BRIDGE STRAIN GAGES OF THE FINAL CONFIGURATION ON NIMONIC 90 TEST SPECIMENS

Cycle and Gage	1 600° F		2 800° F		3 1000° F		4 1000° F		5 800° F	
	Drift Rate*	Zero Shift**	Drift Rate*	Zero Shift**	Drift Rate*	Zero Shift**	Drift Rate*	Zero Shift**	Drift Rate*	Zero Shift**
1	none	-76	2.32	1073	-.57	-830	-.23	1193	-1.32	-44C
2	none	-78	.32	16	--	--	--	--	--	--
3	none	-78	2.07	1011	-.71	-610	-.17	286	-.14	-252
4	none	40	1.42	669	--	-232	-.12	1132	-.12	-46

* Drift rate at maximum test temperature, measured over a period of two hours, micro inches per inch per minute.

**Zero shift in units of micro inches per inch.

For runs 4 and 5, a 120 ohm resistance was put in series with each arm of the Half-Bridge Strain Gage. This has two effects: first, it decreases the sensitivity of the circuit to changes in gage resistance by a factor of $R / (R + 120)$, or approximately one-half and, second, it decreases the voltage drop through each arm of the Half-Bridge strain gage. The latter causes a decrease in the temperature difference between the active and compensating arms of the gage. Since the coefficient of thermal expansion of Nimonic 90 is similar to that of Inconel, a decrease in the temperature difference between the two arms should reduce the apparent strain of the gage. These effects are borne out by the data obtained.

The data for five Half-Bridge strain gages mounted onto 316 Stainless Steel are shown in Figures 24 and 25. These data were obtained in the same fashion and with the same equipment as the data reported for gages mounted on Nimonic 90. The coefficient of thermal expansion of 316 Stainless Steel is higher than that of Nimonic 90 so that it is to be expected that the apparent strain of the Half-Bridge strain gage on 316 Stainless Steel will be higher than that of the gage on Nimonic 90. The data shows that this is indeed the case.

The data for the five gages on stainless steel is summarized in Table VII. Examination of this table shows that there is excellent agreement between four of the five gages tested. For example, on cycle 1, the temperature coefficients of the gages were 2.14, 4.46, 1.92, 2.12 and 2.08 micro-inches per inch per degree Fahrenheit while the value of total drifts in two hours at the maximum test temperature were -110, -173, -107, -125, -180 micro inches per inch.

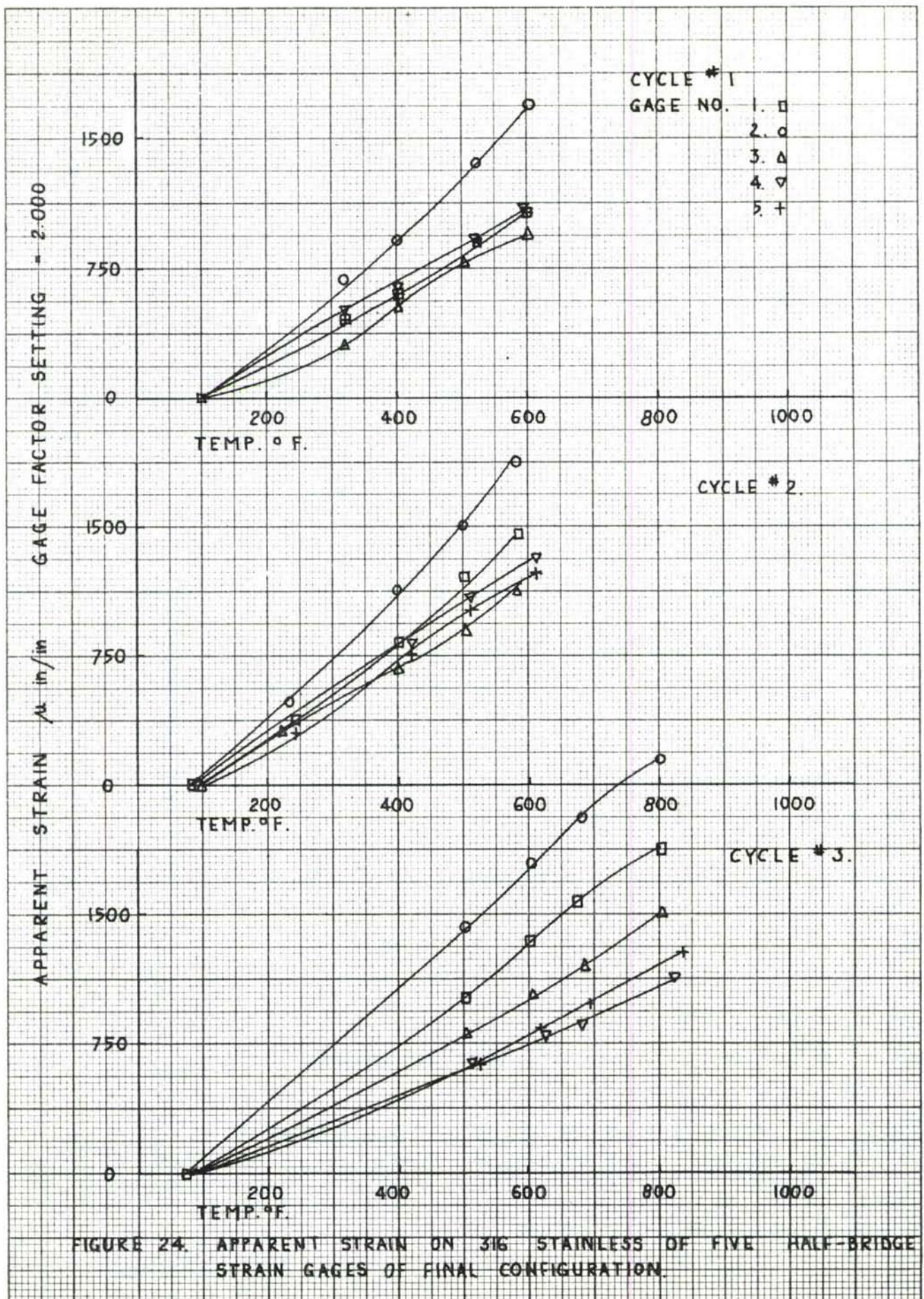
TABLE VII

PERFORMANCE OF FIVE HALF-BRIDGE STRAIN GAGES OF THE FINAL CONFIGURATION ON TYPE 316 STAINLESS STEEL TEST SPECIMENS.

Cycle	1	2	3	4	5
1B					
Max. Temp.	600	580	800	750	825
* Drift	-110	-16	+259	+24	+190
**Temp.Coeff.	2.14	2.88	2.55	2.34	2.25
2B					
Max. Temp.	600	580	800	750	825
* Drift	-173	-36	+ 6	+20	-63
**Temp.Coeff.	4.46	5.08	4.36	4.25	4.07
3B					
Max. Temp.	600	580	800	750	825
* Drift	-107	+72	+399	+34	+439
** Temp.Coeff.	1.92	2.11	2.07	2.01	1.84
4B					
Max. Temp.	600	600	830	780	950
* Drift	-125	-121	-230	-73	-147
** Temp.Coeff.	2.12	2.57	1.48	1.27	1.21
5B					
Max. Temp.	600	600	830	780	850
* Drift	-180	+ 7	-49	-69	+ 9
** Temp.Coeff.	2.08	2.35	1.62	1.57	1.56

* Measured at T maximum over a 2 hour period, - total drift in two hours, micro inches per inch.

** From room temperature to T maximum, micro inches per inch per degree F.



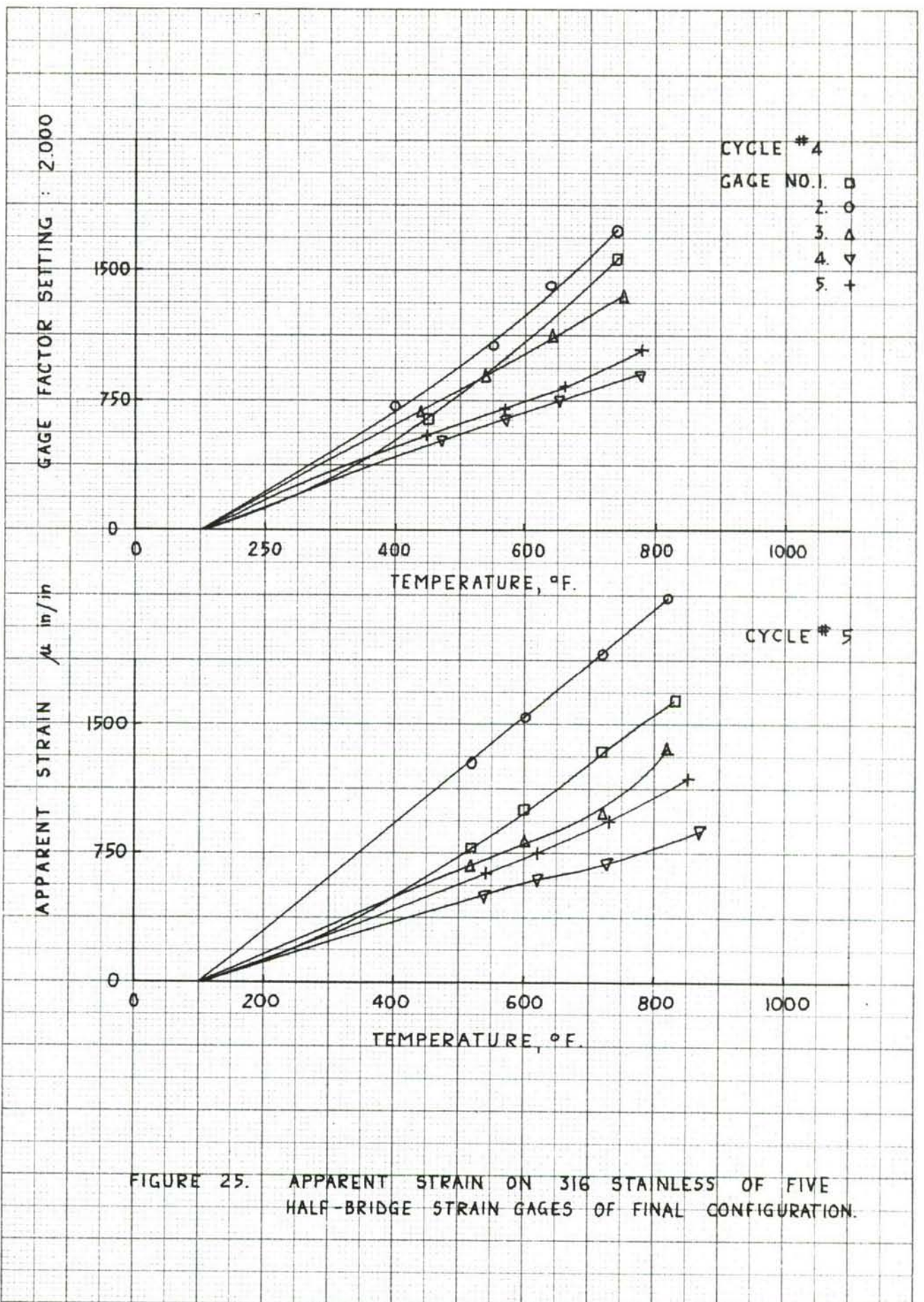


FIGURE 25. APPARENT STRAIN ON 316 STAINLESS OF FIVE HALF-BRIDGE STRAIN GAGES OF FINAL CONFIGURATION.

The binder used in the assembly of the standard configuration Half-Bridge strain gage is Allen PBX ceramic cement. The effects of a change in the binder was investigated by manufacturing gages from various other cements which are described in section VIII. The only gages that could be tested were made with Astroceram A and Quigley 1925. The performance of identical gages made with PBX, Astroceram A, and Quigley 1925 is shown in Figures 26, 27 and 28 respectively. All the gages were attached to Inconel specimens with the same cement which was used as the binder. The data were recorded on the heating part of the cycle and were read from a different Baldwin Type N Strain Indicator than the prior data. The bridge voltage of this indicator was 0.9. As can be seen from the curves drawn, the performance of Astroceram and Quigley 1925 as a binder for the Half-Bridge strain gage is not as good as that of PBX ceramic cement.

An effort was made to improve the zero shift of a Half-Bridge on the first cycle by heat treating the wire from which the gage is made. The apparent strain of a gage made from Nichrome wire that had been heat treated at 1200° F for one hour is shown in Figure 29. This gage was made in the standard configuration and attached with PBX cement.

For the sake of comparison, the apparent strain of two standard Nichrome Half-Bridge strain gages made from the same wire without heat treatment and bonded to identical specimens is shown in Figures 30 and 31. The apparent strain curves for these two gages are very close and very low. These gages also show excellent cycle-to-cycle repeatability after the first cycle.

The drift rate of the standard gages was measured at various temperatures in a series of tests using an X-Y Plotter and 2.5 volts across the bridge. The apparent strain from room temperature to 1100° F of one of the gages on Inconel is shown in Figure 32 and the drift rate for various temperatures and heating cycles is given in Table VIII. The maximum observed drift rate was 10.8 micro inches per inch per minute at 1000° F and occurred the first time the gage was heated to this temperature. This low drift rate, combined with the almost flat apparent strain, would make it feasible to conduct static strain measurements at temperatures as high as 1100° F.

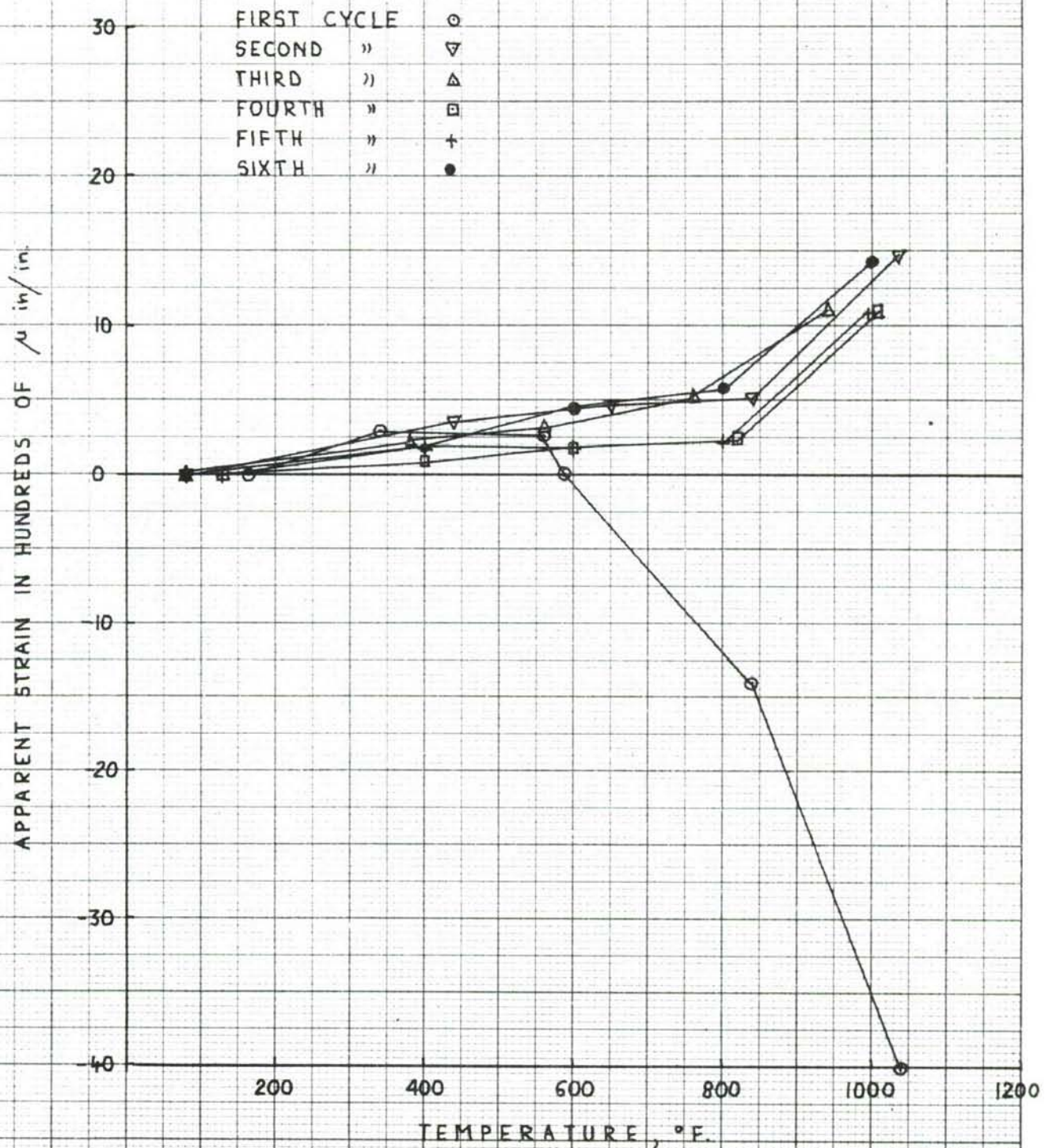


FIGURE 26. APPARENT STRAIN ON INCONEL OF APBX HALF-BRIDGE STRAIN GAGE OF FINAL CONFIGURATION

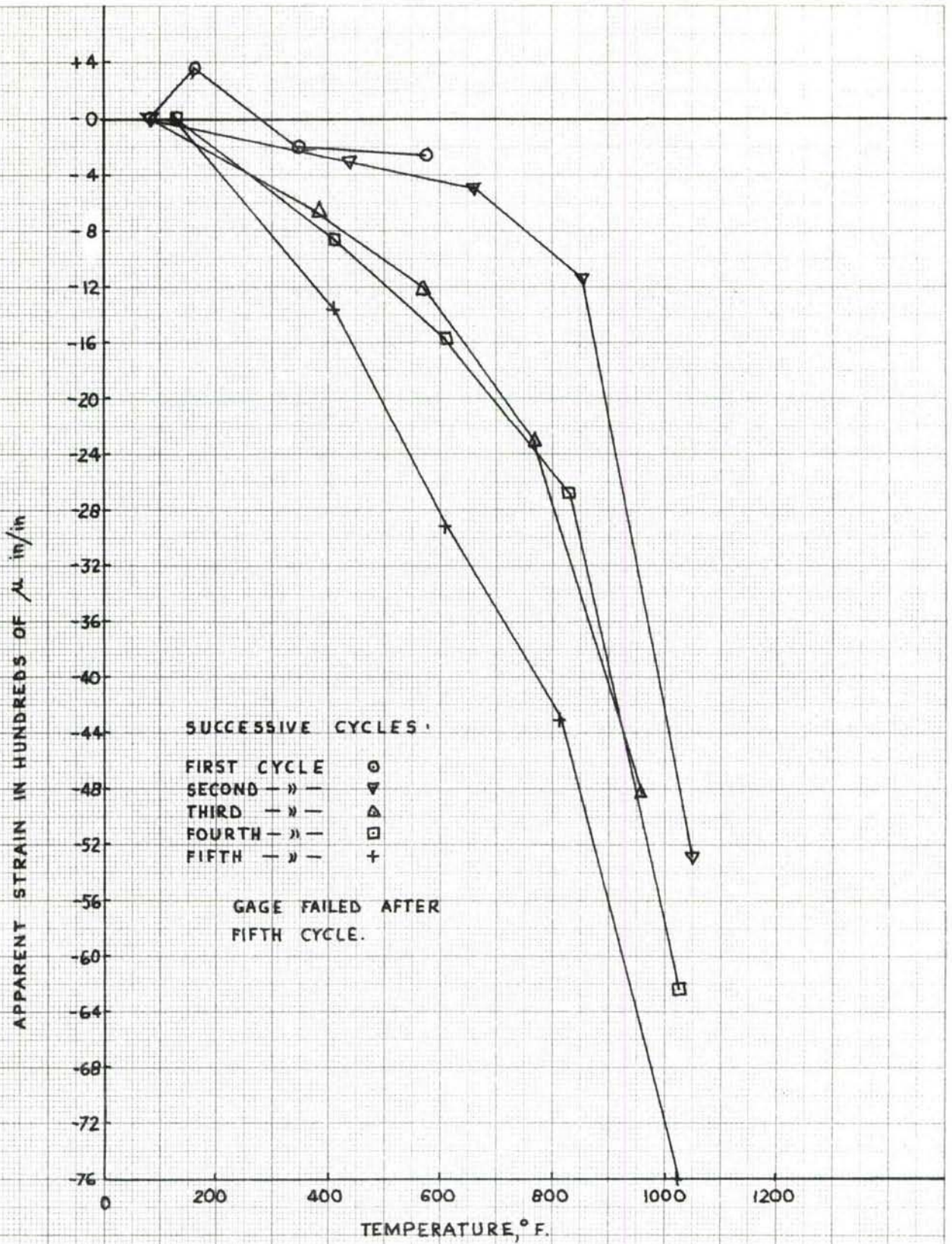


FIGURE 27. APPARENT STRAIN ON INCONEL OF AN ASTROCERAM HALF-BRIDGE STRAIN GAGE OF FINAL CONFIGURATION.

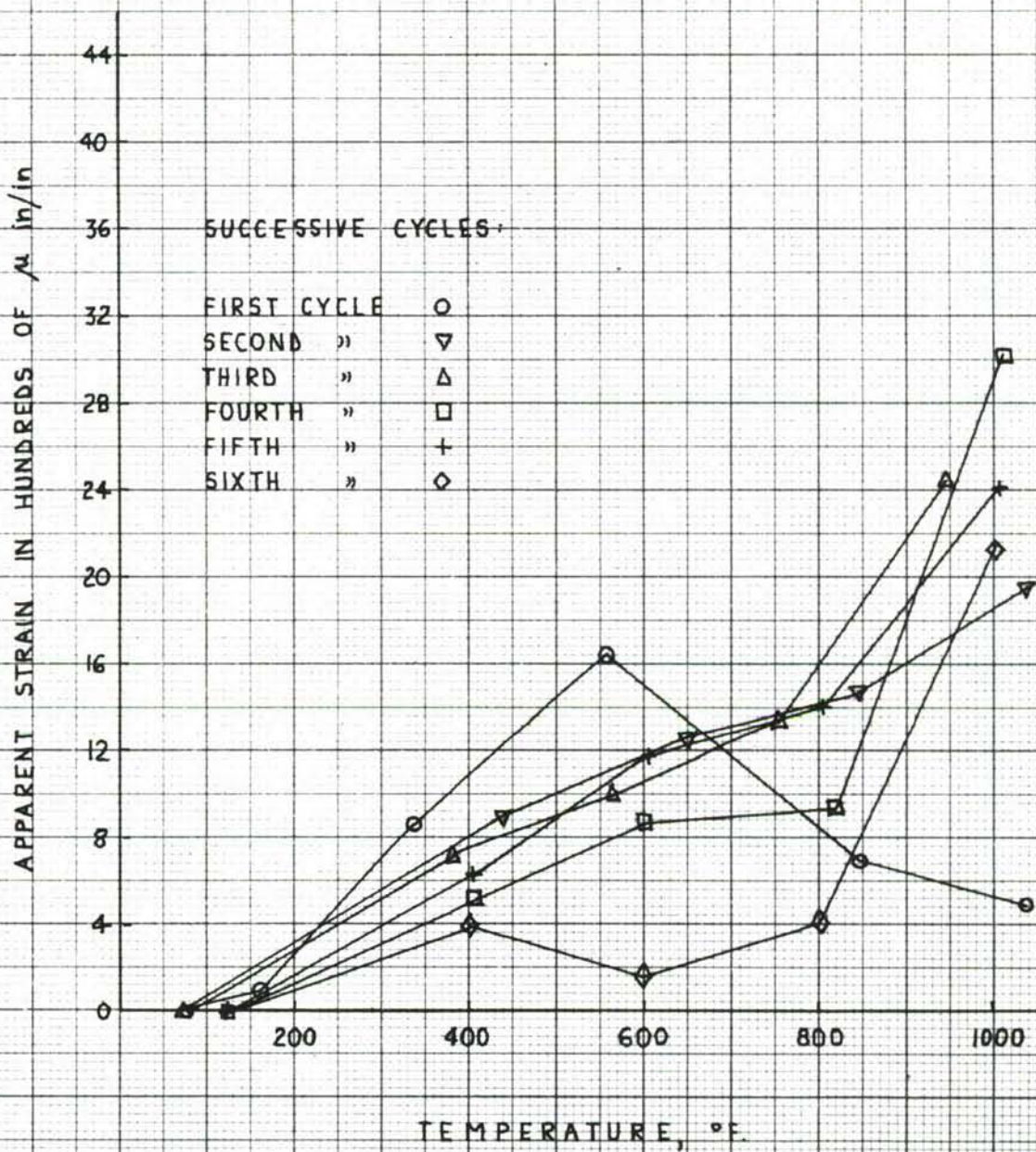


FIGURE 28. APPARENT STRAIN ON INCONEL OF A GUIGLEY 1925 HALF-BRIDGE STRAIN GAGE OF FINAL CONFIGURATION.

APPARENT STRAIN IN HUNDREDS OF μ in/in GAGE FACTOR SETTING : 2.00

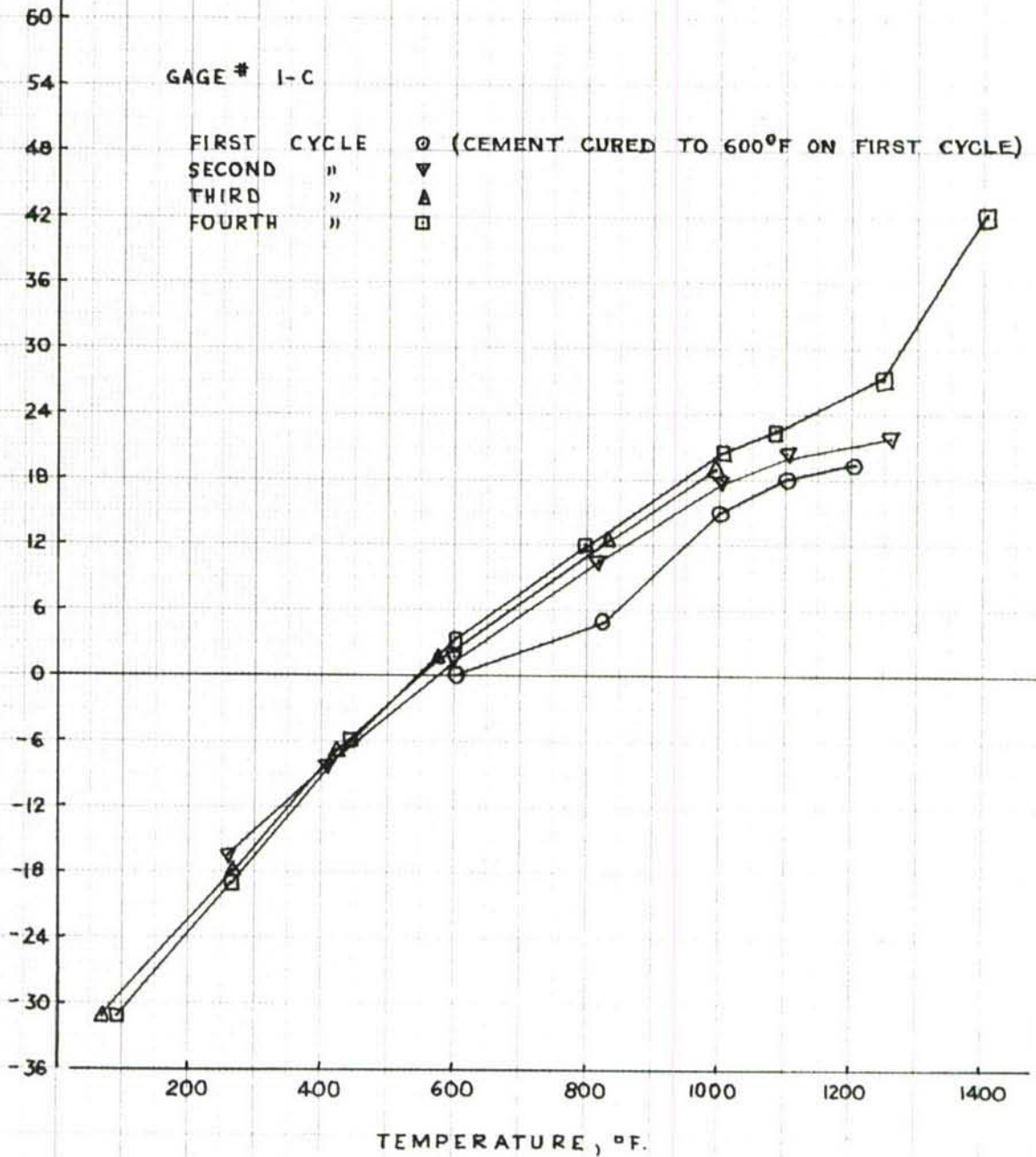


FIGURE 29. APPARENT STRAIN ON INCONEL OF A HALF-BRIDGE STRAIN GAGE MADE OF HEAT TREATED NICHROME.

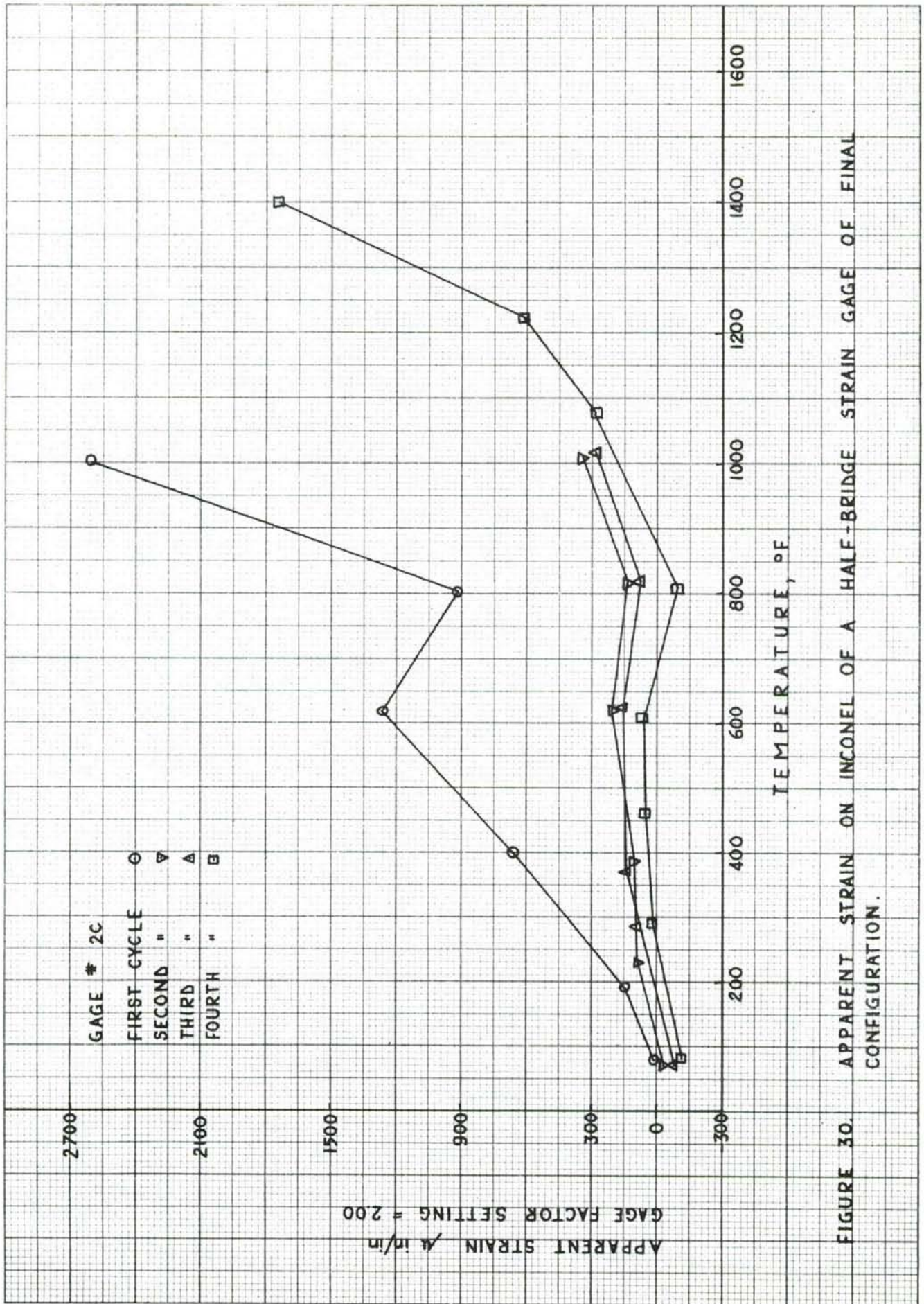


FIGURE 30. APPARENT STRAIN ON INCONEL OF A HALF-BRIDGE STRAIN GAGE OF FINAL CONFIGURATION.

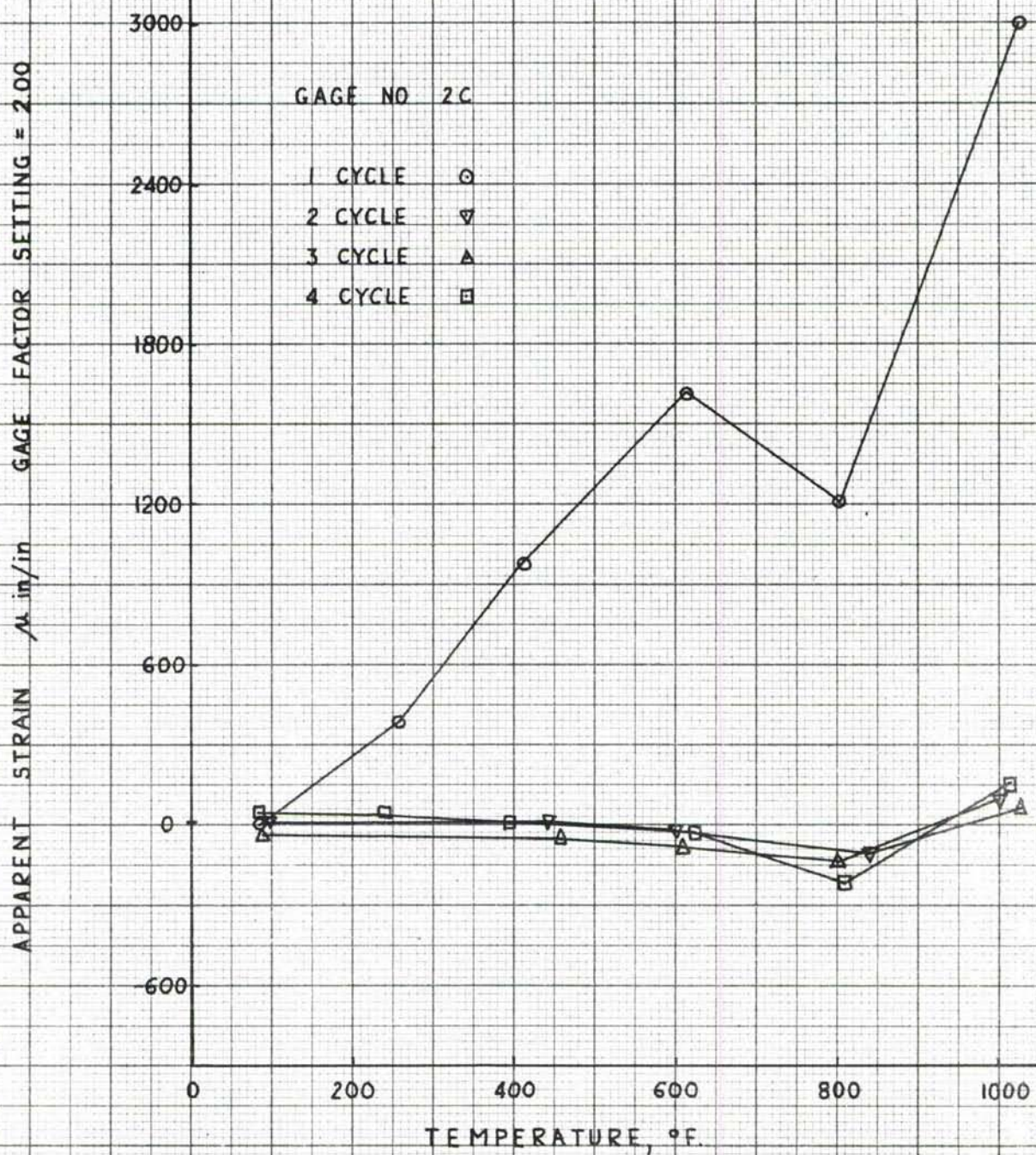


FIGURE 31. APPARENT STRAIN ON INCONEL OF A HALF-BRIDGE STRAIN GAGE OF FINAL CONFIGURATION.

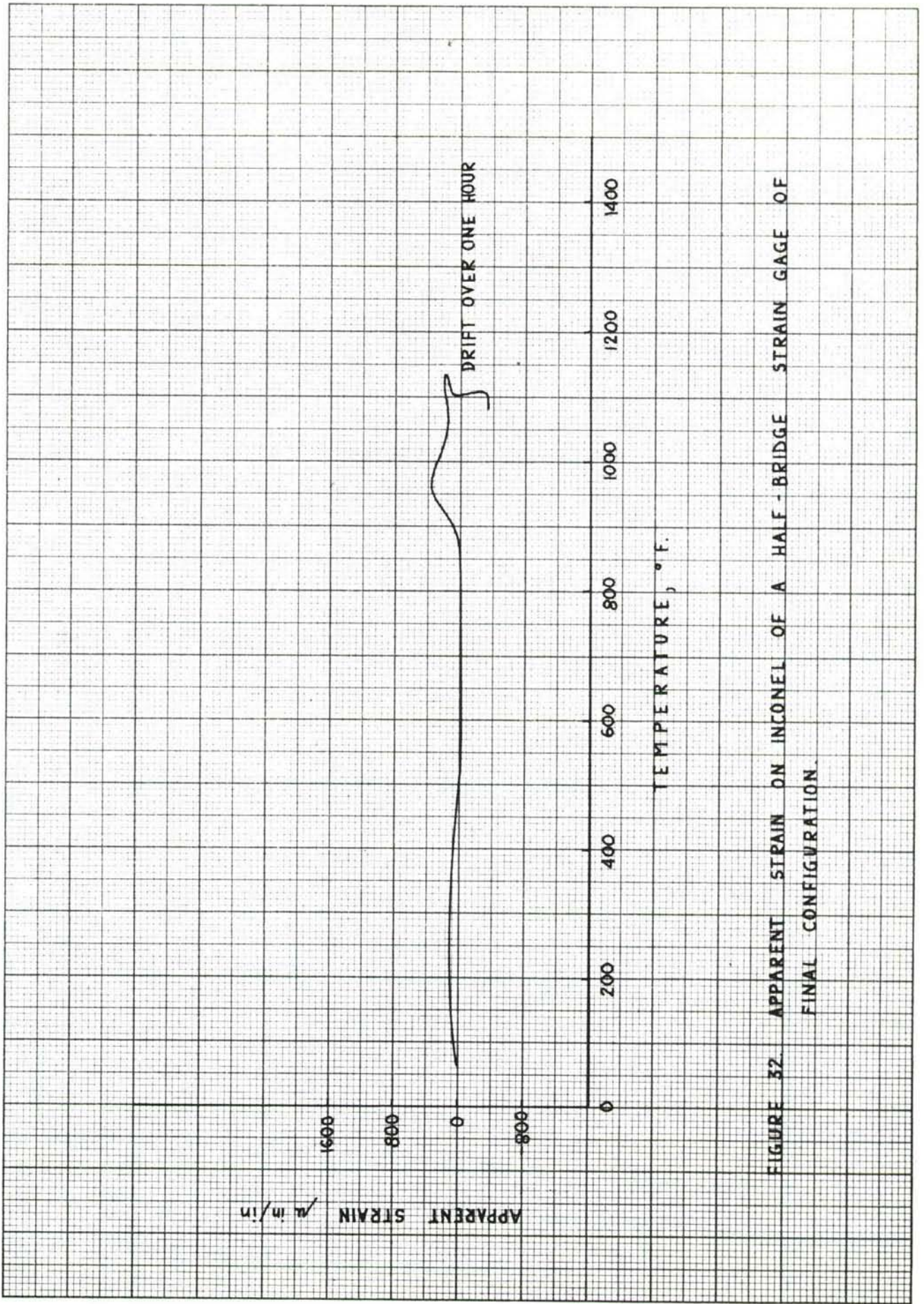


FIGURE 52 APPARENT STRAIN ON INCONEL OF A HALF-BRIDGE STRAIN GAGE OF FINAL CONFIGURATION.

TABLE VIII

DRIFT RATE AT VARIOUS TEMPERATURES FOR A NICHROME HALF-BRIDGE STRAIN GAGE

<u>Heat Cycle</u>	<u>Temperature</u>	<u>Average Drift Rate at Temperature, micro-inches per inch per minute</u>
1	600	Not measurable
2	700	3.2
3	700	Not measurable
4	800	7.5
5	800	7.2
6	800	3.3
	760	Not measurable
	650	" "
7	900	9.4
	800	Not measurable
8	900	2.0
	684	Not measurable
	600	" "
9	1000	10.8
10	600	Not measurable
	700	" "
	800	" "
	900	8
11	1100	-8.9
	880	2.5
	700	Not measurable

Gage factor measurements were also made of the standard configuration Half-Bridge strain gage. Absolute measurements were made of the gage factor at room temperature and relative change measurements made at 600, 800, and 1000° F. These measurements were made at the Baldwin-Lima-Hamilton Corporation and were obtained by means of their standard procedures and equipment. The gage factors of four Half-Bridge strain gages at room temperature were:

Gage 1d - 2.08
 2d - 2.12
 3d - 2.25
 4d - 1.97

which gives an average of 2.10 and a standard deviation of 0.11 or 5.3%.

To obtain the gage factor at elevated temperatures, the response of the installation to a given load was measured at room temperature. The installation was then heated up to the test temperature and the response to the same load was measured. Because the modulus of elasticity of the specimen decreases with increasing temperature, the specimen should elongate more for the same load at elevated temperatures. The strain gage should indicate an increase in strain which is equivalent to the increase in elongation. Any other change in gage output indicates a change in the gage factor of the gage. In Figure 33 the percentage change in the gage output of the four gages mentioned above is given as a function of temperature. Except for the change in gage 3d at 1000° F there is very good repeatability from gage to gage. In terms of actual gage factor, the repeatability is about as good as at room temperature. This is shown in Table IX.

TABLE IX

GAGE FACTOR AT VARIOUS TEMPERATURES FOR
 FOUR NICHROME HALF-BRIDGE STRAIN GAGES

<u>Temperature</u>	<u>1d</u>	<u>2d</u>	<u>3d</u>	<u>4d</u>	<u>Average</u>	<u>Standard Deviation</u>
Room temp.	2.08	2.12	2.25	1.97	2.10	5.3%
600° F.	2.04	2.04	2.17	1.87	2.03	6.0%
800° F.	1.94	2.00	2.11	1.85	1.97	5.9%
1000° F.	1.88	1.91	1.87	1.82	1.87	1.9%

GAGE MATERIAL : NICHROME
 GAGE CONFIGURATION : FINAL
 SPECIMEN MAT'L. : INCONEL X
 BONDING AGENT : ALLEN PBX
 CURE : 1 HOUR IN 600°F.
 APPROX. R.T. STRAIN LEVEL :
 1000 μ in/in

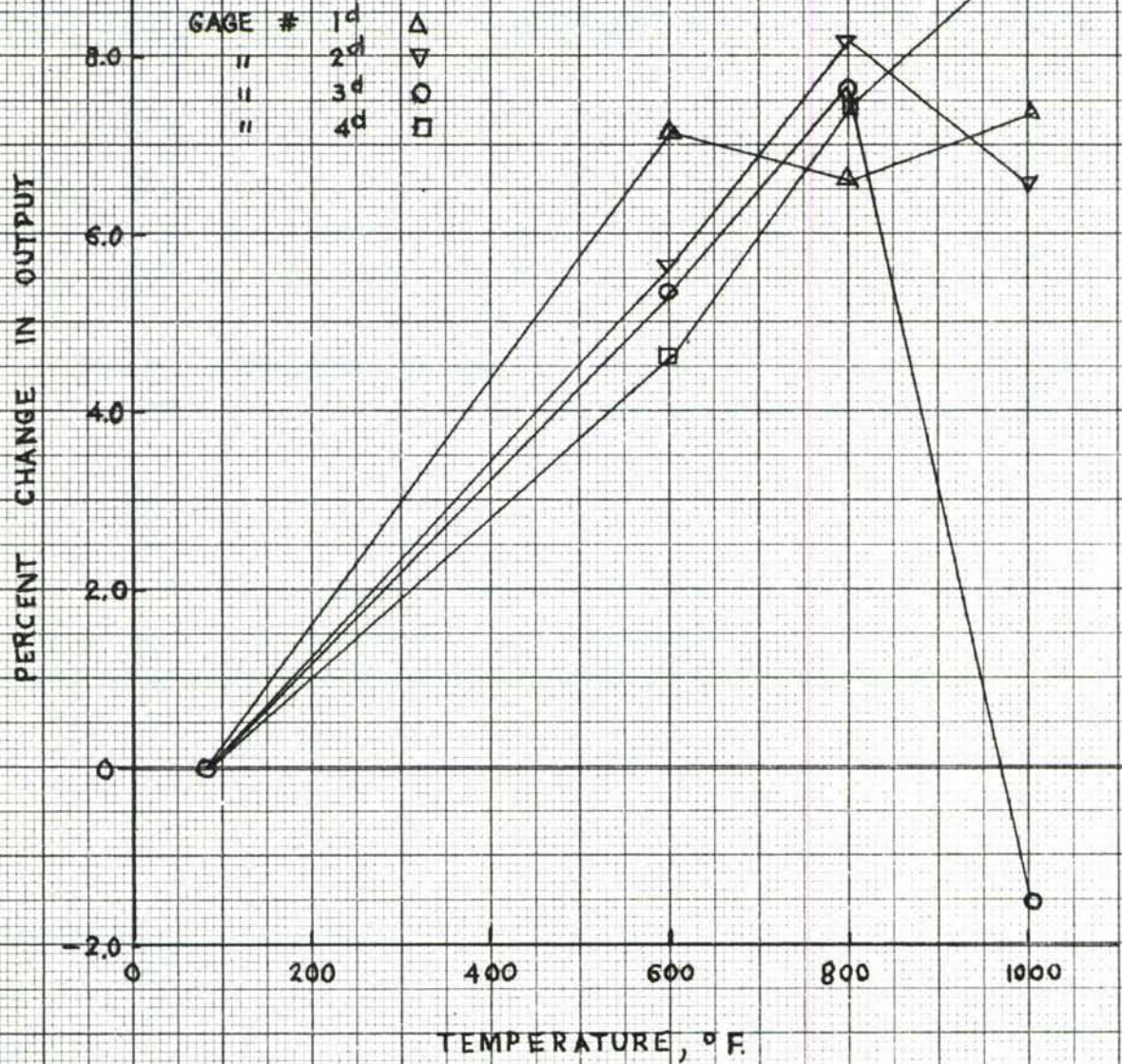


FIGURE 33. PERCENT CHANGE IN OUTPUT VS. TEMPERATURE OF FOUR HALF-BRIDGE STRAIN GAGES OF FINAL CONFIGURATION

VII. GAGE PERFORMANCE UNDER TRANSIENT HEATING CONDITIONS.

The results of the previous program indicated that the most promising material for gage manufacture was Nichrome; consequently, although many gages made from other materials were tested, Nichrome was the material primarily used. For the reasons stated in section VI, data presented here is for five representative Nichrome Half-Bridge strain gages, of final configuration, tested under transient heating conditions. These five gages were tested at different bridge voltages and to successively higher temperatures until failures occurred. In only one instance did the gage itself fail. In all other cases, the bond between gage and metal failed.

Transient Temperature Test Facility

The transient temperature test facility used at the beginning of the program was the same as that described in Reference 1. In mid-May, 1961, additional facilities were received on loan from the United States Air Force. A special area was prepared for this equipment and it was put into operation early in June 1961. The present facility consists of the following equipment:

	<u>Manufacturer</u>	<u>Model No.</u>
Recorder-Controller	Research, Inc.	4080
Power Regulator	" "	4079
Thermocouple Reference Junction	Thermo-Electric, Inc.	150°F Auto Ref.'
Bridge Balance Unit	Century Electronics & Instruments Corp.	1809
Oscillograph	" " " "	408
Radiant Oven	High Temperature Instru- ment Corp.	--
X-Y Plotter	Electronic Associates, Inc.	1100E
D. C. Power Supply	Harrison Labs., Inc.	855A
D. C. Amplifier	Kay Lab.	111

A schematic diagram of the apparatus is shown in Figure 34. A description of each item follows:

A. Radiant Oven. The radiant oven heat source consists of ten General Electric 500 T3 quartz infrared lamps. The oven walls are constructed of sheet transite. The oven ends, which also serve as lamp supports, are also of transite. The ten lamps are held in front

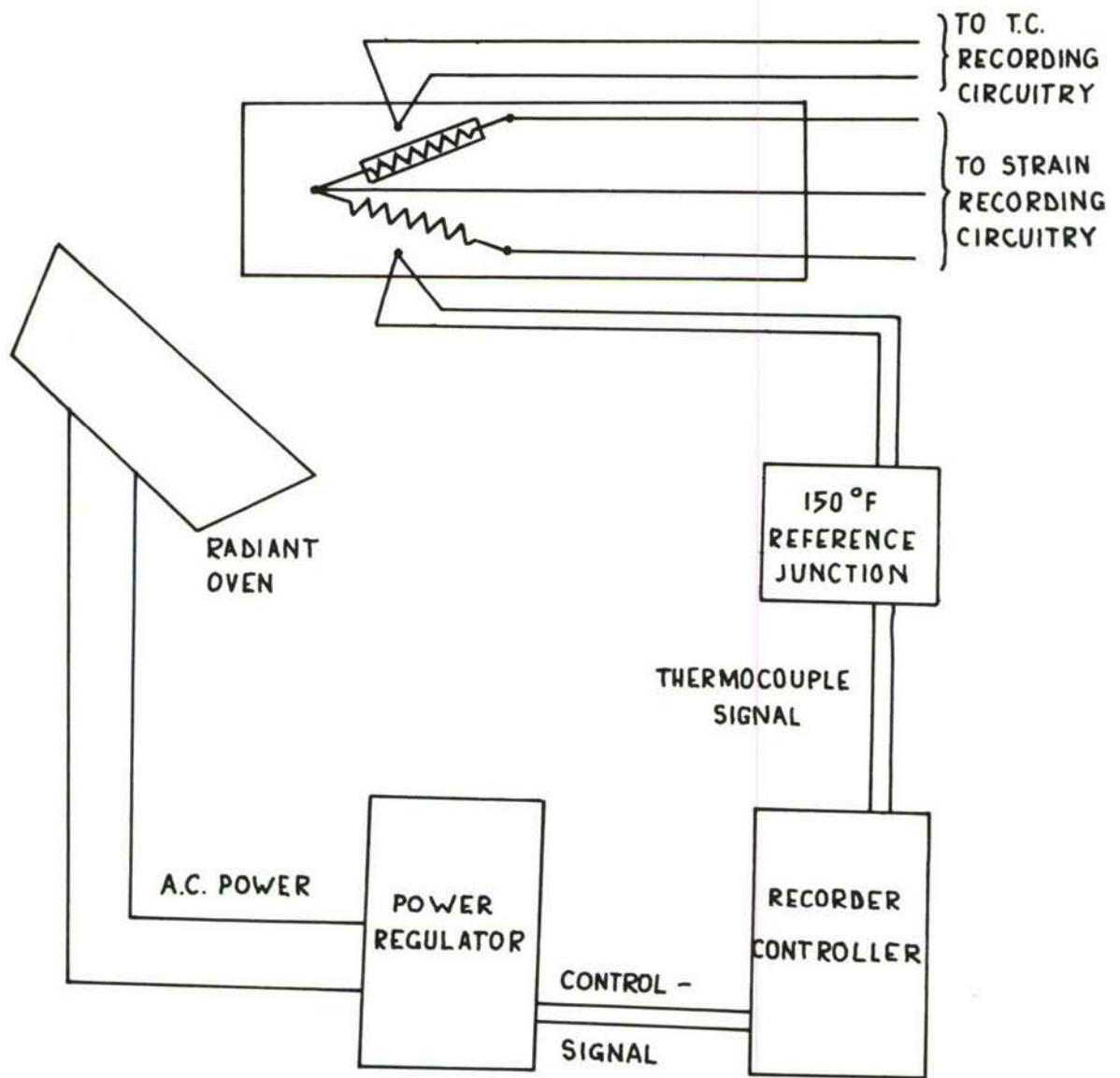


FIG. 34. TRANSIENT TEMPERATURE APPARATUS . DIAGRAM.

of two polished nickel reflectors. These ten lamps are connected in parallel to one module of the thyatron power regulator. At the full line voltage - 220 volts, the lamps draw a total 4C amperes of current.

The oven ends are slotted so that a test specimen may be placed inside. The specimen is supported outside the oven by a clamp so arranged in height that the specimen is held in the center of the oven. The standard specimen size is 6" x 1" x .050".

Before it is placed in the oven, two chromel-alumel thermocouples are welded to the specimen, adjacent to the installed gage. One of these thermocouples is connected to the galvanometer, the other to the thermocouple reference junction.

B. Reference Junction. The Thermo-Electric Auto Ref. Reference Junction is designed to maintain a constant 150° F temperature. Up to 24 chromel-alumel thermocouples can be connected. Measurement indicated that the junction was operating at 149° F. The 150° F reference junction is used instead of an ice bath because the Recorder-Controller has been designed to operate with this reference temperature.

From the reference junction, the low level thermocouple temperature signal is carried by shielded cable to the Recorder-Controller.

C. Recorder-Controller. The Research, Inc., Model 4080 Recorder-Controller is contained in a caster mounted rack. The rack accommodates five modules containing two controllers each. Only one such module was supplied. The module is completely self-contained and operates from a 115 volt a.c. power source.

The main function of the recorder-controller channel is to electrically sum the output of the specimen mounted thermocouple with a reference emf proportional to a desired temperature and amplify any difference emf (error voltage) to a magnitude sufficient to control the output of the associated A-C power regulator. The associated power regulator controls the radiant energy of quartz lamp heaters by proportioning the A-C line power in response to this error signal. The specimen and thermocouple, heated by this radiant energy, will increase in temperature to reduce any system error to within the proportional band of control.

A control mode selector switch is included in each channel to allow selection between temperature control from a set point dial and programmed temperature control from an external digital function generator. The latter mode of operation is referred to as the computer mode. A third mode of control provides for the manual adjustment of A-C power to the heaters with no temperature feedback. A temperature range switch associated with both the recorder and controller circuitry selects between four different thermocouple types and temperature ranges. The temperature band for proportional A-C power control is adjustable from a front panel gain control. A limiter control can be used to limit the load voltage to any given percentage of the line voltage.

Certain controls are shared between the two channels in a module. A common null indicator meter can be selected to read the magnitude of the error signal by depressing a button associated with the channel. A run mode selector simultaneously switches the two associated power regulator channels into a run condition. A common chart switch energizes the two motors in the module. The run mode and the chart switches allow selection between local, off and remote operation.

The chart is part of a Bristol Model RE-1P00663-21 self-balancing potentiometer recorder, constructed as an integral part of each channel. The recorder records the temperature as measured by the thermocouple.

D. Thyatron Power Regulator. The Research, Inc., Model 4079 Thyatron Power Regulator regulates the power delivered to the radiant oven. Two regulator modules were received, mounted in a caster-mounted rack designed to hold ten such modules.

The thyatron power regulator module consists of two gas thyratrons in an inverse parallel connection wired in series with a radiant heating load. Smooth power control is achieved by synchronous switching of the thyatron within the cycle of A-C power and in response to a D-C control signal. The individual modules also contain a current transformer and meter for the measurement of A-C load current, a voltmeter to indicate the load voltage, and a magnetic firing circuit. The magnetic firing circuit converts a D-C control signal of 0 to 1.7 milliamperes to a sharp rising pulse which will fire the thyatron at a point within the cycle of line frequency corresponding to the magnitude of this control current.

Each module will control 40 amperes of current at the 220 volt line voltage. The above units constitute the items necessary for controlling the power supplied to the radiant oven. The following items are used in obtaining and recording the strain and temperature information.

E. Bridge Balance Unit. The Century Model 1809 Bridge Control unit provides facilities for: individually powering up to 12 two-arm strain gage channels; compensating for their initial unbalance; calibrating, manually or automatically, the magnitude of input voltage level by reference to separate, or a common, calibration resistor(s); and matching and distributing the outputs from these gages to recording or indicating galvanometers.

The automatic functions of the bridge control unit were not employed since the automatic features require 22-28 volts D-C at 100 m.a. for their operation. This voltage is not available at the High Temperature Instruments Corp. facility.

F. Oscillograph. The Century Model 408 Oscillograph was equipped to record 18 channels of information on paper 8 inches wide. Variable paper speeds may be selected, but throughout this investigation a speed of 0.5 inches per second was used. Full width timing lines are photographed on the recording paper at 10 millisecond intervals.

The Model 408 was equipped with Century Galvanometers Model 210 C 50-1, which have a natural frequency of 100 cps., a coil resistance of 60 ohms and a D-C deflection sensitivity of 23 micro-amperes per inch (at 12 inch writing distance.)

G. X-Y Plotter. The Electronic Associates Model 1100-E Vari-plotter is a self-balancing, potentiometer type of recorder that plots one variable D-C voltage as a function of a second D-C voltage. The thermocouple signal is applied to the servo amplifier that controls the position of the arm on the abscissa axis. Output of the strain gage bridge is applied to the servo amplifier that controls the position of the motor driven pen along the ordinate.

H. Power Supply. The Harrison Laboratories Model 855A is a regulated power supply supplying 0-15 volts D-C.

I. D-C Amplifier. The Kay Lab Model III D-C Decade Amplifier is a high gain, wide band, D-C amplifier specifically designed to accept a small D-C voltage from a strain gage or other electro-mechanical device and amplify this signal, providing a voltage output which can be used to drive conventional recording potentiometers or voltmeters. A large amount of feedback provides a very precise and stable gain.

The equipment immediately above comprises the recording portion of the transient temperature test facility. The operation of the recording section will be described under "Test Procedure" below.

Test Procedure.

A gage undergoing test is cemented in the center of a test specimen, one-half inch from the end. The standard test specimen size is 6" x 1" x .050". Gages reported on herein were mounted on Inconel, but 304 Stainless Steel, Titanium, and Aluminum have been used. Inconel was normally used for the specimens because of its ability to withstand repeated exposure to higher temperatures without degradation. Electrical connection to the gage is made by swaging gage leads into 30 mil nickel tubes. The nickel tubes are inserted into a section of a 4-hole Alumina ceramic tube for electrical insulation.

Outside the oven, the nickel leads are connected to a shielded 3-conductor cable, which is connected to the other half of the Wheatstone bridge in the bridge balance unit. The power supply is connected to the bridge balance unit. The output of the Wheatstone bridge is connected by shielded cable to the Oscillograph or the X-Y Plotter.

Two 36 ga. Chromel-Alumel thermocouples are welded to the specimen, one on either side of the gage and at the center of its long dimension. One of these thermocouples is connected to the Auto Ref Reference Junction for control, as described above. The other thermocouple is connected to copper leads in an ice bath reference junction, thence to the Oscillograph through a 350 ohm resistor or directly to the X-Y Plotter. The function of the resistor is to attenuate the thermocouple signal for suitable galvanometer deflection.

Oscillograph Calibration.

The thermocouple channels were calibrated by using a known potential from a Leeds & Northrup D. C. Potentiometer as a calibrating voltage. However, the coil resistance of the galvanometer is so low that the potentiometer output gave erroneous calibrations. Also, the fine wire thermocouples used for temperature measurement were so fine that the resistance is significant compared with the galvanometer coil resistance; consequently temperature calibrations were determined as follows:

The Bristol recorder readings on the recorder-controller module were compared with the output of the recording thermocouple, as read by a balanced potentiometer, at several temperatures. Agreement was found within 2% of reading. Comparison between the Bristol recordings and the Oscillographic data established a calibration curve for the temperature trace.

Calibration of the strain trace was accomplished by connecting a Baldwin-Lima-Hamilton SR-4 Strain Calibration Unit into the circuit in place of the Half-Bridge strain gage. This 120 ohm unit simulates precise strain outputs (assuming a gage factor of 2.0) in steps of 2000 microinches per inch per step. Since the galvanometer resistance is finite, a correction factor was calculated to adjust the calibration for a 60 ohm gage.

Strain Sensitivity.

After the test gage is mounted on the specimen, and before the specimen is mounted in the oven, the gage is tested for strain sensitivity in the compensating arm. The specimen is mounted in a stand with the gage and clamped. Loads of 100 gm., 200 gm., 300 gm., and 500 gm., are progressively suspended from the other end. The resistance changes of the sensitive arm and the compensating arm are separately measured, using a Baldwin Type N Strain Indicator. The gage is rejected if the compensating arm exhibits strain sensitivity greater than ten percent that of the sensitive arm.

Test Results.

The transient heating tests measured apparent strain seen by the gage as a function of temperature for three different bridge voltages—1 v., 2 v., and 3 v., and for different peak temperatures. The heating rate for all tests was constant at approximately 47° F per second. The gage was held only momentarily at peak temperature. Gages were cooled

along the "slow" curve as shown in Figure 35. Data was not taken on the cooling portion of the cycle in order to conserve oscillograph paper. After the specimen cooled to room temperature, a short exposure was made to determine the zero shift.

To test the effect of thermally generated emf's, gage 61-5 was run twice to 1400° F with zero bridge voltage. No emfs measurable with the equipment in use were generated.

Original data is shown in Tables X to XIV. The tables show maximum temperature, apparent strain at maximum temperature, and zero shift at the end of the run. All figures shown are in units of microinches per inch, assuming a gage factor of 2.0, an approximation correct to $\pm 5\%$ at room temperature. Curves of apparent strain versus temperature are shown for three voltages in Figures 36 to 40.

Several effects were apparent:

(1) Below 1000° F, the output of the gage under no load conditions is linear with temperature, and in the worst case is less than 3 microohms/ohm per degree F.

(2) Between the temperatures 1000° F to 1300° F, a "hump" occurs in the curve due to a metallurgical transition at these temperatures.

(3) Gage temperature coefficient and "hump" height increase with continued temperature cycling especially to progressively higher temperatures.

(4) Apparent strain is directly related to bridge voltage.

(5) Zero shift upon return to room temperature is most severe the first time the gage experiences a higher temperature, becoming progressively smaller thereafter.

(6) Apparent strain beyond 1600° F becomes progressively smaller with temperature as cement conductivity increases.

(7) Gage installation failure occurs quickly beyond 1600° F.

After observation of these test results, a need for re-orientation of Half-Bridge strain gage philosophy became apparent. The

objective to this time had been to obtain a gage perfectly temperature compensated to 2000° F. It has been shown both theoretically and experimentally that such compensation is unobtainable for bridge voltages higher than 3 volts. Most recent results show lack of perfect compensation for bridge voltages lower than 3 volts even though utilizing the latest manufacturing process, and even though gage construction was of Nichrome, a material with a low temperature coefficient of resistance at the outset. Especially disconcerting is the "hump" that occurs at elevated temperatures due to metallurgical changes.

Consequently, it is now felt that the Half-Bridge strain gage should be manufactured of noble metals or their alloys. Such alloys generally exhibit low drift and negligible zero shift upon heating to elevated temperature. The resistance versus temperature curves are very nearly linear. However, the temperature coefficients of resistance are high (4000 ppm./° C for Platinum, 600 ppm./° C for Platinum-30% Iridium.) It is felt that the Half-Bridge strain gage will be most successful if it can be built to have a linear, reproducible, drift-free resistance versus temperature curve.

As a result of this thinking, just prior to the time of this report, several gages were manufactured using Platinum-30% Iridium as the strain sensitive alloy. These gages all failed immediately upon being subjected to radiant heating. Dissection of the gages showed this due to poor manufacturing techniques, as a result of inexperience with this material.

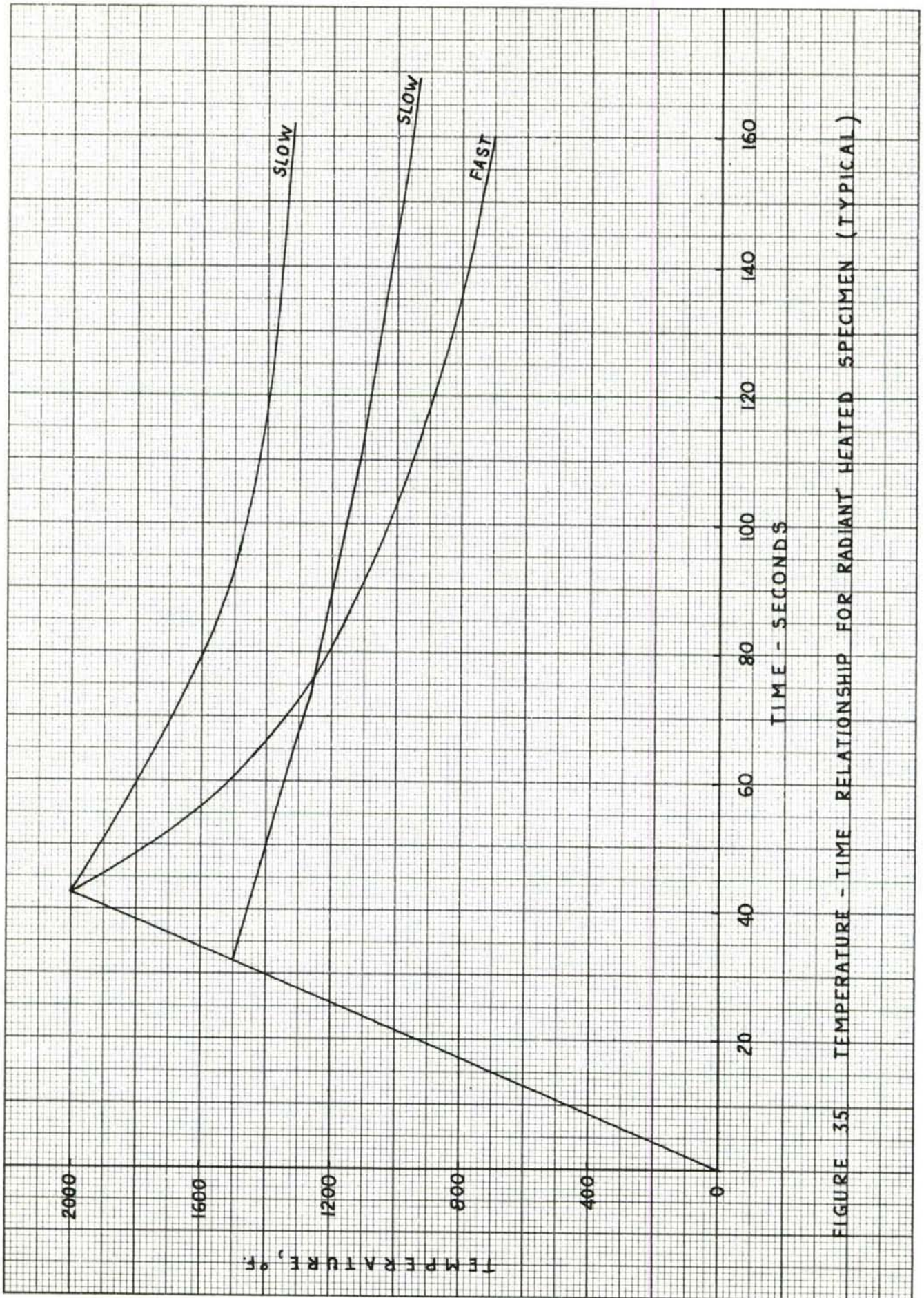


FIGURE 35 TEMPERATURE - TIME RELATIONSHIP FOR RADIANT HEATED SPECIMEN (TYPICAL)

TABLE X

HALF-BRIDGE STRAIN GAGE

DATA SHEET

Gage Number: 61-1
 Gage Wire: Nichrome Wire Size: Standard
 Lead Material: Nickel Cement: PBX
 Silicon Tubing Size: Standard Specimen Size: Standard
 Specimen Material: Inconel
 Gage Length: 1"
 Configuration: Standard
 Heat Treatment: None
 Cure: Standard
 Resistance: $R_a = 60.3$
 $R_c = 58.7$

LOAD CHECK

<u>Load</u>	<u>Arm 1</u>	<u>Δ 1</u>	<u>Arm 2</u>	<u>Δ 2</u>	<u>Total Gage</u>	<u>Δ t</u>
0 gms	15245 $\mu\%$		15270 $\mu\%$		10940 $\mu\%$	
100 "	15365	120	15273	3	11060	120
200 "	15490	125	15278	5	11180	120
300 "	15610	120	15280	2	11300	120
500 "	15850	240	15300	20	11520	220

Bridge rebalanced after each run.

<u>Cycle</u>	<u>Voltage</u>	<u>Max.Temp. Degrees F</u>	<u>Apparent Strain at Maximum Temp. Micro Inches per in.</u>	<u>Zero Shift Micro Inches per inch</u>
1	1	1000	0	-300
2	1	1000	+150	+200
3	1	1000	+100	+100
4	1	1000	+ 50	+200
5	2	1000	+400	+ 50
6	2	1000	+375	+ 50
7	2	1000	+350	+ 50
8	3	1000	+700	+130
9	3	1000	+480	0
10	3	1000	+610	60
11	3	1000	510	30
12	1	1200	200	1100
13	1	1200	150	450
14	1	1200	0	300
15	2	1200	800	

-- Gage noisy

TABLE XI

HALF-BRIDGE STRAIN GAGE

DATA SHEET

Gage Number: 61-2
 Gage Wire: Nichrome
 Lead Material: Nickel
 Gage Length: 1"
 Configuration: Standard
 Heat Treatment: None
 Resistance: $R_a = 58.6$
 $R_c = 58.3$

Cement: PBX
 Specimen Size: Standard

LOAD CHECK

<u>Load</u>	<u>Arm 1</u>	<u>$\Delta 1$</u>	<u>Arm 2</u>	<u>$\Delta 2$</u>	<u>Total Gage</u>	<u>Δt</u>
0 gms	10700 $\mu\%$		10510 $\mu\%$		12310 $\mu\%$	
100 "	10820	120	10520	10	12410	100
200 "	10935	115	10530	10	12500	90
300 "	11045	110	10532	2	12620	120
500 "	11280	245	10538	6	12850	230

Bridge rebalanced after each run.

<u>Cycle</u>	<u>Voltage</u>	<u>Max. Temp. Degrees F</u>	<u>Apparent Strain at Maximum Temperature Micro inches per in.</u>	<u>Zero Shift Micro Inches per inch</u>
1	1	1000	+ 200	-400
2	2	1000	+ 550	-200
3	3	1000	+1150	- 90
4	1	1200	+1600	+2300
5	2	1200	+1000	+ 100
6	3	1200	+1890	No record
7	1.5	1400	+ 700	+ 700
8	2	1400	+ 750	- 50
9	3	1400	+1600	0
10	1	1600	+ 400	Gage installa- tion failed.

TABLE XII

HALF-BRIDGE STRAIN GAGE

DATA SHEET

Gage Number: 61-3
Gage Wire: Nichrome
Lead Material: Nickel
Specimen Material: Inconel
Gage Length: 1"
Configuration: Standard
Heat Treatment: None
Resistance: $R_a = 61.5$
 $R_c = 58.7$
Cement: PBX
Specimen Size: Standard

LOAD CHECK

<u>Load</u>	<u>Arm 1</u>	<u>Δ 1</u>	<u>Arm 2</u>	<u>Δ 2</u>	<u>Total Gage</u>	<u>Δ t</u>
0 gms	15360 μ %"		15140 μ %"		11210 μ %"	
100 "	15480	120	15145	5	11335	125
200 "	15615	135	15155	10	11460	125
300 "	15750	135	15160	5	11580	120
500 "	16020	270	15170	10	11835	255

Bridge rebalanced after each run.

<u>Cycle</u>	<u>Voltage</u>	<u>Max. Temp. Degrees F</u>	<u>Apparent Strain at Maximum Temperature Micro Inches per in.</u>	<u>Zero Shift Micro Inches per in.</u>
1	1	1200	- 700	- 700
2	2	1200	+ 650	+ 200
3	3	1300	+1050	+ 60
4	1	1300	+ 300	+ 200
5	2	1300	+ 200	+ 50
6	3	1300	+1056	+ 30
7	1	1400	- 500	- 100
8	2	1400	+ 100	- 150
9	3	1400	+ 850	+ 60
10	1	1500	- 200	- 100
11	2	1500	+ 550	- 250
12	3	1500	+1375	- 130
13	1	1500	--Gage installation failed on heating portion.	

TABLE XIII

HALF-BRIDGE STRAIN GAGE

DATA SHEET

Gage Number: 61-4	Resistance: $R_a = 58.8$
Gage Wire: Nichrome	$R_c = 58.6$
Lead Material: Nickel	Wire Size: Standard
Gage Length: 1"	Cement: PBX
Heat Treatment: None	Specimen Size: Standard

LOAD CHECK

<u>Load</u>	<u>Arm 1</u>	<u>$\Delta 1$</u>	<u>Arm 2</u>	<u>$\Delta 2$</u>	<u>Total Gage</u>	<u>Δt</u>
0 gms	16010 $\mu\%$		14865 $\mu\%$		12140 $\mu\%$	
100 "	16120	110	14875	10	12245	105
200 "	16240	120	14890	15	12355	110
300 "	16340	100	14891	1	12460	115
500 "	16545	205	14905	14	12655	195

Bridge rebalanced after each run.

<u>Cycle</u>	<u>Voltage</u>	<u>Max. Temp. Degrees F</u>	<u>Apparent Strain at Maximum Temperature Micro Inches per in.</u>	<u>Zero Shift Micro Inches per inch</u>
1	3	1200	+1980	+1600
2	2	1200	+ 600	No record
3	1	1200	+ 900	+ 400
4	3	1300	+2050	+ 440
5	2	1300	+1400	+ 200
6	1	1300	+ 900	+ 150
7	3	1400	+1440	+2100
8	2	1400	+1050	+ 650
9	1	1400	+ 700	+ 450
10	3	1500	+ 830	+ 380
11	2	1500	+ 600	+ 400
12	1	1500	0	+ 300
13	3	1500	+1380	+ 640
14	2	1500	+ 300	+ 200
15	1	1500	+ 100	+ 200
16	3	1600	0	+1200
17	2	1600	0	+1000
18	1	1600	- 100	+ 900
19	3	1700	--	Gage Failed.

TABLE XIV

HALF-BRIDGE STRAIN GAGE

DATA SHEET

Gage Number: 61-5	Configuration: Standard
Gage Wire: Nichrome	Heat Treatment: None
Lead Material: Nickel	Cure: Standard
Specimen Material: Inconel	Cement: PBX
Gage Length: 1"	Specimen Size: Standard
Resistance: $R_a = 59.2$	
$R_c = 58.8$	

LOAD CHECK

<u>Load</u>	<u>Arm 1</u>	<u>$\Delta 1$</u>	<u>Arm 2</u>	<u>$\Delta 2$</u>	<u>Total Gage</u>	<u>Δt</u>
0 gms	13960 $\mu"/\text{in}$		18920 $\mu"/\text{in}$		5980 $\mu"/\text{in}$	
100 "	14090	130	18935	15	6100	120
200 "	14230	140	18945	10	6220	120
300 "	14370	140	18950	5	6350	130
500 "	14645	275	18958	8	6610	260

Bridge rebalanced after each run.

<u>Cycle</u>	<u>Voltage</u>	<u>Max. Temp. Deg. F</u>	<u>Apparent Strain at Max. Temp. Micro Inches per in.</u>	<u>Zero Shift Micro in.per in.</u>
1	0	1400	0	0
2	0	1400	0	0
3	3	1500	0	+ 450
4	2	1500	+ 100	+ 750
5	1	1500	- 100	+ 100
6	5	1500	+1700	+ 64
7	2	1500	+1500	+ 200
8	1	1500	+1300	+ 400
9	3	1500	+2500	+ 350
10	2	1500	+1950	+ 200
11	1	1500	+1500	+ 100
12	2	1500	+2100	+ 150
13	1	1500	+1700	0
14	2	1500	+2720	Gage failed.

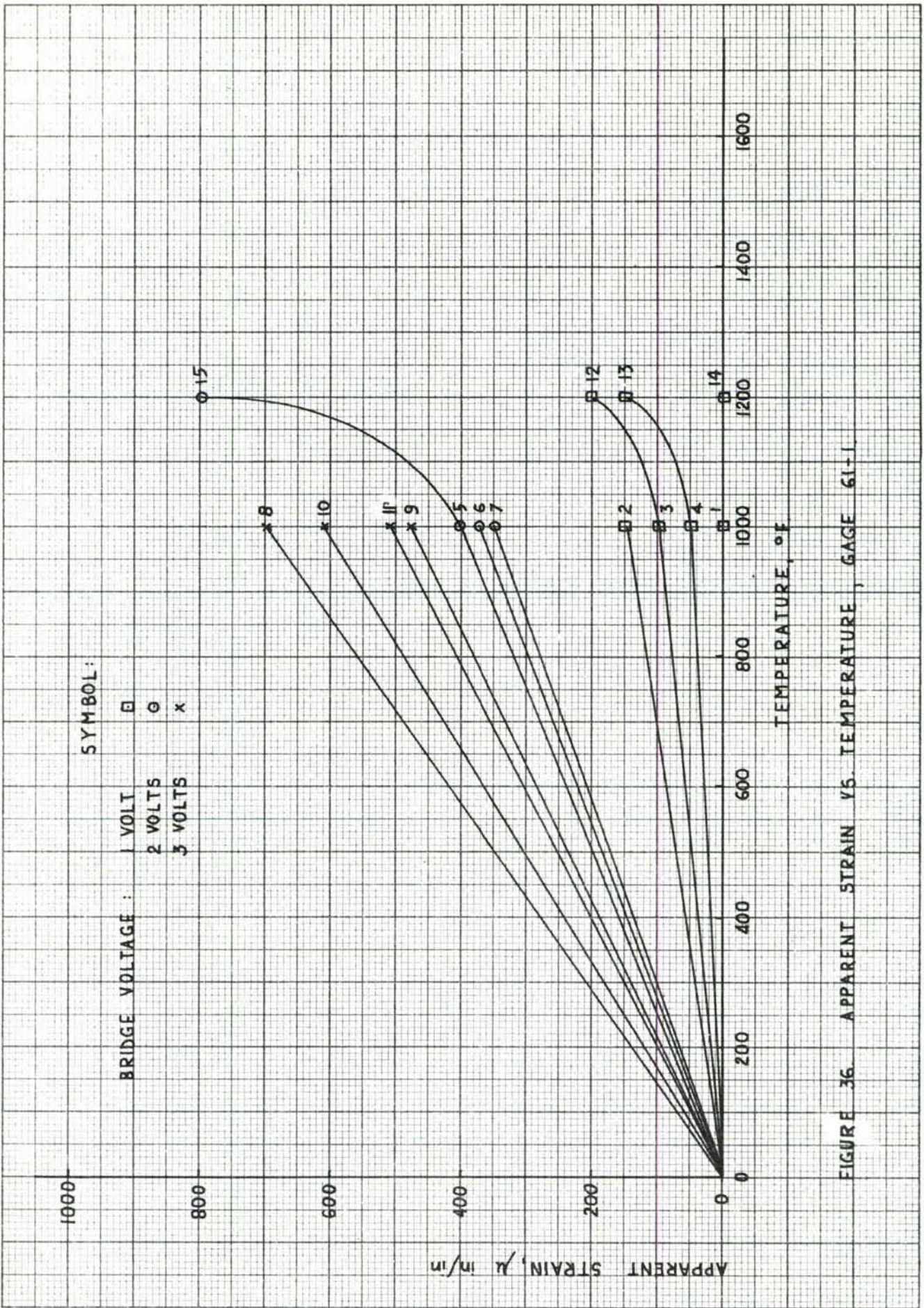


FIGURE 36. APPARENT STRAIN VS. TEMPERATURE, GAGE 61-1.

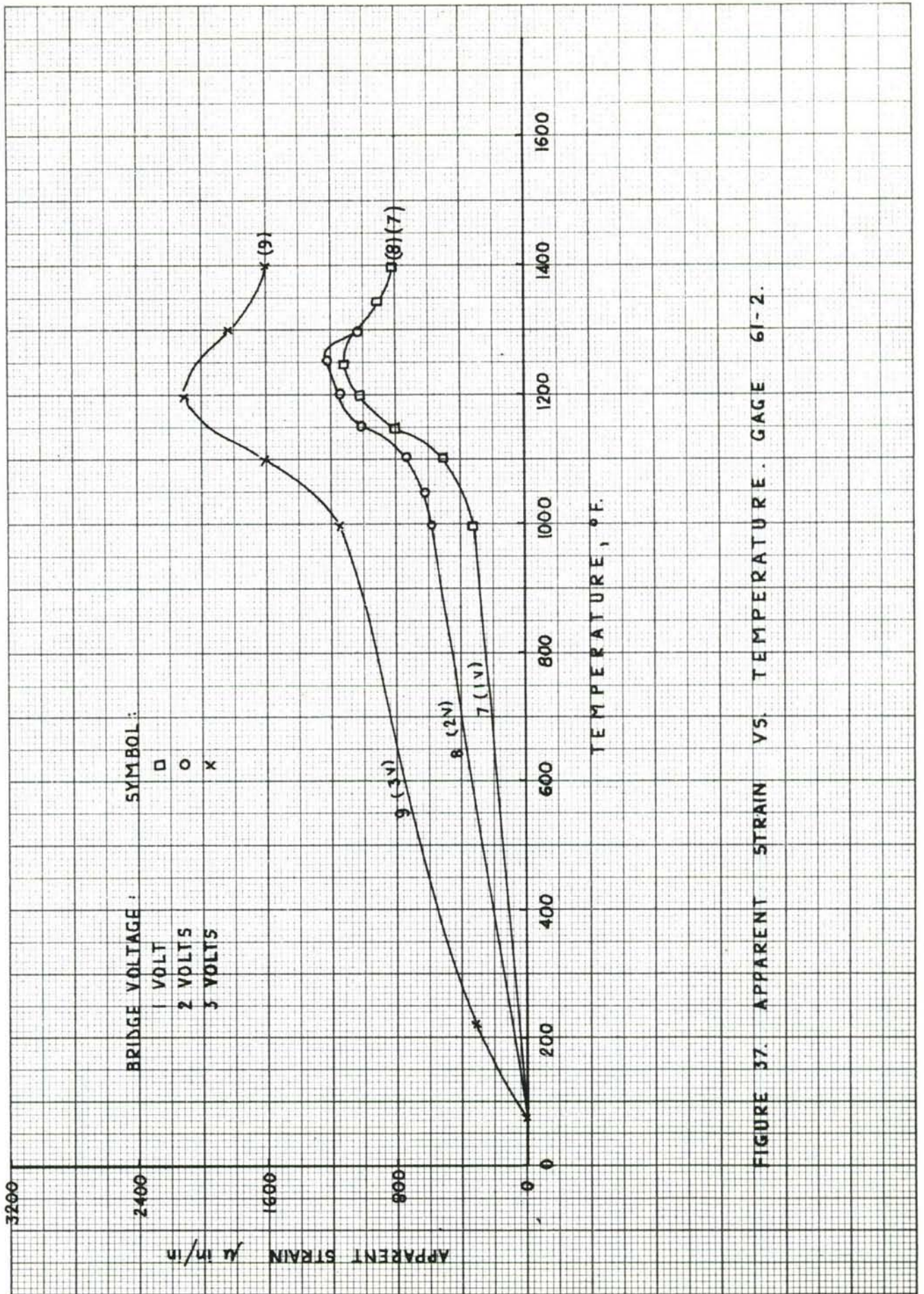


FIGURE 37. APPARENT STRAIN VS. TEMPERATURE. GAGE 61-2.

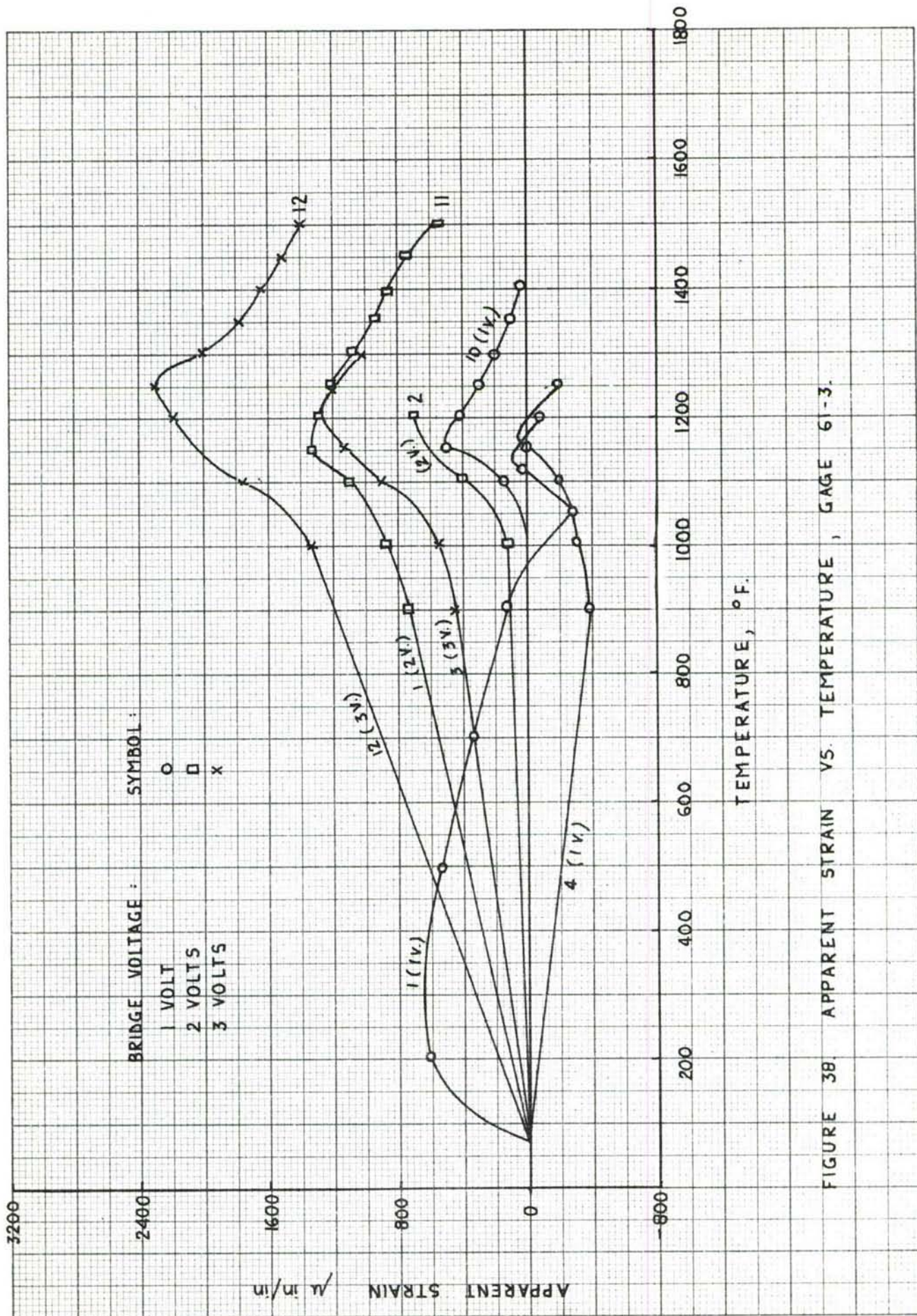


FIGURE 38. APPARENT STRAIN VS. TEMPERATURE, GAGE 61-3.

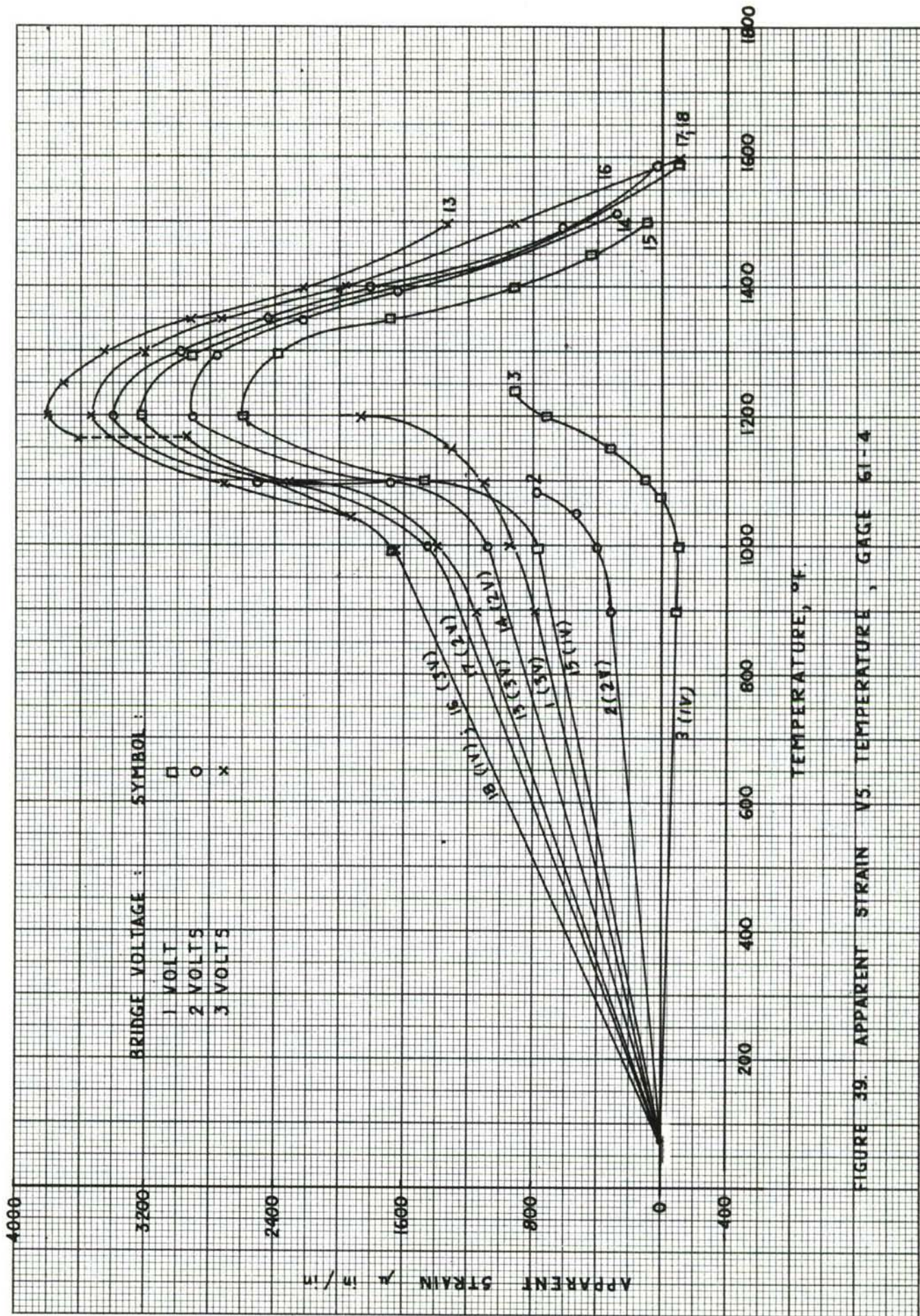
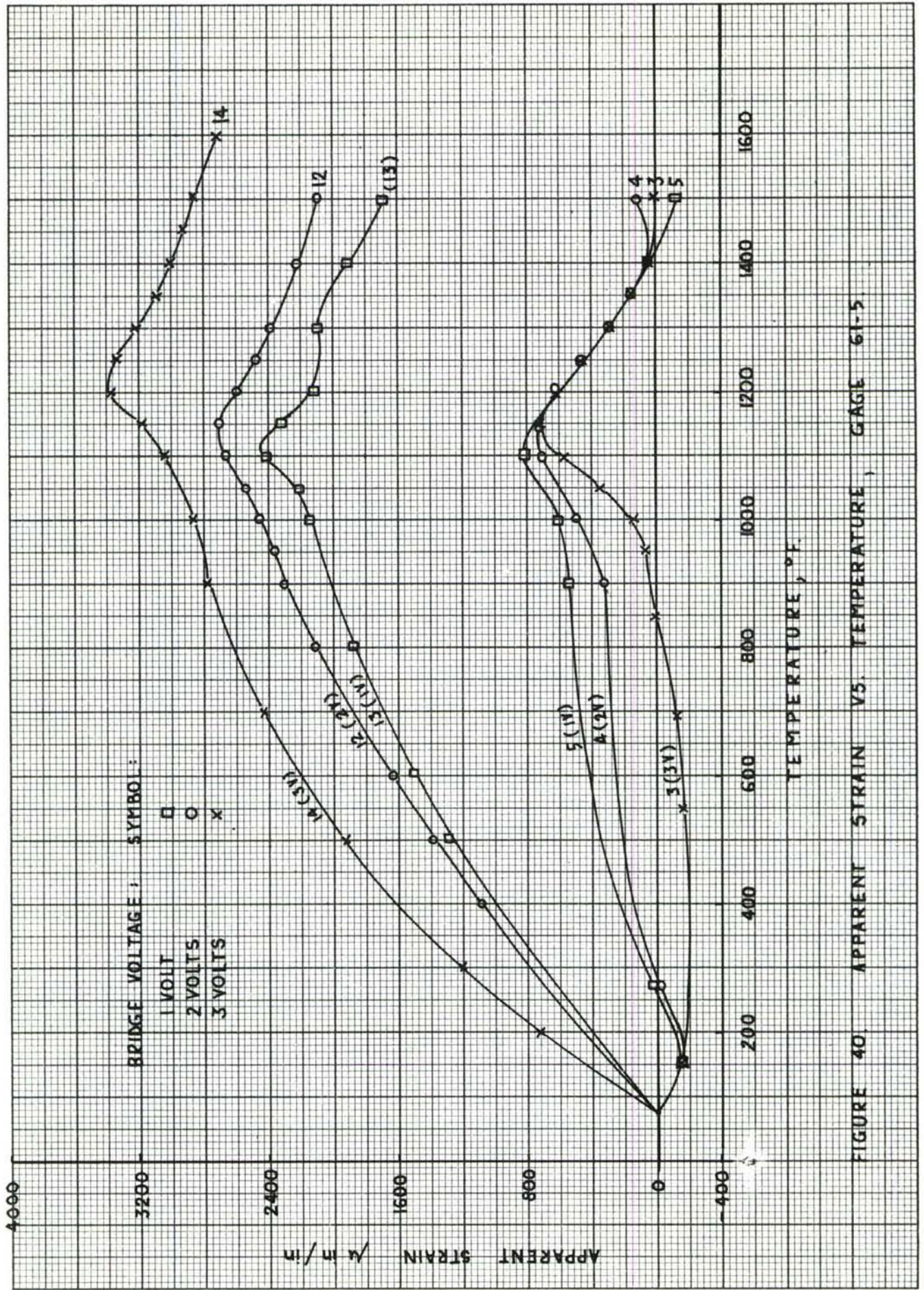


FIGURE 39. APPARENT STRAIN VS TEMPERATURE, GAGE 61-4



VIII. GAGE CEMENTS AND GAGE BONDING TECHNIQUES

A considerable amount of work has been done in the past on high temperature strain gage cements, references 5, 6, 7 and 8. As a result of this work, during most of the contract period, Allen PBX cement was used as both binder and adhesive.

Investigation during this contract period showed, however, that PBX would not reliably hold a gage attached to Inconel, 304 Stainless Steel or Titanium surfaces under rapid heating conditions in air for more than one heating cycle above 1500° F maximum temperature. Consequently, during the latter days of the contract period, several newly marketed cements as well as two flame-sprayed ceramic coatings were investigated to determine their performance in strain gage manufacture and installation.

The following proprietary ceramic cements and flame-sprayed coatings were investigated:

<u>Cement</u>	<u>Manufacturer</u>
Astroceram A	American Thermocatalytic Corp., Mineola, N.Y.
Astroceram B	" " " "
Baymal	E.I. Du Pont de Nemours & Co. Inc., Wilmington, Del.
Melbond CA-100	Melpar, Inc., Falls Church, Va.
Quigley 1925	Quigley, Inc., New York City
B-144	Armour Research Foundation
Flame Sprayed Alumina	
Flame Sprayed Zirconia	

The above materials were tested for their ability to withstand repeated exposure to high temperatures in the following manner:

Two parallel strips of cellophane tape are applied lengthwise on a standard test specimen (.050" thick x 1" wide x 6" long), with a one-half inch gap between them. A quantity of the cement to be tested is placed in this gap, and is smoothed off with a razor blade or plastic strip which "rides" on the cellophane tape. When

the tape is removed, a uniform .003" thick coating remains. The cement is then cured. A chromel-alumel control thermocouple is welded to the metal alongside the cement coating approximately 1/2" from the end of the specimen. When the specimen is placed in the radiant oven and the thermocouple connected to the reference junction, the specimen is ready for testing.

The test consists of heating the specimen from room temperature at a rate of 47° per second until the upper test temperature is reached. The specimen may then be held at this temperature, or cooled immediately. Two cooling rates were used: fast cooling, in which the specimen was removed from the oven immediately, and slow cooling, in which the specimen remained in the oven during cooling. Heating, constant temperature, and cooling constitute one thermal cycle. Figure 35 shows temperature-time relationships during a thermal cycle and shows the heating rate as well as the slow and fast cooling rate.

Table XV shows the materials tested, the maximum test temperature, the test specimen materials, the time-at-maximum temperature through which the cement survived, and the number of survived thermal cycles. A vertical subdivision shows whether the cement was used for the manufacture of gages, for attachment of gages, or only as a coating. A detailed description of each cement follows.

Astroceram: Astroceram cements have been advertised by the manufacturer as being suitable for use on metallic and non-metallic surfaces, at temperatures up to 5300° F. Two types are available: Astroceram A and Astroceram B. The Astroceram A is an air-drying cement, advertised usable to 4300° F, while the Astroceram B must be cured at high temperature, after which it should be usable to 5300° F (Reference 5). The cements should withstand heating rates up to 500° F per second (Reference 6).

Both Astroceram cements, as received, were too coarse grained for use either in gage installation or as coatings. However, fifteen minutes of grinding in a mortar and pestle produced a mixture which could be applied as a coating. Inconel and Titanium specimens were coated, and cured for one hour at 125° F followed by one hour at 400° F. Even the reduced consistency, however, produced grainy, uneven coatings, approximately .005" thick instead of the desired .003". After the cure, the Astroceram A had hardened, but the Astroceram B was still soft. The "B" samples were replaced in the oven for two additional hours of curing at 400° F. At the end of this time, all Astroceram B coatings cracked and flaked off the specimens. This occurrence, coupled with the manufacturer's recommended 2200° F cure, caused discontinuation of further work with Astroceram B.

TABLE XV

EFFECT OF TEMPERATURE CYCLING ON SELECTED CERAMIC CEMENTS AND FLAME-SPRAYED COATINGS

Cement	Applica- tion	Max. Test Temp.	Max. Time at Temp.	Specimen Materials	Max. No. of Cycles Survived	Cure Cycle	Remarks
Astroceram	Coating	2000°F	Inst.	1, 2, 3	0	1 hr. @ 125° F plus	
A	Ga.cement	2000°F	"	3, 2	0	1 hr. @ 400° F	
	Ga. mfg.	1000°F	2 hours	2	-		
Astroceram	Coating	400°F	3 hours	2	0	1 hr. @ 125°F plus	
B					0	3 hrs. @ 400°F	
Baymal	Coating	1000°F	Inst.	1, 2	0	(A) Heat Lamp	
	Gage Cem.	Room	--	2	0	(B) 1 hr. @ 125°F plus 1 hr.	@400°F
	Gage mfg.	Room	--	--	0		
Melbond	Coating	2000°F	Inst.	1, 2, 3, 4	0	1 hr. @ room temp. plus 4 hrs.	
CA-100	Ga.cement	2000°F	"	2, 3	0	gradual rise from 100 to 250°F	
	Ga. mfg.	Room	--	--	--	plus 1 hr. @ 250° F	
Allen PBX	Ga.cement	2000°F	Inst.	1, 2, 3, 4	2	Dry at room temperature plus	
	Ga. mfg.	2000°F	"	1, 2, 3, 4	2	1 hour @ 600° F	
Quigley	Coating	2000°F	"	1, 2	2	1 hour @ 125°F plus	
	Ga. mfg.	1000°F	2 hours	2	-	1 hour @ 400°F	
	Ga.cement	1000°F	2 "	2	-	Best cement coating tested	
Armour B-144	Coating	2000°F	3 min.	2, 1	7	1 hr. @ 125° plus 1 hr. @ 400°F	
Flamesprayed							
Alumina	Coating	2000°F	90 sec.	2, 3	7	No failures observed	
Flamesprayed							
Zirconia	Coating	1700°F	90 sec.	Low carbon steel	3	Severe thermal shock on cooling	

Material Legend: 1-Stainless Steel; 2-Inconel; 3-Titanium; 4-Aluminum.

The Astroceram A samples were tested to 2000° F maximum temperature. Cooling followed the slow curve (Figure 35) until the temperature reached 700° F, at which time the specimen was removed from the oven. After removal, all coatings cracked and flaked off the specimen.

Several 1/4" gages were manufactured from Astroceram A and cemented to Inconel test specimens with the same cement. These gages were tested at slow heating rates to 1000° F in a large oven. The test results were discussed previously in section VI (p.59). Results of the tests indicated a general inferiority to standard gages made with Allen PBX.

Melbond CA-100: Melbond CA-100 appeared attractive for strain gage work because of its advertised low curing temperature (250° F). Coatings of CA-100 were made using standard procedure on Inconel, 304 Stainless Steel, Titanium and Aluminum. The cement has the consistency of a thick paste and forms a uniform, thin, smooth coating. The cement reacted chemically with aluminum, and no testing was done on this material. The other samples were tested in the radiant oven to 2000° F and cooled along the slow curve to 700° F, at which time the specimens were removed from the oven. All coatings failed by cracking and flaking after removal.

CA-100 was also used for the manufacture of gages, simultaneously with the above tests. The first gages were unsatisfactory because of air bubbles in the cement. Since the manufacturer does not recommend the cement for use on metal, and since the tests showed it unsuitable for adhesion to the metals tested, further investigation was suspended. However, when the flame sprayed coatings became available, CA-100 was used to cement PBX gages to the coating. The manufacturer recommends CA-100 for adhesion to Alumina, Pyrophyllite, K-30 brick, and Graphite to 2000° F.

In all the tests above, and in gage installation, the manufacturer's cure cycle was followed. This cycle consists of air drying for one hour, followed by oven drying for four hours, during which the temperature is raised from 100° F to 250° F, followed by 1/2 hour at 250° F.

All gages installed with CA-100 were tested to 2000° F and cooled following the slow curve. All failed on the cooling portion of the first thermal cycle.

Baymal: Baymal is not an adhesive in the usual sense of the term. It is a fine powder of pure alumina; so fine that it forms a colloidal dispersion in water. The manufacturer advertises the material as a cement based on interlocking of the particles as the dispersing medium evaporates.

Experimental dispersions were mixed using water, Allen P-1 Solvent, and Phosphoric Acid as the dispersing media. The Allen P-1 Solvent and the Phosphoric Acid formed dispersions which would not harden when applied as coatings. Two types of curing were used: (1) applications of heat by a heat lamp; (2) air drying followed by curing for one hour at 125° F followed by one hour at 400° F.

Even using the standard coating procedure carefully, two thicknesses of coating were obtained: "thick" or "milky" coatings and "thin" or transparent coatings. All thick coatings cracked and became detached during curing, and usually during air drying.

The thin coated specimens were tested to 1000° F and cooling followed the slow curve. When the specimens were removed from the oven, all had cracked and flaked off.

The Baymal dispersion in water was also used in gage manufacture and as a gage adhesive. Gages were unsatisfactory because of air bubbles in the cement. As an adhesive, the material developed no bond strength. Further use and investigation was discontinued.

Quigley 1925: Several Inconel and 304 Stainless Steel samples were coated with Quigley 1925, cured for one hour at 125° F, followed by one hour at 400° F, and tested to 2000° F following standard procedure. Three samples failed by detaching and flaking on the first thermal cycle. However, one specimen, on Inconel, remained intact, although with discoloration and some flaking along the edges, until failure on the third thermal cycle.

Several 1/4" gages were manufactured from Quigley 1925 and cemented to Inconel with the same cement. These gages were statically tested simultaneously with the Astroceram A gages described above. Test results are reported in section VI. These gages were also generally inferior to gages made with PBX.

Flame Spray. The flame spray technique deposits metal or ceramic coatings on virtually any substrate from a special gun. The ceramic, in powder or rod form, depending upon the equipment manufacturer, is fed into a chamber in the gun. Acetylene gas and oxygen are mixed in this chamber, and ignited. The flame vaporizes the ceramic. The ceramic particles are ejected from the gun nozzle, and deposited on the target. Alumina and Zirconia are the most commonly used ceramics, although other ceramics are available on special order.

Several Inconel and Titanium specimens were coated with flame sprayed Alumina by the Atlas Metal Spraying Company, of Philadelphia. Specimens must be sandblasted before coating. The entire coating process takes less than five minutes per specimen. One standard Half-Bridge strain gage was attached by flame spraying to an Inconel specimen coated with sprayed Alumina. Because of the unusual nature of this installation in Atlas's experience, the gage installation was made very thick, and the entire Alumina coating detached from the metal. However, it was felt that more experience will result in reliable gage installation by this method.

Scheduling problems resulted in several days delay before the above mentioned samples were prepared. In the interim, the Atlas Company supplied High Temperature Instruments Corp., with a sample of Zirconia 201, .010" thick, sprayed on a low carbon steel specimen 3" x 1" x 1/8". This specimen was tested as follows: the specimen was heated to 1700° F and cooled following the fast cycle. The coating remained intact. On the second cycle the specimen was heated to 1700° F, cooled along the fast cycle to 700° F, removed from the support, and held under a running cold water tap. The coating remained intact. On the third cycle, the specimen was heated to 1700° F, removed immediately from the oven, and placed under the cold water tap. The coating cracked and lifted from the specimen. Apparently, the zirconia coating will withstand all but the most severe thermal shock.

Inconel specimens received with an alumina coating were tested to 2000° F and cooled along the fast curve three times. The coating remained intact with no visible degradation. Attempts were now made to attach PBX gages to this coating, using PBX, Melbond CA-100 and Astroceram A as adhesives. The alumina coating was very porous, and absorbed some of the cement rapidly. Each gage installation was tested to 2000° F instantaneously, and cooled along the slow curve. Each gage installation lifted on the first cycle, taking with it that part of the coating which had absorbed the cement. All failures occurred during cooling.

No degradation was observed in the coatings themselves following these tests.

Armour B-144. During the last week of this reporting period, samples of Armour Research Foundation cement B-144 were received through the courtesy of Mr. C. R. Nelson, of the Aeronautical Structures Laboratory, Naval Air Material Center, Philadelphia Naval Base. This cement is tan and of very thin consistency, making a very smooth coating. Four coatings were made on Inconel and one on 304 Stainless Steel.

The Stainless Steel specimen was heated to 2000° F and held at temperature for two minutes. Cooling took place along the slow curve. The specimen was removed from the oven at 900° F. Part of the coating was gone when removed. The remainder continued to pop off on subsequent cooling.

The first Inconel specimen (first specimen tested) was heated to 2000° F and cooled along the slow curve. The cement remained intact, although a color change occurred from tan to violet. Four more cycles were run, employing the fast cooling. There were no signs of degradation. The coating was hard and firm, even when tested with a razor blade at high temperature. On the sixth cycle, the specimen was held for one minute at 2000° F before fast cooling. The seventh cycle was identical, except that the specimen remained two minutes at maximum temperature. On the eighth cycle, the specimen was held at maximum temperature for three minutes. The coating remained intact until the specimen had cooled below 800° F, after which it detached and flaked off.

The second specimen survived one cycle of heating to 2000° F, holding for one minute, and fast cooling. On the second such cycle, the coating detached immediately on beginning of cooling.

The third specimen was tested in the same manner as the second. On the second cycle, however, it was held 90 seconds at 2000° F. Failure occurred immediately on cooling.

The fourth specimen survived three successive cycles to 2000° F, holding for three minutes, and slow cooling without apparent degradation. On the fourth cycle, several lamps in the radiant oven failed, and temperatures higher than 1700° F could not be obtained. Testing was discontinued with the coating intact.

Conclusions:

(1) Allen PBX is unsatisfactory for reliable use on Inconel in air above 1500° F, through more than one thermal cycle, although very satisfactory for use below 1500° F.

(2) Melbond CA-100, Baymal, Astroceram A and B, and Quigley 1925 are unsatisfactory for use above 1500° F on Inconel, Titanium, or 304 Stainless Steel under transient heating. These cements are generally inferior to PBX under static conditions below 1500° F.

(3) Flame sprayed coatings and Armour B-144 have the greatest potential for strain gage installation above 1500° F under transient heating conditions.

(4) All investigations show that failure of gage installations occurs on the cooling portion of a thermal cycle.

IX. GAGE INSTALLATION TECHNIQUES

Surface Preparation

The surface of the structure or specimen on which the gage is to be installed must be scrupulously cleaned. A properly cleaned surface will exhibit no "water break."

Surfaces may be prepared for gage installation either by vapor blasting or by scouring with medium grit emery cloth. In either case, the surface should be thoroughly rinsed with distilled water. After drying, the vapor-blasted surface is ready for gage installation. Surfaces prepared by scouring with emery cloth should not be allowed to dry, however. A lint-free swab impregnated with Allen PBX ceramic cement is used to apply a coating of cement, which is allowed to air dry for a few minutes. The ceramic cement is then completely removed with a clean cloth wet with distilled water. This procedure etches the surface lightly and provides an excellent surface for bonding the gage.

Gage Installation

While the Half-Bridge strain gage is simple to install, it must be handled with care. The back of the gage is coated with wet cement, and the gage is pressed lightly against the prepared surface. The cement is dried under an infra-red lamp for about an hour.

The gage is then lightly coated with cement (Figure 41, A). After further air drying, the specimen is placed in a furnace, and the temperature raised to 300° F. Specimens should be held at this temperature for at least 30 minutes, after which the temperature is raised to 600° F, and held at this temperature for one hour.

Lead Wire Installation

Lead wires are required to connect the light gauge (.005" dia.) leads of the Half-Bridge strain gage to the bridge and power supply. These lead wires must be capable of withstanding the temperatures to which the specimen will be exposed. Since the leads on the Half-Bridge strain gage of the final configuration are nickel, .025" diameter grade A nickel tubing having an inside diameter of not more than .010" was chosen for the leads. The .005" diameter gage leads were cold swaged into the heavy nickel tubes, to withstand the thermal shocks that the installation would be subjected to.

It was further realized that a suitable connector containing three appropriate lead wire tubes in the dimensions previously stated would be a fine accessory for field instrumentation. Work is progressing in this area and a prototype connector will be available in the near future. This type of connector is illustrated in Figure 41, B.

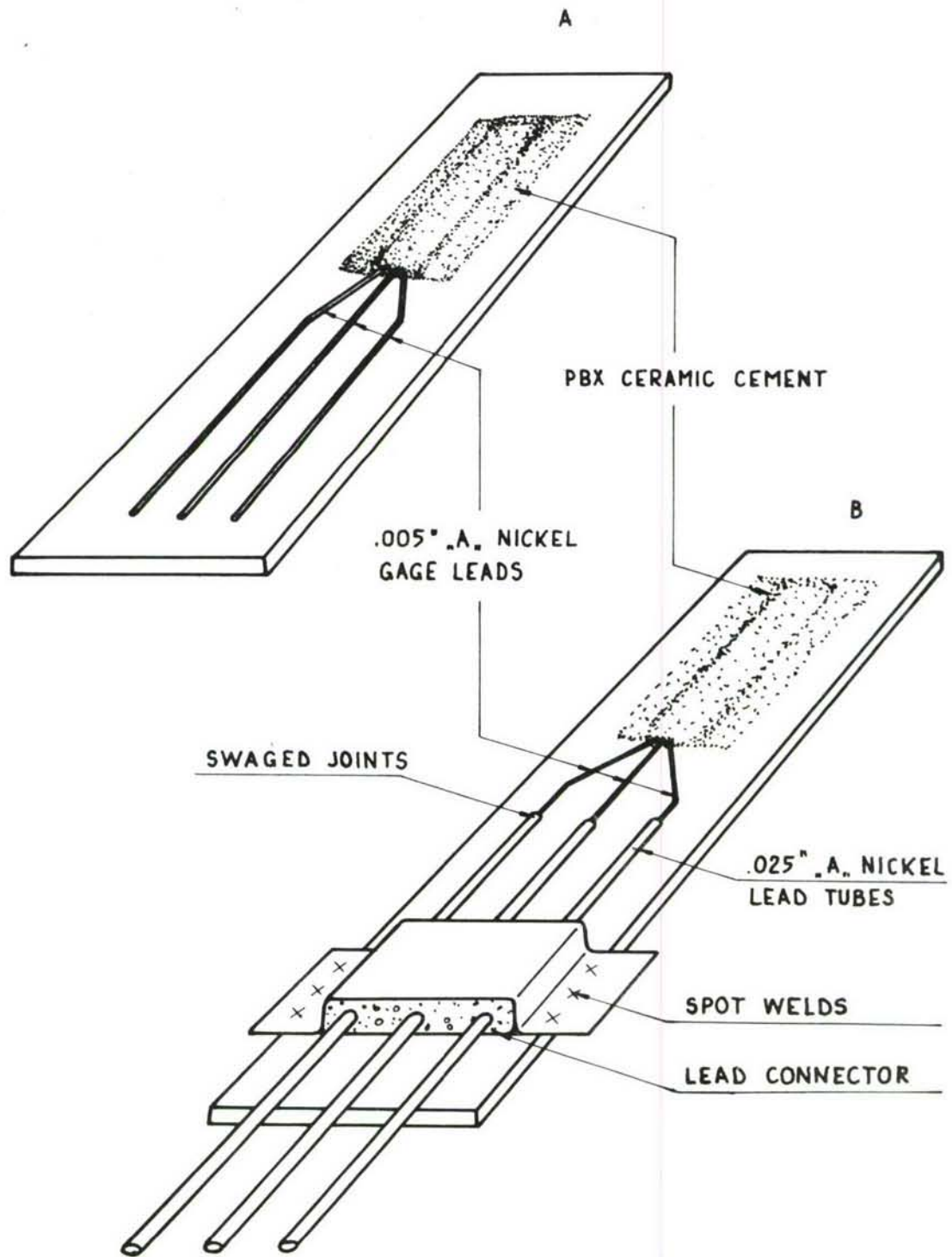


FIGURE 41. HALF-BRIDGE STRAIN GAGE INSTALLATION.

X. SUMMARY AND CONCLUSIONS

The theoretical and experimental investigations documented herein have shown that:

1. The Nichrome Half-Bridge strain gage is presently usable to temperatures of 1100° F with very low temperature coefficients of resistance.
2. The Half-Bridge strain gage is usable in the regions between 1100° and 1500° F if the rapid change in temperature coefficient is taken into account.
3. The gage is not presently usable beyond 1500° F because of the failure of the bonding techniques and because of the increase in cement conductivity above this temperature.
4. The Half-Bridge strain gage should be operated at bridge voltages of 2 volts or less to minimize the effects of self-heating.
5. Investigations of Armour B-144 and flame-spraying techniques indicate that these ceramics have the potential for overcoming the bonding problems above 1500° F.
6. The Half-Bridge strain gage with its present binder and cement will withstand at least ten, and usually more, excursions to 1500° F at heating rates of approximately 50° per second.

APPENDIX I

DERIVATION OF EQUATION 16

$$\frac{E_o}{E} = \frac{R_t}{R_t + L_b} \left[\frac{R_a + L_a}{R_a + L_a + R_1} - \frac{R_c + L_c}{R_c + L_c + R_2} \right] \quad (15)$$

$$\frac{\Delta E_o}{E} = \frac{R_t}{R_t + L_b} \left[\frac{R_a + \Delta R_a + L_a}{R_a + \Delta R_a + L_a + R_1} - \frac{R_c + \Delta R_c + L_c}{R_c + \Delta R_c + L_c + R_2} \right]$$

$$- \frac{R_t}{R_t + L_b} \left[\frac{R_a + L_a}{R_a + L_a + R_1} - \frac{R_c + L_c}{R_c + L_c + R_2} \right]$$

$$= \frac{R_t}{R_t + L_b} \left[\left(\frac{R_a + \Delta R_a + L_a}{R_a + \Delta R_a + L_a + R_1} - \frac{R_a + L_a}{R_a + L_a + R_1} \right) \right.$$

$$\left. + \left(\frac{R_c + L_c}{R_c + L_c + R_2} - \frac{R_c + \Delta R_c + L_c}{R_c + \Delta R_c + L_c + R_2} \right) \right]$$

let $a = R_a + L_a$, and $c = R_c + L_c$

$$\frac{\Delta E_o}{E} = \frac{R_t}{R_t + L_b} \left[\left(\frac{a + \Delta R_a}{a + \Delta R_a + R_1} - \frac{a}{a + R_1} \right) \right.$$

$$\left. + \left(\frac{c}{c + R_2} - \frac{c + \Delta R_c}{c + \Delta R_c + R_2} \right) \right]$$

$$\begin{aligned}
&= \left[\frac{a^2 + a \Delta R_a + a R_1 + R_1 \Delta R_a - a^2 - a \Delta R_a - a R_1}{a^2 + a \Delta R_a + a R_1 + a R_1 + R_1 \Delta R_a + R_1^2} \right. \\
&\quad \left. - \frac{c^2 + c \Delta R_c + c R_2 - c^2 - c \Delta R_c - c R_2 - R_2 \Delta R_c}{c^2 + c \Delta R_c + c R_2 + c R_2 + R_2 \Delta R_c + R_2^2} \right] \\
&= \frac{R_t}{R_t + L_b} \left[\frac{R_1 \Delta R_a}{(a + R_1)^2 + a \Delta R_a + R_1 \Delta R_a} - \frac{R_2 \Delta R_c}{(c + R_2)^2 + c \Delta R_c + R_2 \Delta R_c} \right]
\end{aligned}$$

The values of $a \Delta R_a$, $R_1 \Delta R_a$, $c \Delta R_c$ and $R_2 \Delta R_c$ can be neglected since they are small when compared to $(a + R_1)^2$ and $(c + R_2)^2$.
Substitute for a and c :

$$\frac{\Delta E_o}{E} = \frac{R_t}{R_t + L_c} \left[\frac{R_1 \Delta R_a}{(R_a + L_a + R_1)^2} - \frac{R_2 \Delta R_c}{(R_c + L_c + R_2)^2} \right] \quad (16)$$

APPENDIX II

DERIVATION OF EQUATION 28

When the temperature of the compensating arm is increased from the reference temperature, t_0 , to the ambient temperature, t_1 , the resistance changes and is given by

$$R_{c,1} = R_{c,0} [1 + \alpha_1 (t_1 - t_0)]$$

where α_1 is an integrated, average temperature coefficient of resistance over the temperature range t_0 to t_1 . Now, when current is passed through the wire the temperature will rise above the ambient to the operating temperature, t_2 , and the resistance will be given by

$$R_{c,2} = R_{c,1} [1 + \alpha_2 (t_2 - t_1)]$$

Here, α_2 , is the average value of the temperature coefficient of resistance between t_1 and t_2 . (For small values of $t_2 - t_1$, this will be the slope of the curve of α versus t). If $R_{c,2}$ is now written in terms of $R_{c,0}$ and $t_1 - t_0$, equation 28 results.

APPENDIX III

DERIVATION OF EQUATION 33

The justification for the approximation

$$T_c^4 - T_s^4 \cong 4T_s^3 (t_c - t_s) \quad (33)$$

may be seen by writing

$$T = T_o - \Delta T$$

then $T^4 = (T_o + \Delta T)^4$

$$= T_o^4 + 4T_o^3 (\Delta T) + 6T_o^2 (\Delta T)^2 + 4T_o (\Delta T)^3 + (\Delta T)^4$$

or $T^4 - T_o^4 = 4T_o^3 (\Delta T) + 6T_o^2 (\Delta T)^2 + 4T_o (\Delta T)^3 + (\Delta T)^4$

Since $\Delta T = T - T_o$ is assumed to be small, we neglect the higher order terms and obtain

$$T^4 - T_o^4 = 4T_o^3 (T - T_o)$$

and, since

$$T - T_o = (t + 459.6) - (t_o + 459.6) = t - t_o$$

equation 33 results.

REFERENCES

- (1) W.A.D.D. TR. 60-680, "Half-Bridge Strain Gage".
- (2) Kreith, Frank, "Principles of Heat Transfer" International Textbook Co., Scranton, Pa., 3rd printing 1960.
- (3) Anon., "Nichrome and Other High Nickel Electrical Alloys" Driver-Harris Co., Harrison, N. J. 1957.
- (4) Anon., "Properties of Some Metals and Alloys" International Nickel Co. Inc., New York.
- (5) Baldwin-Lima-Hamilton Corp., Waltham, Mass. Technical Brochure 4310-9, "High Temperature Cement Evaluation".
- (6) Pitts, J. W., Bullard, F., and Moore, D. G. "Resistance Measurement of Ceramic Type Strain Gage Cements," ASTM Special Publication No. 230, 1958, p. 67.
- (7) Pitts, J.W., & Moore, D.G., "Development of High Temperature Strain Gages," NBS Monograph 26, 1951, p. 12 et. seq.
- (8) Pitts, J.W. & Moore, D.G., "Development of Ceramics for Improved Electrical Insulation of High Temperature Strain Gages", NBS Report 5970, 1958.
- (9) Missiles & Rockets, 24 April 1961, p. 40.
- (10) Keith W. Cornely, American Thermocatalytic Corp., Chief Chemist, private communication.
- (11) Chen-Ya Liu, "Natural Convection Heat Transfer in Long Horizontal Cylindrical Annuli," D.S.Thesis, New York University, Sept. 1959.

NATIONAL BUREAU OF STANDARDS REPORT

NBS PROJECT

NBS REPORT

0604-20-06441

June 1963

8004

EVALUATION OF RESISTANCE STRAIN GAGES AT ELEVATED TEMPERATURES

Progress Report No. 15

by

J. T. Trumbo and R. L. Bloss

Engineering Mechanics Section
Division of Mechanics

Technical Report

to

Bureau of Naval Weapons
Aeronautical Systems Division

Order No. IPR19-62-8020-WEPS

IMPORTANT NOTICE

NATIONAL BUREAU OF STANDARDS REPORTS are usually preliminary or progress accounting documents intended for use within the Government. Before material in the reports is formally published it is subjected to additional evaluation and review. For this reason, the publication, reprinting, reproduction, or open-literature listing of this Report, either in whole or in part, is not authorized unless permission is obtained in writing from the Office of the Director, National Bureau of Standards, Washington 25, D. C. Such permission is not needed, however, by the Government agency for which the Report has been specifically prepared if that agency wishes to reproduce additional copies for its own use.



U. S. DEPARTMENT OF COMMERCE
NATIONAL BUREAU OF STANDARDS

FOREWORD

In recent years the use of structures at elevated temperatures has increased greatly. If the safe design and efficient use of structural materials are to be assured, a knowledge of the properties of materials and of structural configurations is essential. In determining these properties, the measurement of strains and deformations is important. Strain gages to measure these quantities must be capable of operating satisfactorily over a wide temperature range.

In order to determine the characteristics of strain gages that are available for use at elevated temperatures, the Department of the Navy and the Department of the Air Force have sponsored a program for the evaluation of these gages. Results obtained from only one gage type are given in this report so that performance information may be made available without undue delay. Results obtained from other gage types have been presented in earlier reports of this series.

There is a continuing effort on the part of manufacturers and research organizations to develop improved strain gages for use at elevated temperatures. Therefore the results given in this report would not necessarily show the performance of similar gages which may differ in characteristics due to differences in materials, treatments, or methods of fabrication.

L. K. Irwin
Chief, Engineering Mechanics
Section

B. L. Wilson
Chief, Mechanics Division

CONTENTS

	Page
FOREWORD -----	II
SYNOPSIS -----	1
1. INTRODUCTION -----	1
2. DESCRIPTION OF GAGES -----	2
3. TEST EQUIPMENT AND METHODS -----	2
4. RESULTS AND DISCUSSION -----	2
4.1 Strain Sensitivity -----	3
4.2 High Strains -----	3
4.3 Drift -----	4
4.4 Temperature Sensitivity -----	4
4.5 Transient Heating -----	5
4.6 Leakage Resistance -----	5
5. CONCLUSIONS -----	5
6. REFERENCES -----	7

EVALUATION OF RESISTANCE STRAIN GAGES
AT ELEVATED TEMPERATURES

Progress Report No. 15

by

J. T. Trumbo and R. L. Bloss

Synopsis

Resistance strain gages of an experimental type, furnished by the High Temperature Instruments Corporation in accordance with their contract with the Aeronautical Systems Division, were evaluated. The results of these tests indicate that the gage factor may vary considerably from gage to gage and that it is affected by the power dissipated by the gage; that the gages can sustain strains greater than 0.005 without failure at 75° and 600° F; that the drift behavior is affected by the voltage across the gage and gage history as well as by temperature; that the temperature sensitivity is affected by gage voltage and, to some extent, by heating rate; and that the leakage resistance is a function of the thermal history of the gage. Attempts to measure the variation of gage factor with temperature were not successful.

1. INTRODUCTION

In the continuing evaluation of resistance strain gages designed for use at elevated temperatures, gages of an experimental type developed by the High Temperature Instruments Corporation in accordance with their contract No. AF33 (616) - 6897 with the Aeronautical Systems Division were tested to determine the following characteristics:

- (1) Gage factor at room temperature,
- (2) Relative change of resistance with time at a constant temperature,
- (3) Resistance-temperature relationship,
- (4) Behavior under transient heating conditions,
- (5) Behavior when subjected to large strains, and
- (6) Resistance between the gage and the test strip.

Attempts to measure the variation of gage factor with increasing temperature were unsuccessful due to failure of the gages before the tests could be completed.

The results of previous evaluations of other types of gages are given in references 1 through 13.

2. DESCRIPTION OF GAGES

The gages which are reported on ~~herein~~ were furnished by the High Temperature Instruments Corporation. It is understood that these gages were manufactured and installed by the Baldwin-Lima-Hamilton Corporation. Due to gage failure during variation of gage factor tests, gages manufactured and installed by High Temperature Instruments Corporation personnel were obtained. However, these gages also failed during test and no results are included in this report. The gages were furnished installed on test specimens specified or furnished by the National Bureau of Standards. Each gage contained two resistance elements arranged to be connected as adjacent arms of a Wheatstone Bridge circuit. One element, referred to as the "active arm", was to be sensitive to dimensional changes in the test strip. The other element, referred to as the "compensating arm", was to be insensitive to such changes but affected by other environmental conditions in the same manner as the active arm. Compensation for all effects except strain, thermal expansion and dimensional instability of the test strip was to be obtained by connecting the elements as adjacent arms of a bridge circuit.

Gages for drift, temperature sensitivity, transient heating and leakage resistance tests were mounted on Inconel test strips. Gages for gage factor and high strain tests were mounted on type 303 stainless steel. For all elevated temperature tests, the gage leads were passed through fine porcelain tubing. The ends of this tubing and all exposed parts of the gage leads were covered with Allen PBX cement which was then cured at 300° F for fifteen minutes. External leads for elevated temperature tests were of "A" nickel wire furnished by the High Temperature Instruments Corporation. For room temperature tests, external leads of copper wire were used. The gage leads were connected to the nickel by spotwelding and to the copper by soldering.

3. TEST EQUIPMENT AND METHODS

The equipment and methods used for all evaluation tests have been described in references 5, 8, 14, 15 and 16.

4. RESULTS AND DISCUSSION

The number of gages subjected to the various tests and the voltages applied to the active arms of the gages are shown in table 1. The heating rates used for the transient heating tests are given in table 2. The results of the evaluation tests are given in tables 3 and 4 and in figures 1 through 24.

4.1 Strain Sensitivity

Gage factor values were obtained at about 75° F from four gages at a maximum strain of about 0.001 in both tension and compression. Gage factor determinations were first made with 0.5 volt across the active arm of the gage and then with 3.0 volts across the active arm. The results of these tests are given in tables 3 and 4 where:

K_u = gage factor for increasing load

K_d = gage factor for decreasing load

\bar{K} = average gage factor

Gages 41 and 46 were tested in tension before being tested in compression. Gages 42 and 44 were tested in compression first.

The differences between the experimental gage factor values and a nominal value are shown in figure 1. The nominal values of 2.03 and 1.76 were chosen as being representative of the three gages that were in best agreement with each other. The departure of a plotted point from the origin shows the difference between the experimental value and the nominal value as a percentage of the nominal value. The departures of the points from the diagonal line show the differences between gage factor values for tension and compression loading.

Figures 2 and 3 show the departure from linearity of the gage response and the zero shift for the first loading cycle of three gages. The maximum strain was about 0.001. The gage factors, K , used in the data reduction were the averages obtained from tests of these gages. These values were 2.03 for the tests at 0.5 volt and 1.76 for the tests at 3.0 volts. In the figures, open symbols indicate an increasing load and solid symbols are for decreasing loads. No corrections were applied for temperature fluctuations during the tests.

Attempts to determine the variation of gage factor with increasing temperature were unsuccessful. Gage element failure occurred in less than ten minutes when the gages were subjected to dynamic strains of about ± 0.0004 at 40 cps. In most tests a failure occurred in less than three minutes.

4.2 High Strains

The results of tests in which gages were subjected to tensile strains greater than those used for gage factor determinations are shown in figures 4 and 5. The gage factor values used to compute the strains indicated by the resistance gages, ϵ_{ind} , were the average values determined from preloads to approximately 1000 microinches per inch at the test temperature.

One gage, tested at room temperature, showed an error less than 50 microinches per inch for strains less than 5000 microinches per inch. Another gage tested at 600° F showed an error of less than 80 microinches per inch for strains less than 6000 microinches per inch and continued to indicate strain to about 10,000 microinches per inch, but with increasing error. Other gages tested at room temperature and at 600° F, showed greater errors indicating more change of gage resistance than expected.

4.3 Drift

Records of relative change of gage resistance with time at constant temperatures up to 1600 ° F are shown in figures 6 through 16. The results were obtained after heating the gage installation at about 10 deg F per second from room temperature or the next lower test temperature. Recording was started one minute after the desired test temperature was reached. The second series of tests (results labeled "Run 2") were made after the gages had been tested once at each test temperature up to 1200° F. The temperature fluctuations during the tests exceeded ± 5 deg F during only three test runs. The data was not corrected for temperature fluctuations.

Three gages were tested with 0.5 volt across the active arm of the gage and three gages were tested with 3.0 volts across the active arm. The drift (resistance change) of the gages tested at 0.5 volt was less than 0.2 percent for thirty minutes at temperatures up to 1200° F except at 900° F where a drift of about 0.3 percent occurred. Gages tested at 3.0 volts also showed drifts of less than 0.2 percent below 1200° F except at 800° and 900° F where resistance changes of about 0.4 and 0.6 percent, respectively, were recorded.

The greater noise for the tests at 0.5 volt can be attributed to the additional amplification required to record these data. Spurious signals that are not a function of the input voltage, e.g. thermal emfs, are also amplified when greater recording sensitivity is used.

4.4 Temperature Sensitivity

Average values of the change of gage resistance with increasing temperature for three gages are shown in figures 17 and 18. The voltage across each arm of the gage was 0.5 volt for tests of three gages and 3.0 volts for tests of three other gages. Each gage was also tested with no power input to the bridge circuit to ascertain if significant thermal emfs were generated within the circuit. No significant effects from such thermal emfs were detected. The heating rate for these tests was about 10 deg F per second. Tests 1 and 2 were carried to a maximum temperature of about 1200° F and tests 3 and 4 were carried to about 1600° F. Each point on the graphs was determined as the slope of a line drawn tangent to a curve of relative change of gage resistance versus temperature.

4.5 Transient Heating

The results of tests in which the temperature of the test strip to which the gage was attached was increased at about 10 deg, 50 deg and 95 deg F per second are shown in figures 19 and 20. The voltage across each gage arm was 0.5 volt for three gages and 3.0 volts for another three gages. The heating rates for all tests are given in table 2. The results of all tests are not shown because the differences between tests at the same heating rate were not thought to be significant after run 1. Although the total resistance changes were less for tests at 0.5 volt than for tests at 3.0 volts, the gage to gage repeatability was generally better for the 3.0 volt tests. This may be due, at least in part, to the greater amplification required for the 0.5 volt tests and the differences in spurious signals from the various gage installations.

Similar tests were conducted with no power to the gage circuit to determine the possible effect of uncompensated thermal emfs within the circuit. Results of these tests, shown in figure 21, show that care must be taken in using these gages when high heating rates are involved.

4.6 Leakage Resistance

The resistance between the gage and the test strip as a function of temperature is shown in figures 22 through 24. These results were recorded while the test strip was being heated at about 10 deg F per second to the maximum test temperature. Four tests to a maximum temperature of about 1200° F were followed by three tests to about 1600° F. Two of the gages, No. 14 and No. 15, had been given an additional cure of one hour at 600° F prior to the test. Gage No. 15 was found to have separated from the test strip at the end of the fifth test run.

These results show the effect of temperature and thermal history on the insulating properties of the cement. The values shown can be considered to be only a qualitative indication of the insulating properties of the cement since it has been found that ceramic cements do not follow Ohm's law (reference 17).

5. CONCLUSIONS

For gages of this type, the data obtained from the evaluation tests covered by this report indicate that:

- (1) The gage factor values can vary considerably from gage to gage as differences greater than 30 percent of the average were found during tests of four gages. Differences in results from repeated tests of one gage were generally less than 5 percent. The gage factor is affected by the power dissipated by the gage.

- (2) The gages can withstand static strains greater than 0.004 at 75° and 600° F. However, the gages failed quickly (usually in less than three minutes) when subjected to low level dynamic strains (± 0.0004 at 40 cps).
- (3) The drift is low, generally less than 0.002 in 30 minutes, at temperatures as high as 1200° F. The drift is dependent upon the power dissipated by the gage, especially at 800° and 900° F.
- (4) The temperature sensitivity of the gages is dependent upon gage history and, to some extent, upon gage voltage. The greatest effect of temperature was found in the temperature range of 900° to 1200° F.
- (5) Care must be taken to connect the gage circuit so that major uncompensated thermal emfs will be in series with the power source if a d-c system is used.
- (6) The insulating properties of the cement are strongly affected by thermal history.

Acknowledgment

The authors gratefully acknowledge the assistance of T. W. Butler, C. H. Melton, J. S. Steel, M. L. Sundquist, Mrs. C. B. Waldron and R. J. Wall in performing the evaluation tests and in preparing this report.

6. REFERENCES

- (1) R. L. Bloss and C. H. Melton, "An Evaluation of Two Types of Resistance Strain Gages at Temperatures up to 600° F," NBS Report No. 4676, May 1956 (ASTIA No. AD 94696).
- (2) R. L. Bloss and C. H. Melton, "An Evaluation of One Type of Resistance Strain Gage at Temperatures up to 600° F," NBS Report No. 4747, July 1956 (ASTIA No. AD 101079).
- (3) R. L. Bloss and C. H. Melton, "An Evaluation of Two Types of Resistance Strain Gages at Temperatures up to 600° F," NBS Report No. 4843, September 1956 (ASTIA No. AD 107662).
- (4) R. L. Bloss and C. H. Melton, "An Evaluation of Strain Gages Designed for Use at Elevated Temperature -- Preliminary Tests for Temperatures up to 1000° F," NBS Report No. 5286, May 1957 (ASTIA No. AD 135050).
- (5) R. L. Bloss and C. H. Melton, "Evaluation of Resistance Strain Gages at Elevated Temperatures" (Progress Report No. 5), NBS Report No. 6117, August 1958 (ASTIA No. AD 202419L).
- (6) R. L. Bloss, C. H. Melton, and M. L. Seman, "Evaluation of Resistance Strain Gages at Elevated Temperatures" (Progress Report No. 6), NBS Report No. 6245, December 1958, (ASTIA No. AD 211391).
- (7) R. L. Bloss, C. H. Melton, and M. L. Seman, "Evaluation of Resistance Strain Gages at Elevated Temperatures" (Progress Report No. 7) NBS Report No. 6395, April 1959, (ASTIA No. AD 217651).
- (8) R. L. Bloss, C. H. Melton, and J. T. Trumbo, "Evaluation of Resistance Strain Gages at Elevated Temperatures" (Progress Report No. 8) NBS Report No. 6526, August 1959, (ASTIA No. AD 227197).
- (9) R. L. Bloss, C. H. Melton, and J. T. Trumbo, "Evaluation of Resistance Strain Gages at Elevated Temperatures" (Progress Report No. 9) NBS Report No. 6900, July 1960, (ASTIA No. AD 240829).
- (10) R. L. Bloss, J. T. Trumbo, and C. H. Melton, "Evaluation of Resistance Strain Gages at Elevated Temperatures" (Progress Report No. 11) NBS Report No. 7004, November 1960, (ASTIA No. AD 248649).
- (11) J. T. Trumbo, C. H. Melton, and R. L. Bloss, "Evaluation of Resistance Strain Gages at Elevated Temperatures" (Progress Report No. 12) NBS Report No. 7161, May 1961 (ASTIA No. AD 262790).

- (12) R. L. Bloss, J. T. Trumbo, C. H. Melton and J. S. Steel "Evaluation of Resistance Strain Gages at Elevated Temperatures" (Progress Report No. 13) NBS Report No. 7399, December 1961.
- (13) R. L. Bloss, J. T. Trumbo, C. H. Melton and J. S. Steel (Evaluation of Resistance Strain Gages at Elevated Temperatures" (Progress Report No. 14) NBS Report No. 7588, August 1962.
- (14) R. L. Bloss, "A Facility for the Evaluation of Resistance Strain Gages at Elevated Temperatures, Symposium on Elevated Temperature Strain Gages," ASTM Special Technical Publication No. 230, pp. 57-66.
- (15) R. L. Bloss, "Evaluation of Resistance Strain Gages at Elevated Temperatures," Materials Research and Standards, Vol. 1, No. 1, p. 9 (1961).
- (16) R. L. Bloss and J. T. Trumbo, "A Method for Measuring the Instability of Resistance Strain Gages at Elevated Temperatures," ISA Transactions, Vol. 2, No. 2, p. 112 (1963).
- (17) J. W. Pitts and D. G. Moore, "Development of High-Temperature Strain Gages" NBS Monograph 26, 1961.

Table 1 - Number of Gages Tested and Gage Voltage

Type of test	Number gages tested	Voltage across gage arm volts, d-c
Gage factor determination	4	0.5 and 3
High strain	4	1.5*
Resistance instability (drift)	3	0.5
	3	3
Temperature sensitivity	3	0.5
	3	3
Transient heating	3	0.5
	3	3
Leakage Resistance	3	10**

* a-c (1000 cps)

** Maximum voltage between gage and test strip

Table 2 - Heating Rates for Transient Heating Tests

Test No.	Nominal heating rate deg F/sec	Gage circuit*	Power to gage circuit
1 through 5	10	A	yes
6 through 8	50	A	yes
9 and 10	10	A	yes
11 through 13	85 to 98**	A	yes
14 and 15	10	A	yes
16	10	A	No
17	10	B	No
18	50	A	No
19	50	B	No
20	93 to 98**	A	No
21	93 to 98**	B	No

* See figure 21

** Maximum heating rate attainable

Table 3 - Gage Factor Values at About 75° F with 0.5 Volt Across Each Gage Arm

Gage No.	Run No.	Gage factor values					
		Tension			Compression		
		K_u	K_d	\bar{K}	K_u	K_d	\bar{K}
41	1	2.156	2.162	2.159	2.037	2.159	2.098
	2	2.159	2.162	2.160	2.131	2.156	2.144
	3	2.162	2.167	2.164	2.120	2.135	2.128
	Average			2.161			2.123
42	1	1.972	2.042	2.007	1.922	1.903	1.912
	2	2.055	2.041	2.048	1.845	1.855	1.850
	3	2.040	2.034	2.037	1.865	1.888	1.876
	Average			2.031			1.879
44	1	2.156	2.098	2.127	1.830	1.933	1.882
	2	2.077	2.062	2.070	1.911	1.931	1.921
	3	2.089	2.079	2.084	1.884	1.909	1.896
	Average			2.094			1.900
46	1	1.562	1.495	1.528	1.167	1.316	1.242
	2	1.500	1.489	1.494	1.218	1.283	1.250
	3	1.492	1.488	1.490	1.280	1.278	1.279
	Average			1.504			1.257

Table 4 - Gage Factor Values at About 75° F with 3.0 Volts Across Each Gage Arm

Gage No.	Run No.	Gage factor values					
		Tension			Compression		
		K_u	K_d	\bar{K}	K_u	K_d	\bar{K}
41	1	1.767	1.843	1.805	1.847	1.941	1.894
	2	1.877	1.857	1.867	1.959	1.995	1.977
	3	1.876	1.847	1.862	1.932	1.950	1.941
	Average			1.845			1.937
42	1	1.714	1.742	1.728	1.718	1.627	1.672
	2	1.755	1.732	1.744	1.893	1.681	1.787
	3	1.722	1.749	1.736	1.942	1.678	1.810
	Average			1.736			1.756
44	1	1.691	1.689	1.690	1.654	1.624	1.639
	2	1.715	1.688	1.702	1.607	1.606	1.606
	3	1.710	1.690	1.700	1.594	1.557	1.576
	Average			1.697			1.607
46	1	1.236	1.341	1.288	1.258	1.201	1.230
	2	1.313	1.318	1.316	1.163	1.207	1.185
	3	1.314	1.312	1.313	1.185	1.174	1.180
	Average			1.306			1.198

USCOMM-NBS-DC

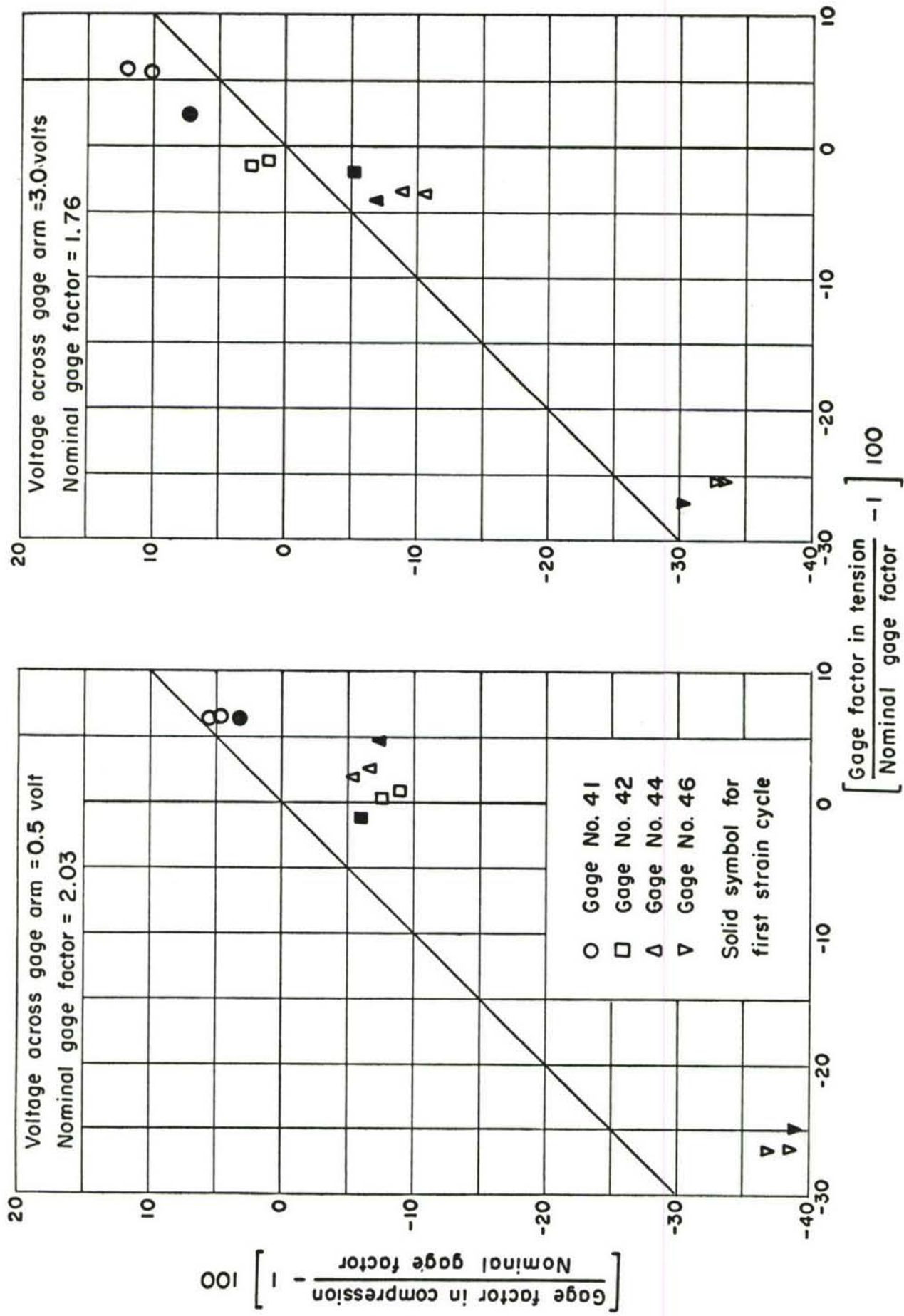


Fig. 1 Gage factor deviation at 75° F

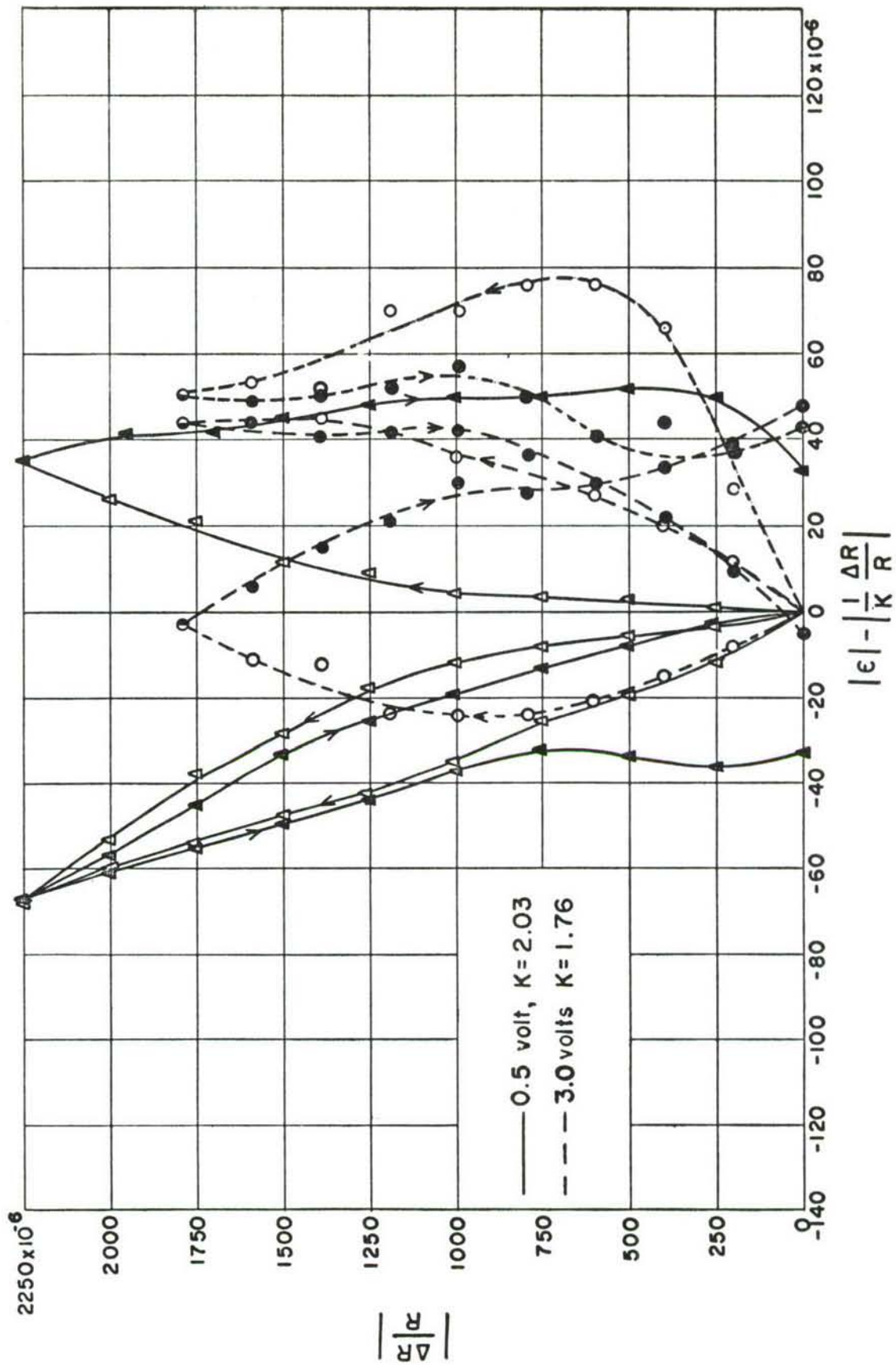


Fig. 2 Strain deviation for tension loading

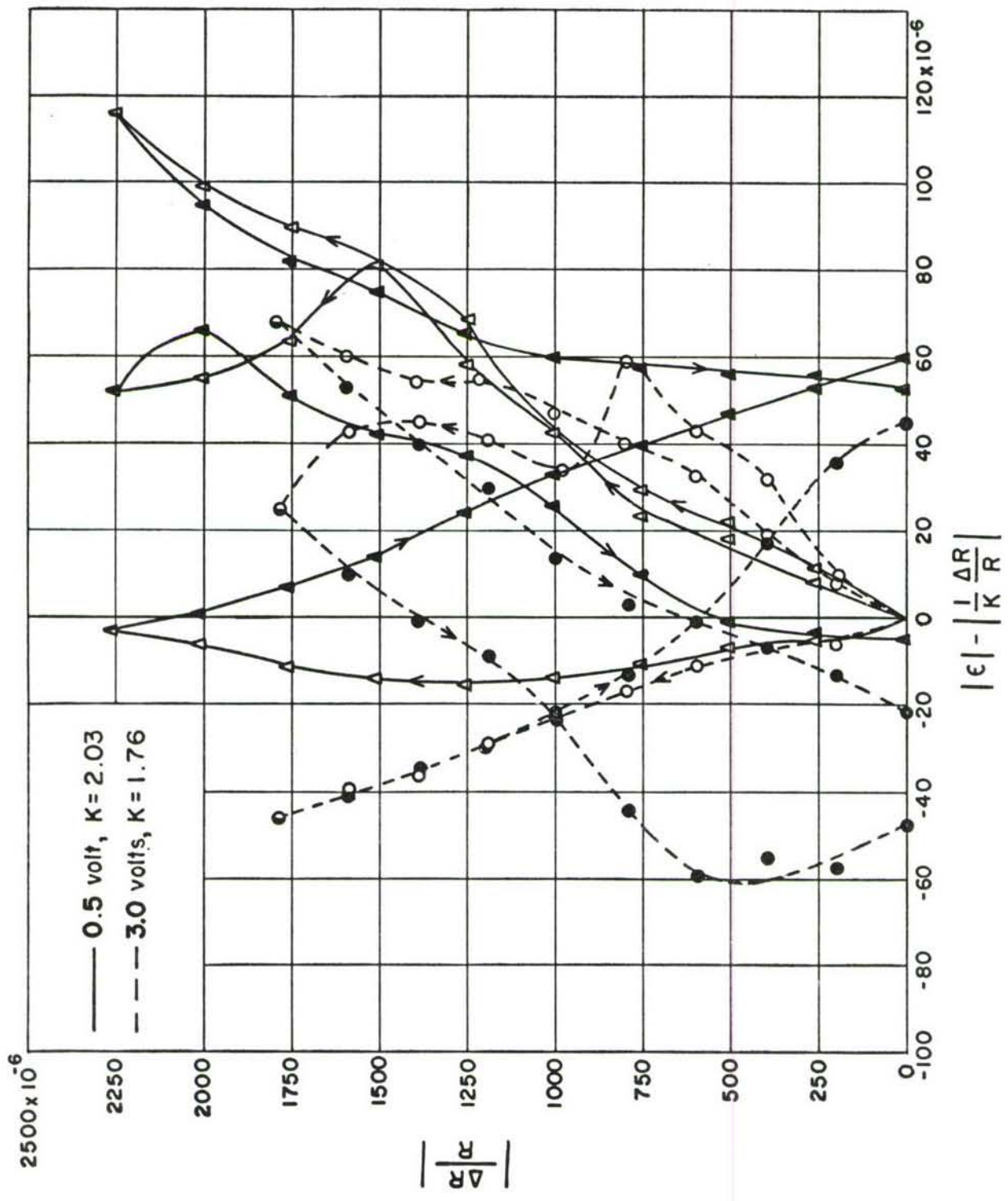


Fig. 3 Strain deviations for compressive loading

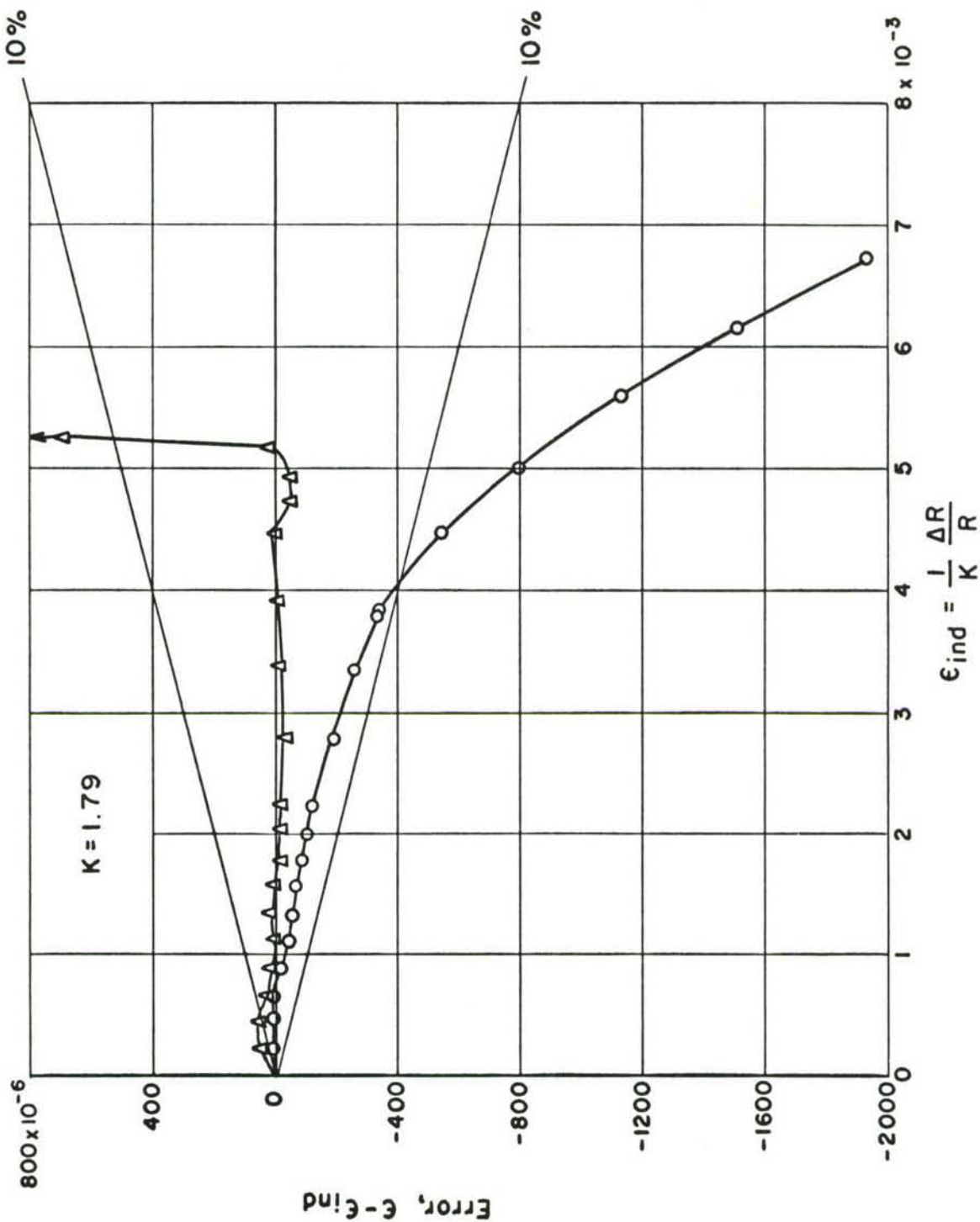


Fig. 4 Gage behavior at high strain at 75° F

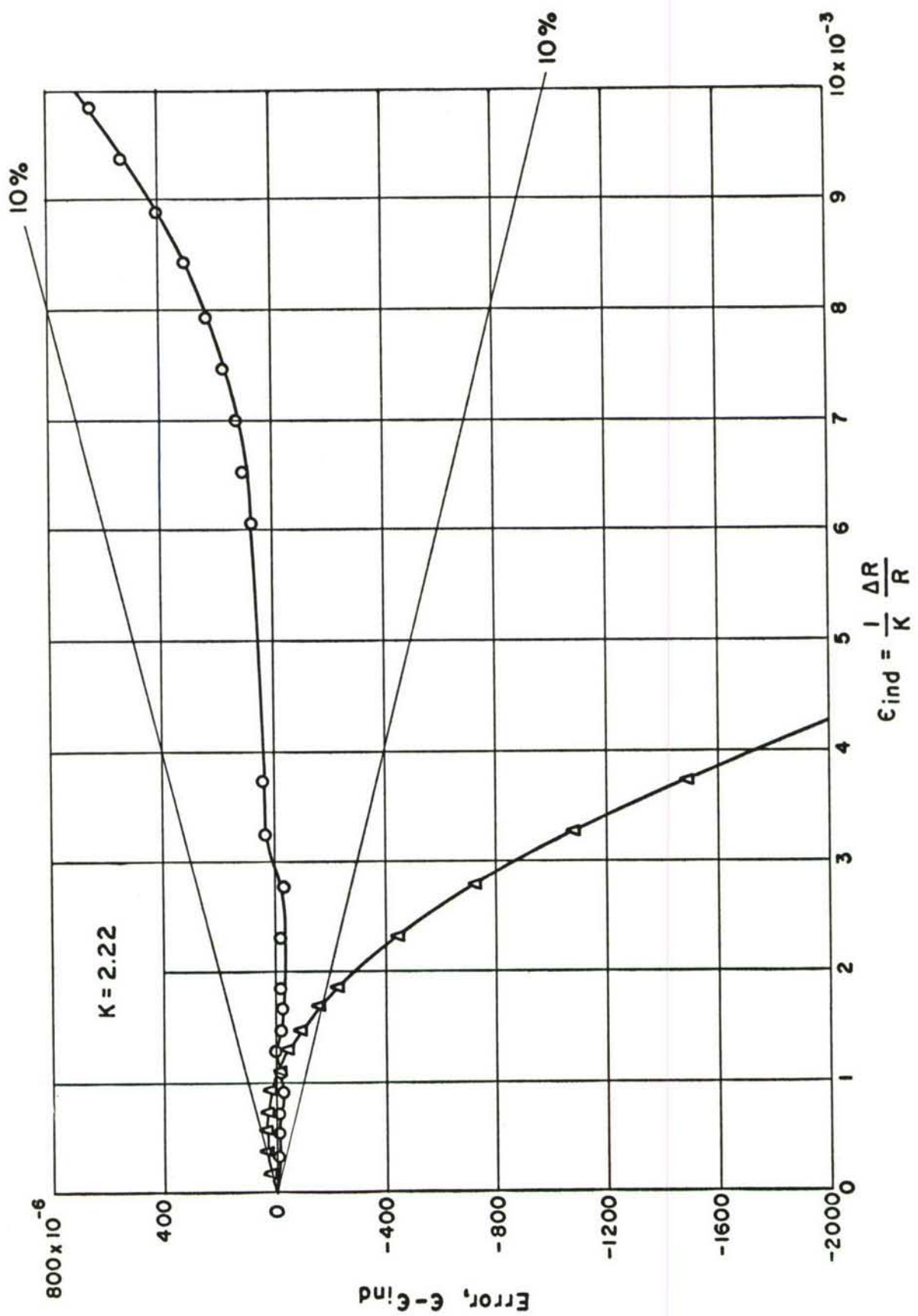


Fig. 5 Gage behavior at high strain at 600°F

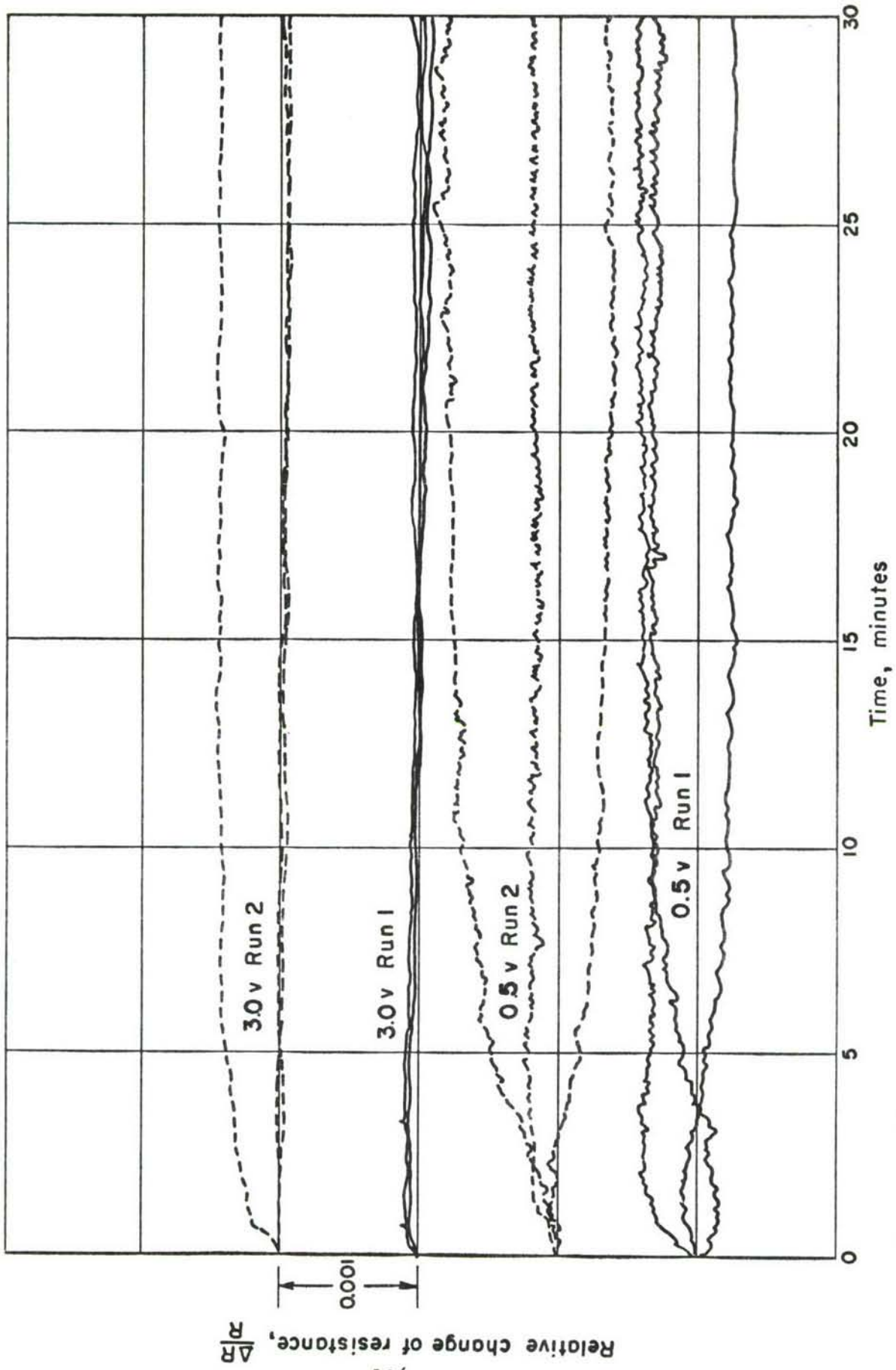


Fig. 6 Drift behavior at 600°F

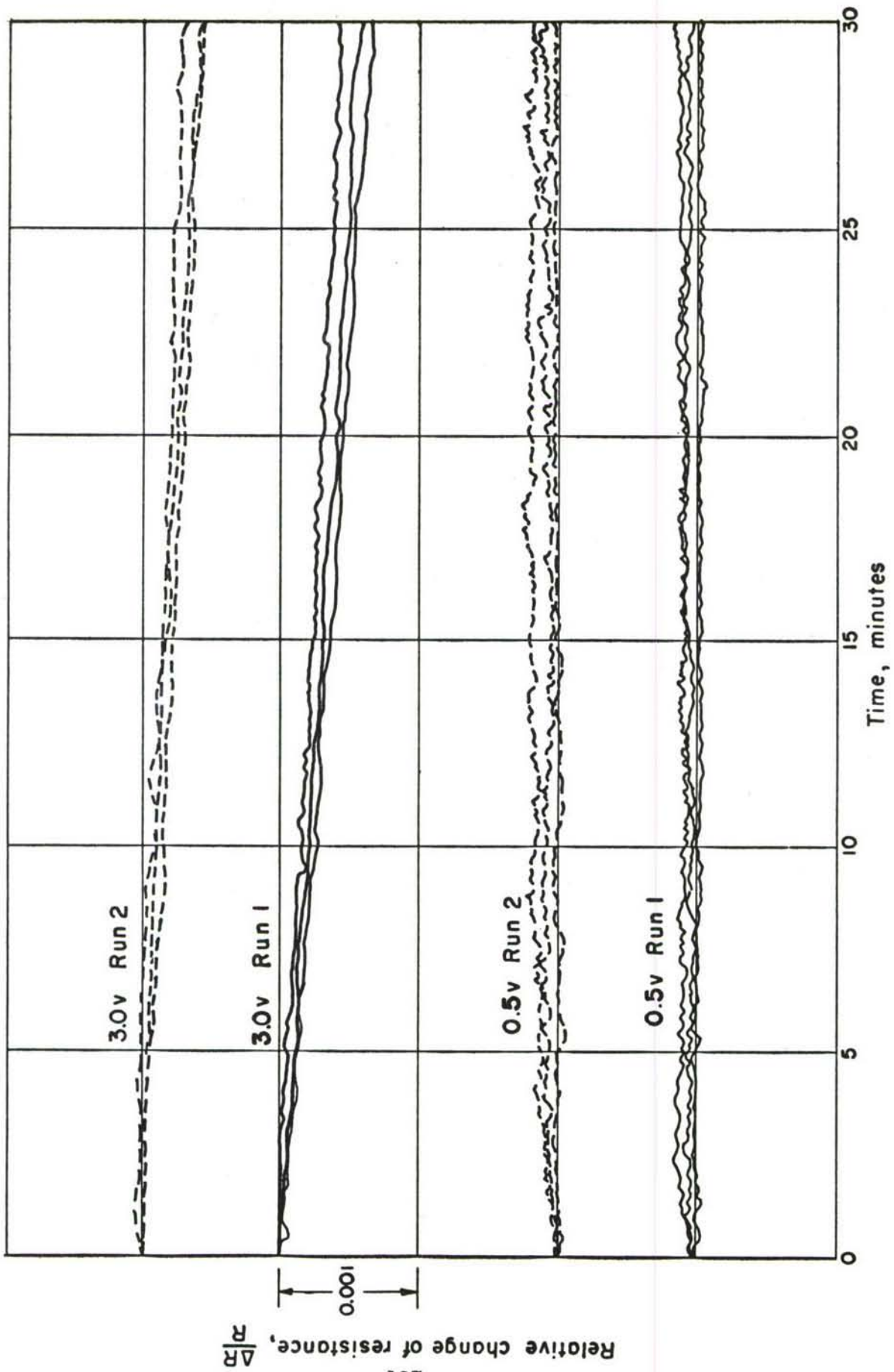


Fig. 7 Drift behavior at 700°F

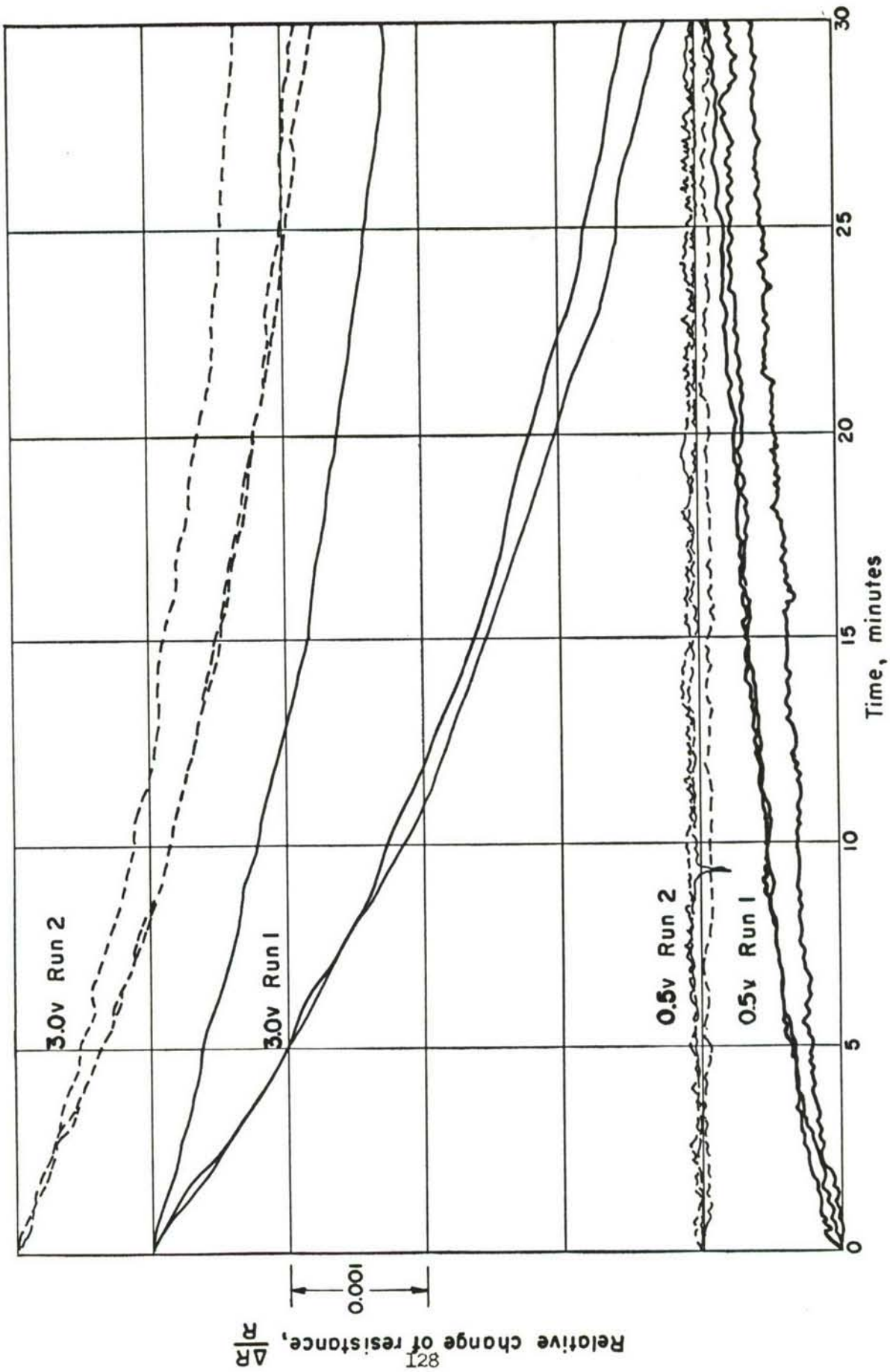


Fig. 8 Drii. behavior at 800°F

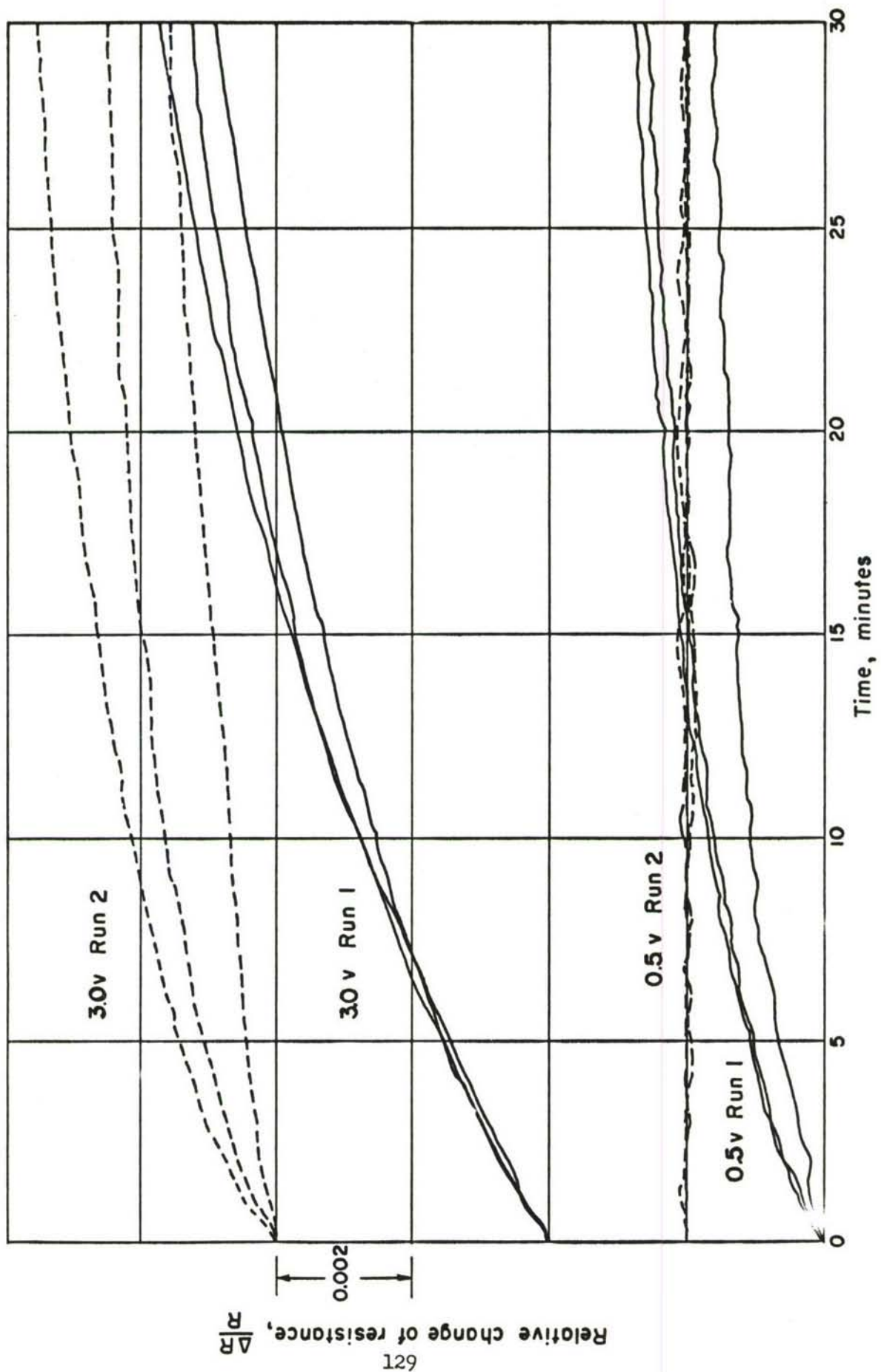


Fig. 9 Drift behavior at 900°F

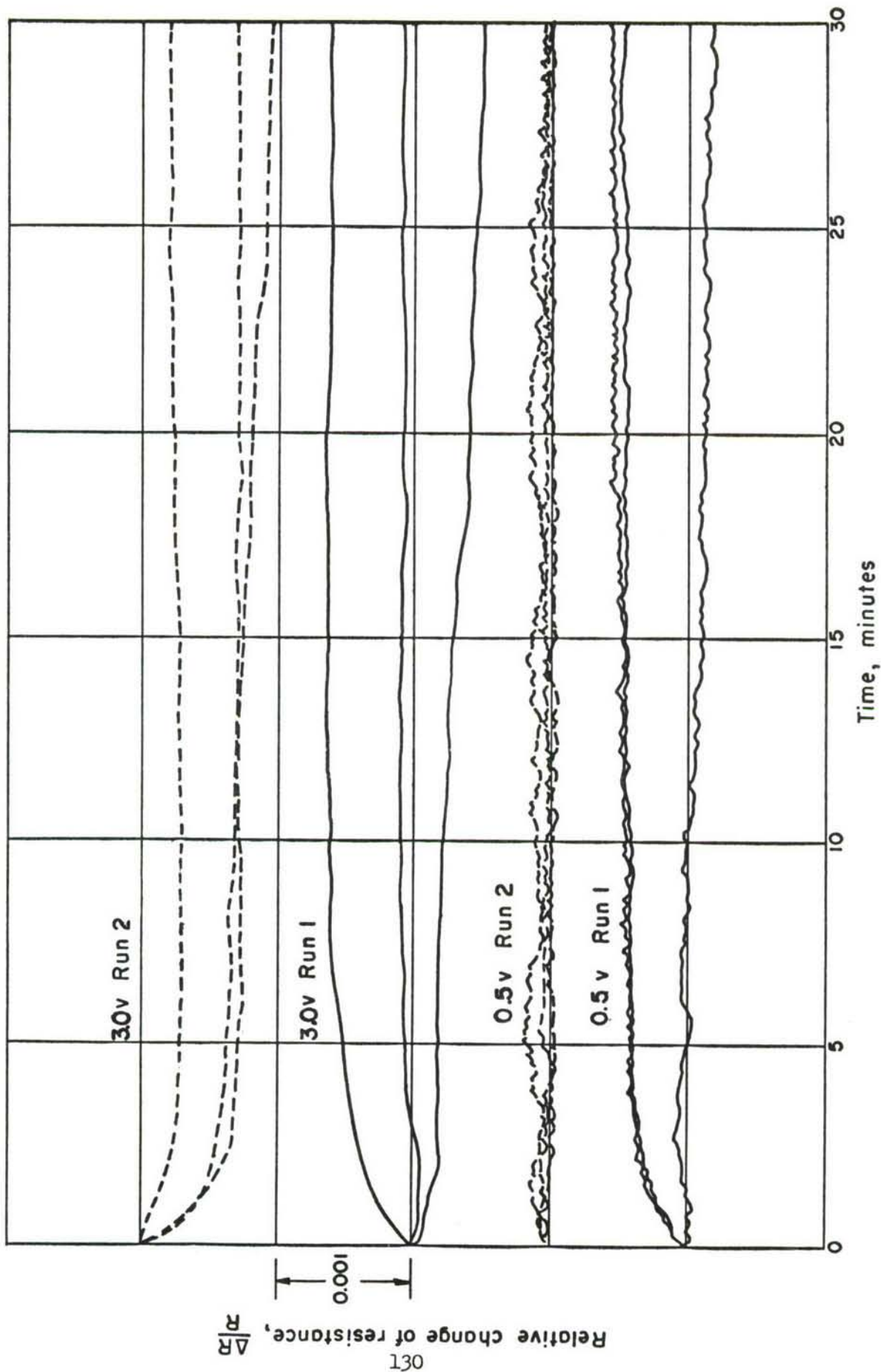


Fig.10 Drift behavior at 1000° F

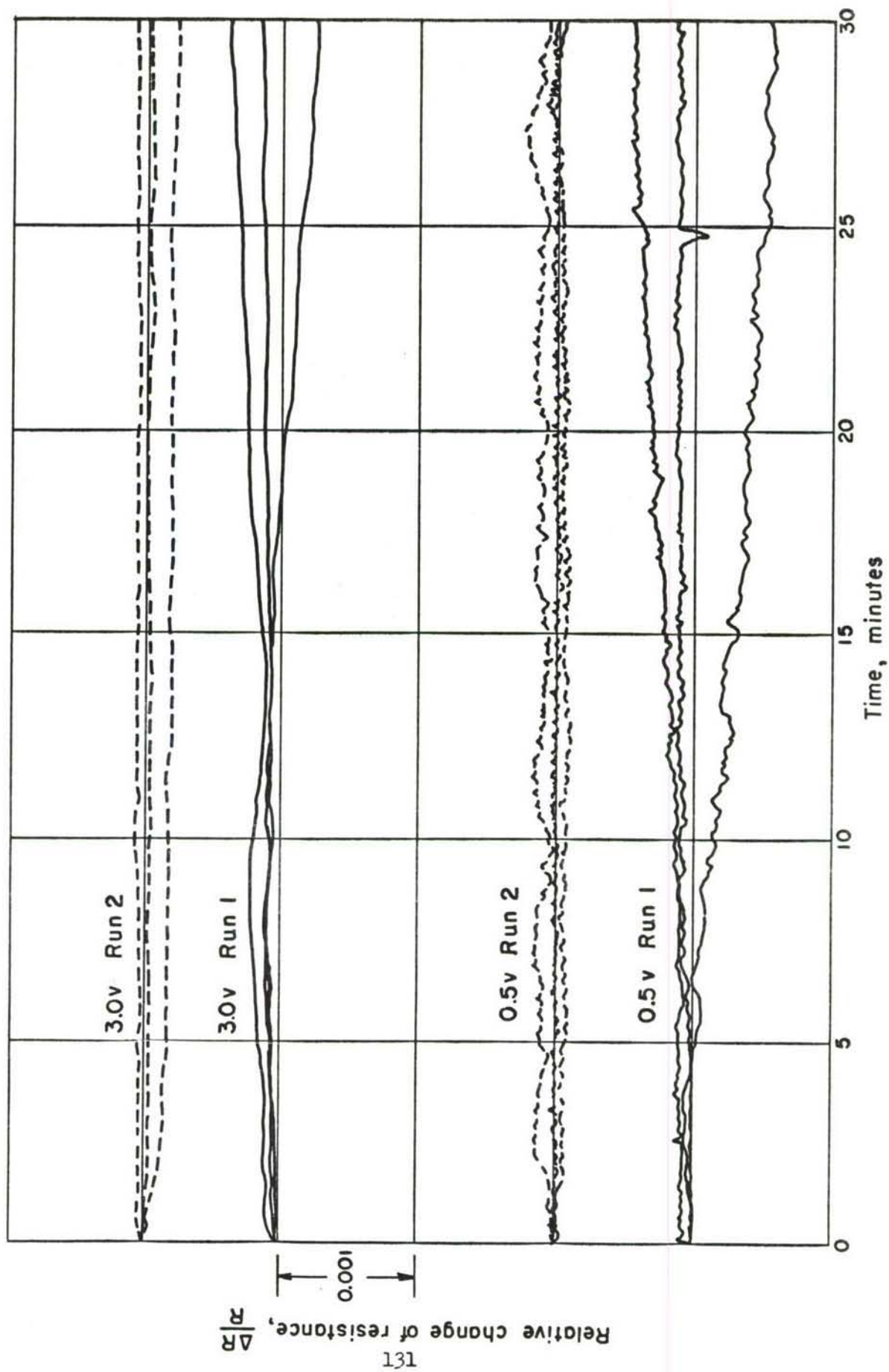


Fig. 11 Drift behavior at 1100° F

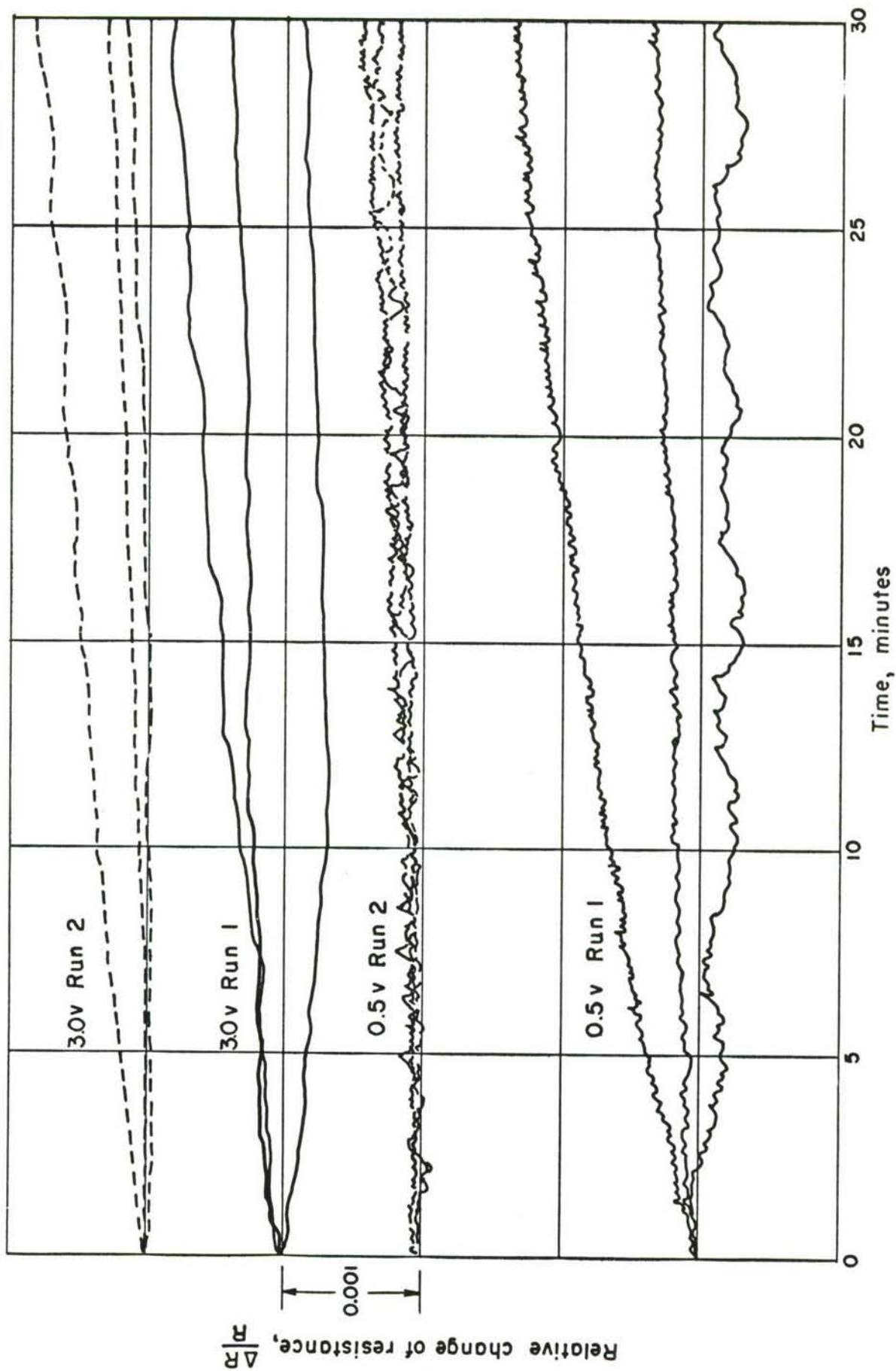


Fig. 12 Drift behavior at 1200° F

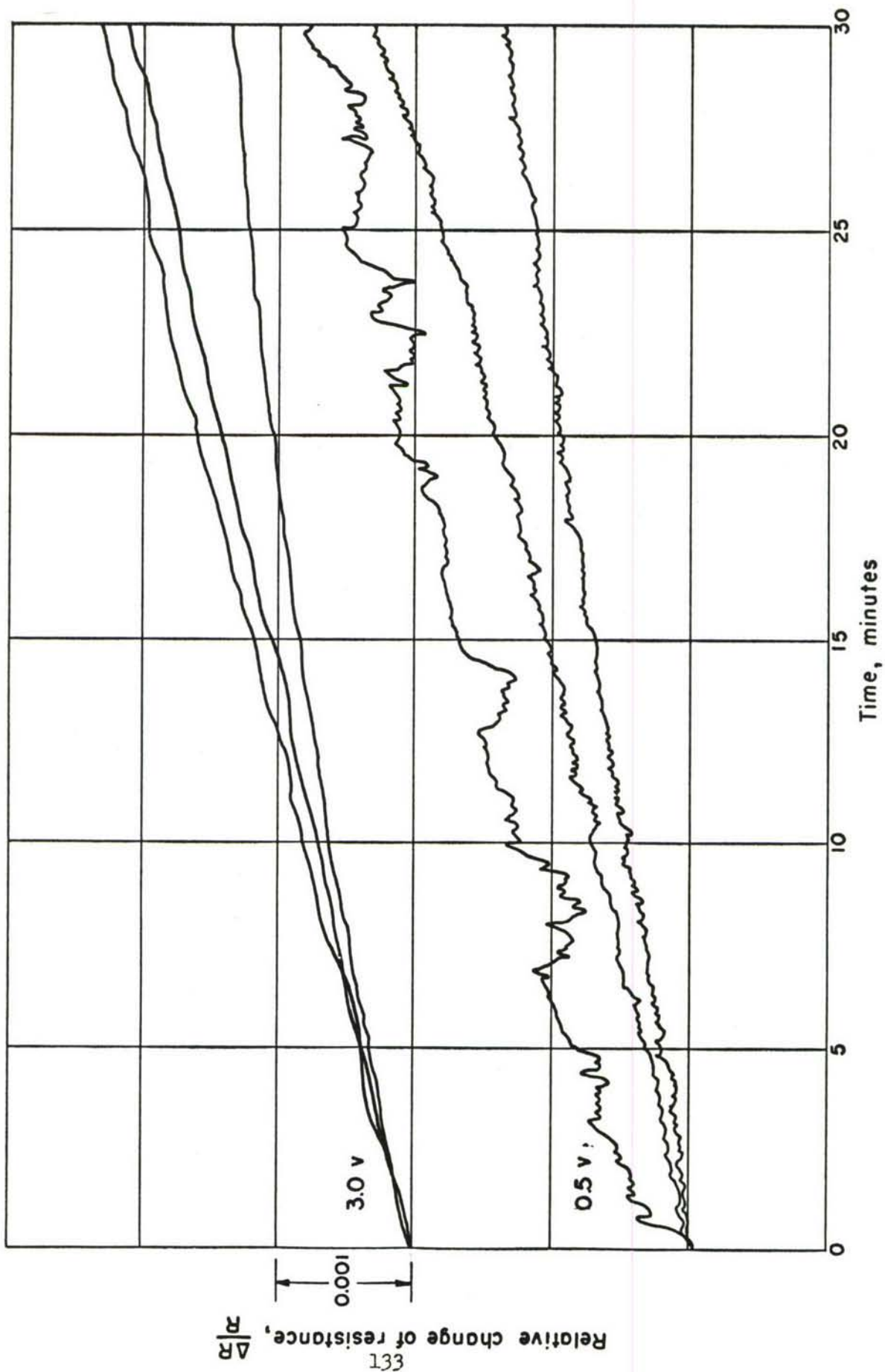


Fig.13 Drift behavior at 1300° F

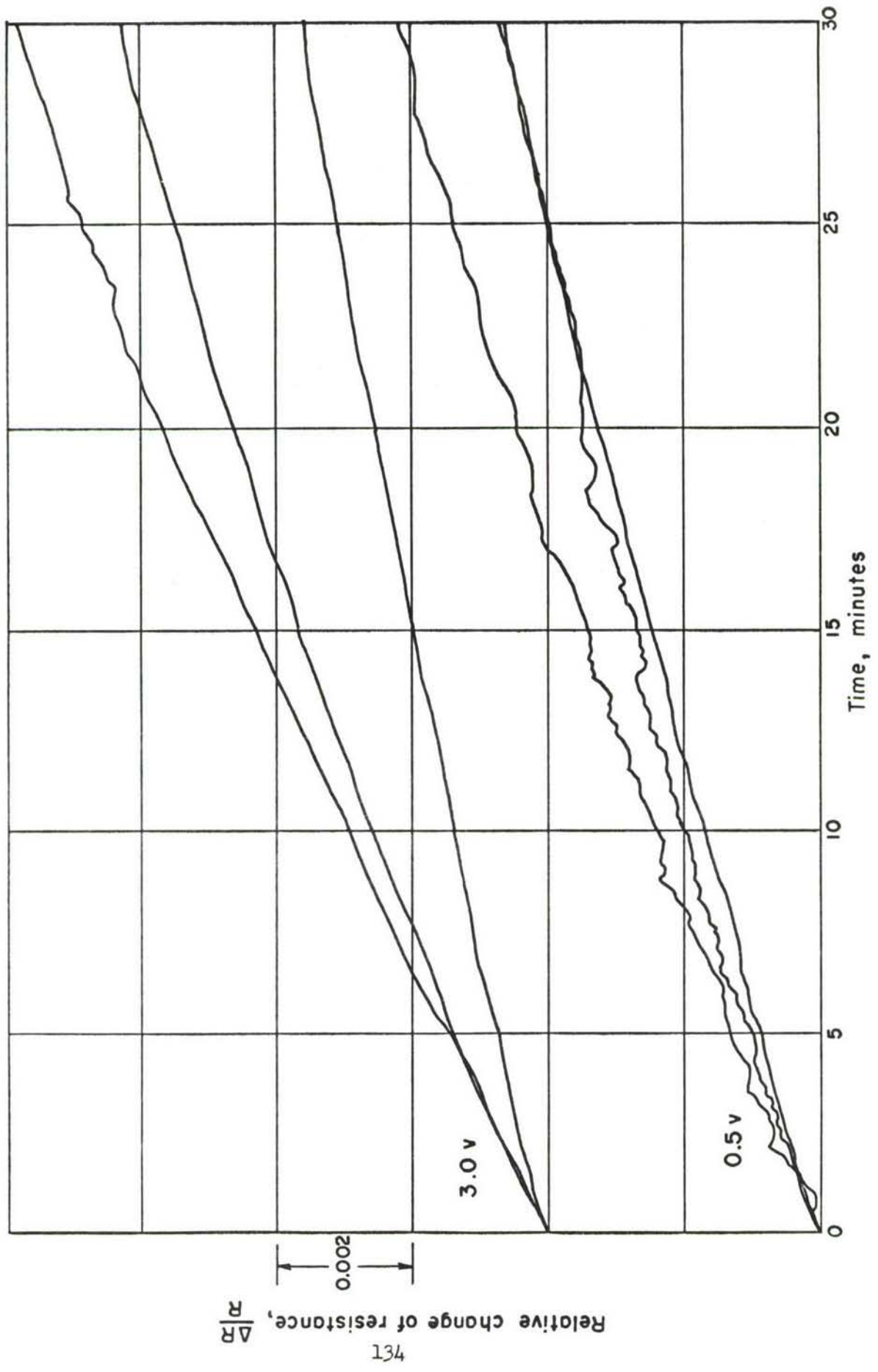


Fig. 14 Drift behavior at 1400° F

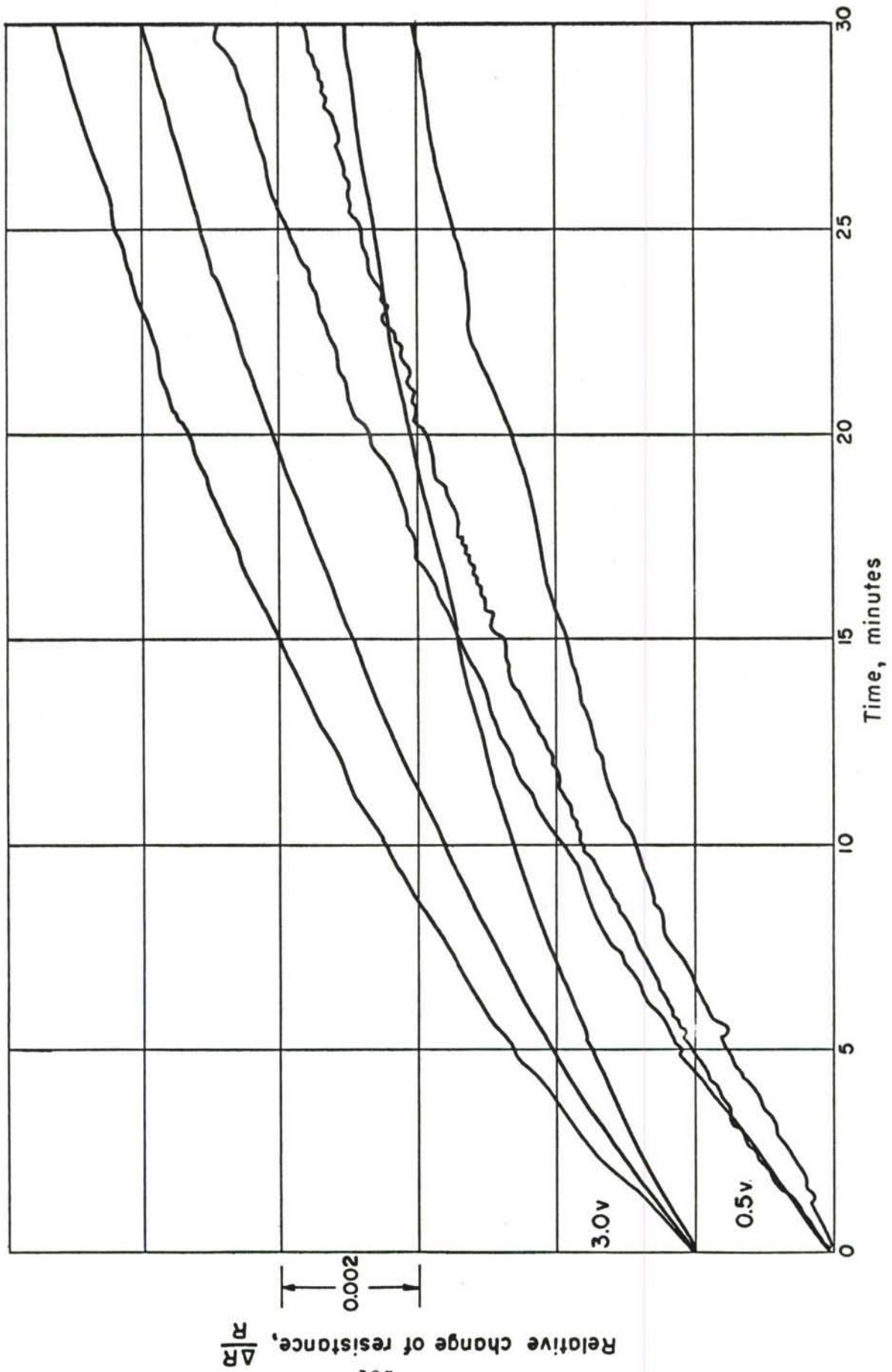


Fig.15 Drift behavior at 1500°F

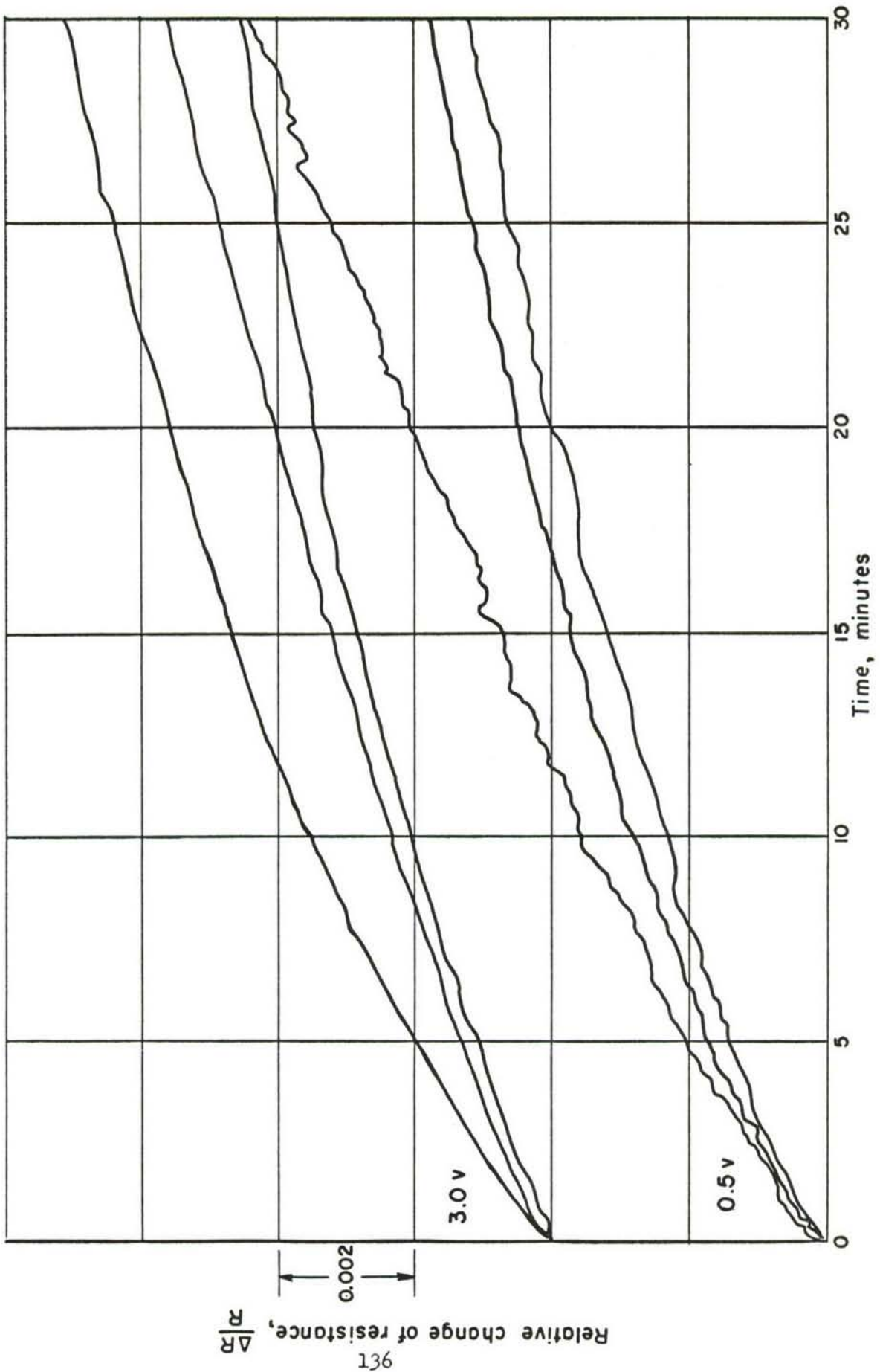


Fig.16 Drift behavior at 1600 °F

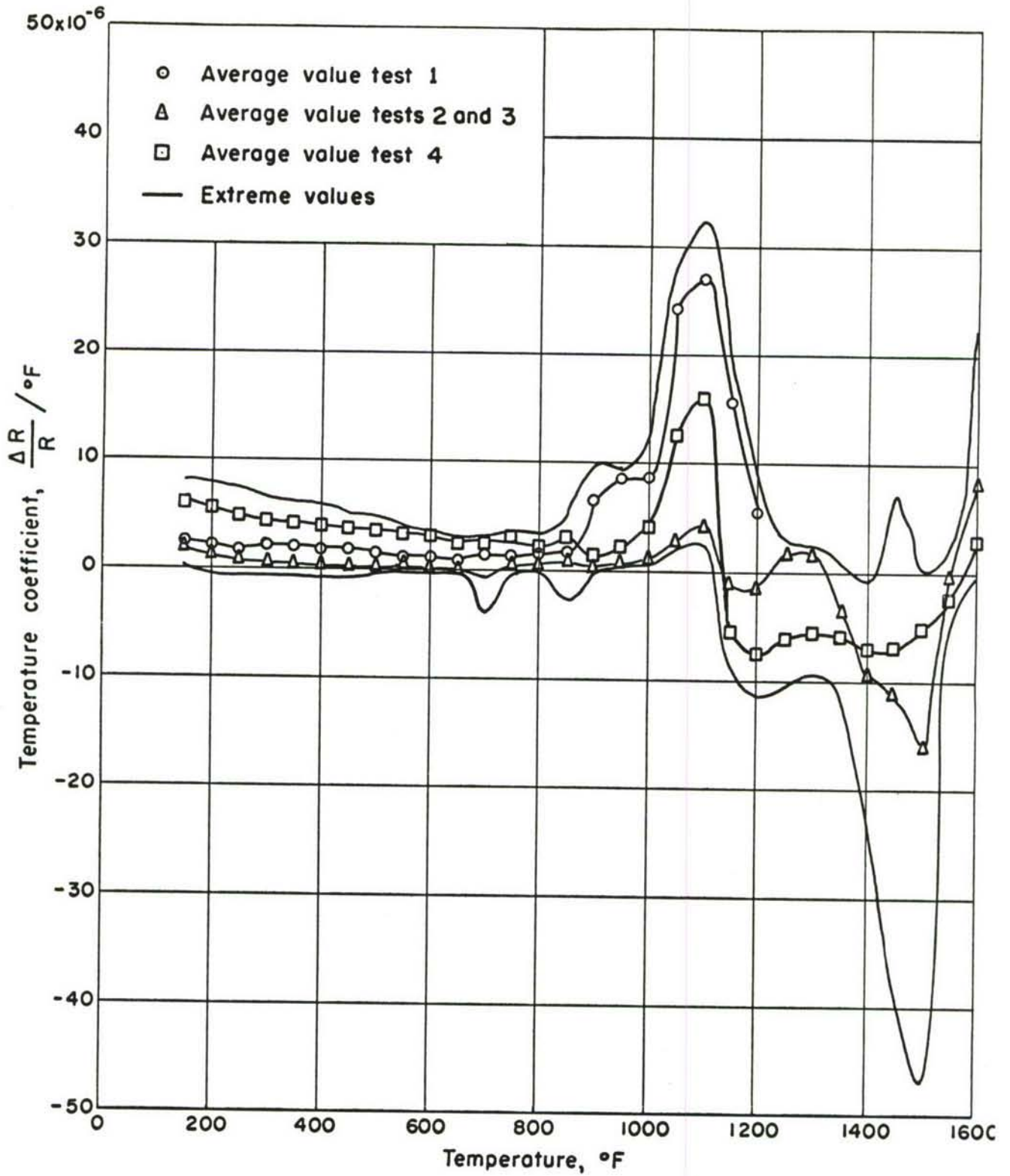


Fig. 17 Temperature sensitivity with 0.5 volt across gage arm

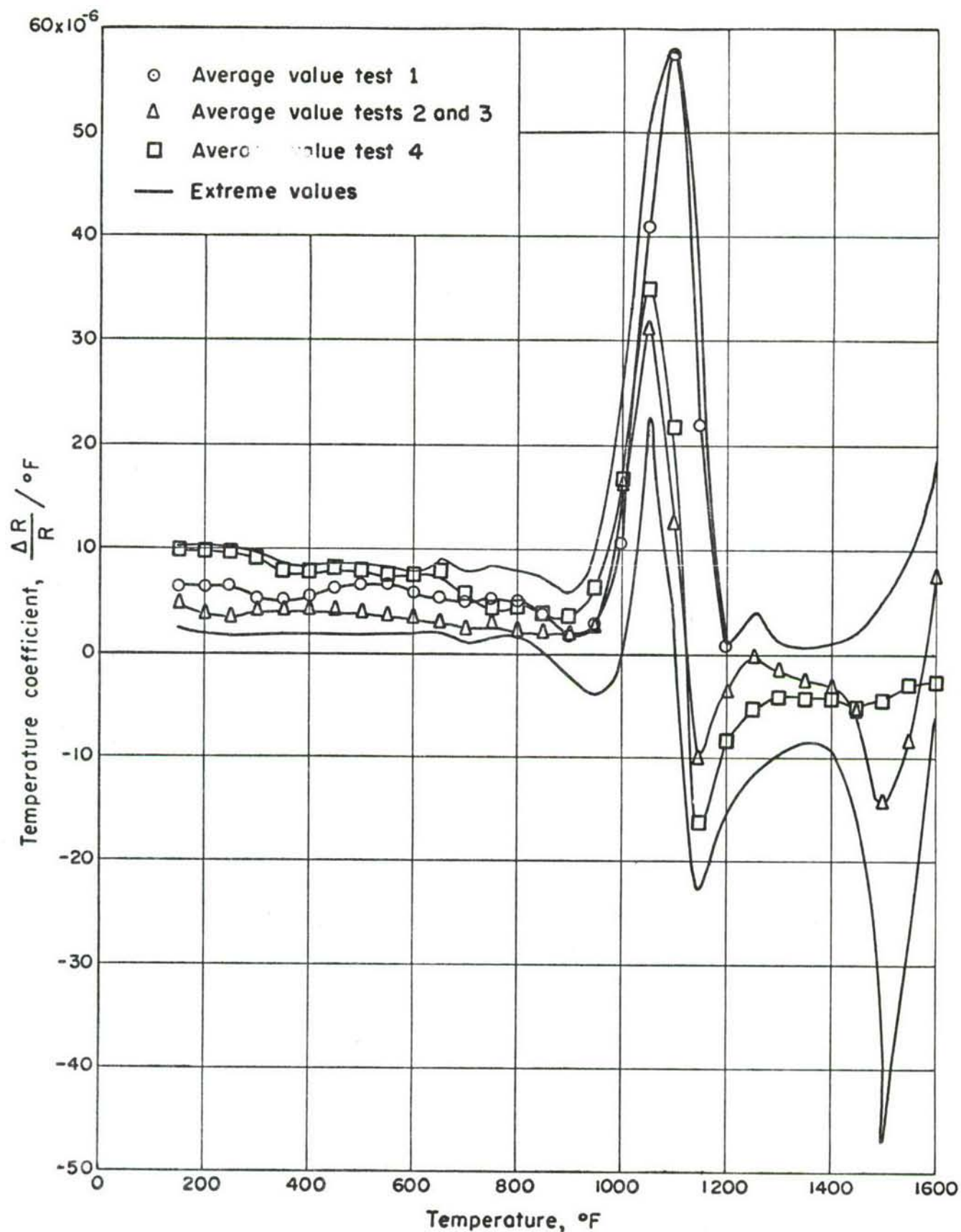


Fig.18 Temperature sensitivity with 3.0 volts across gage arm

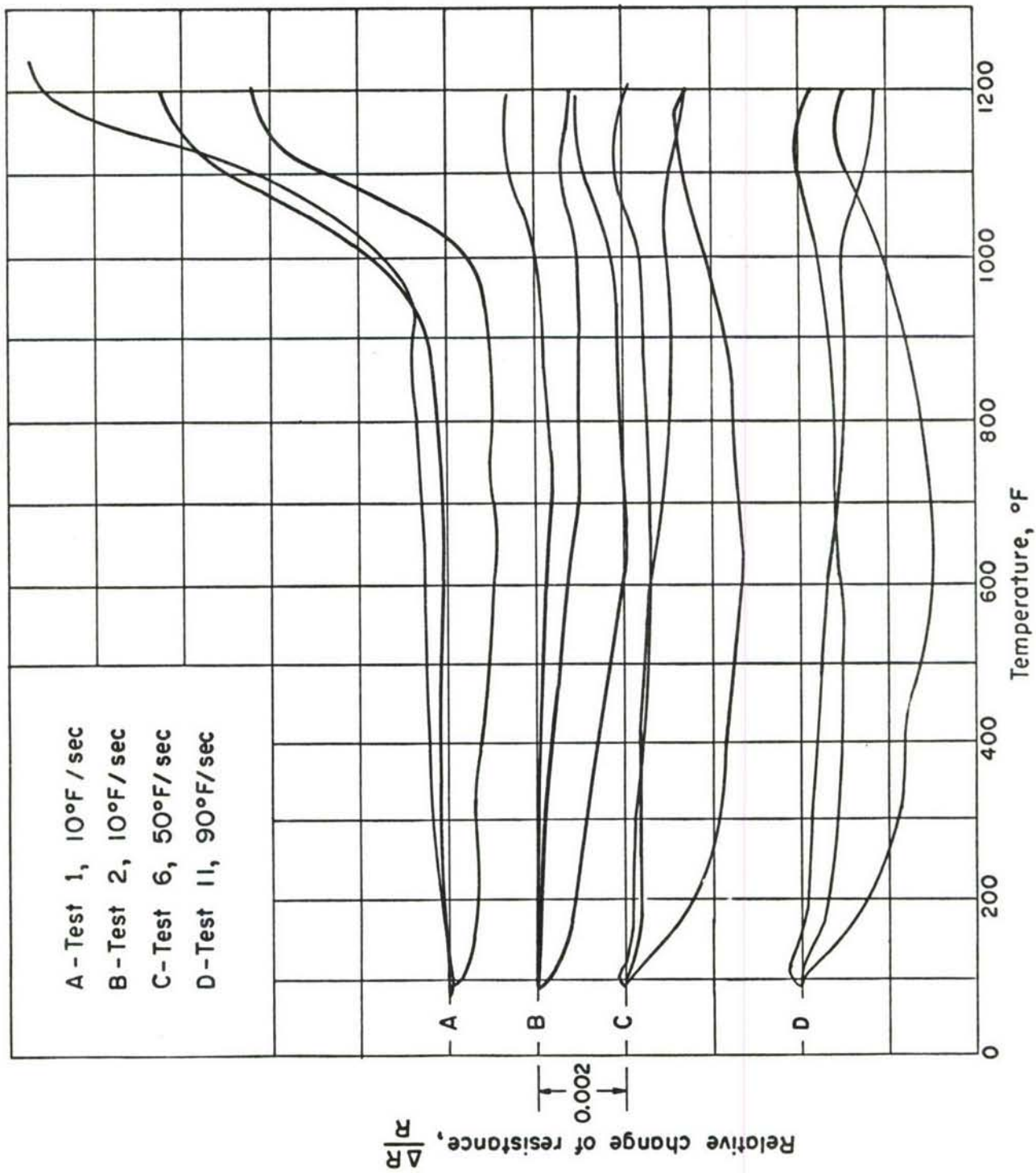


Fig. 19 Gage response at various heating rates with 0.5 volt across gage arm

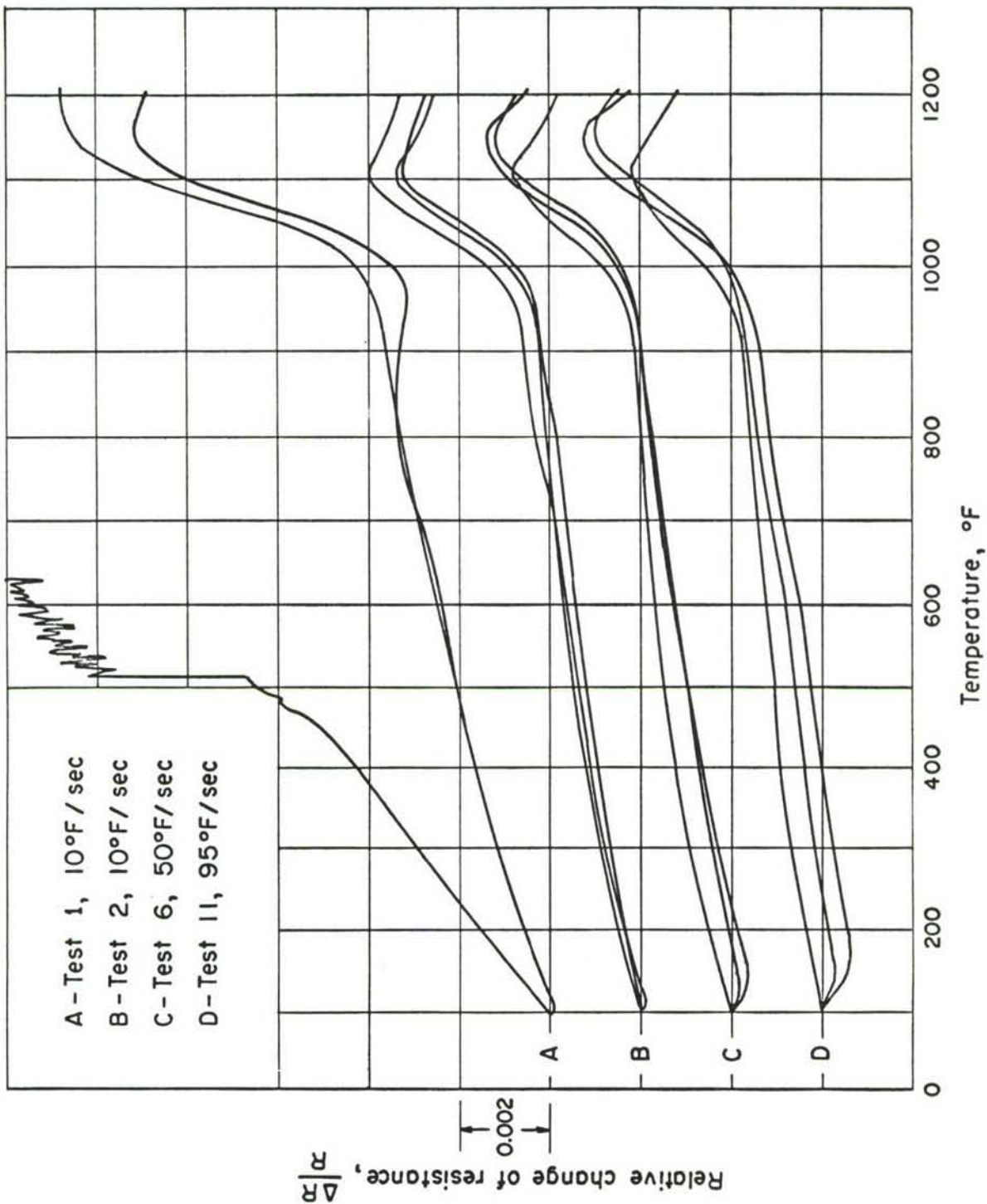


Fig. 20 Gage response at various heating rates with 3.0 volts across gage arm

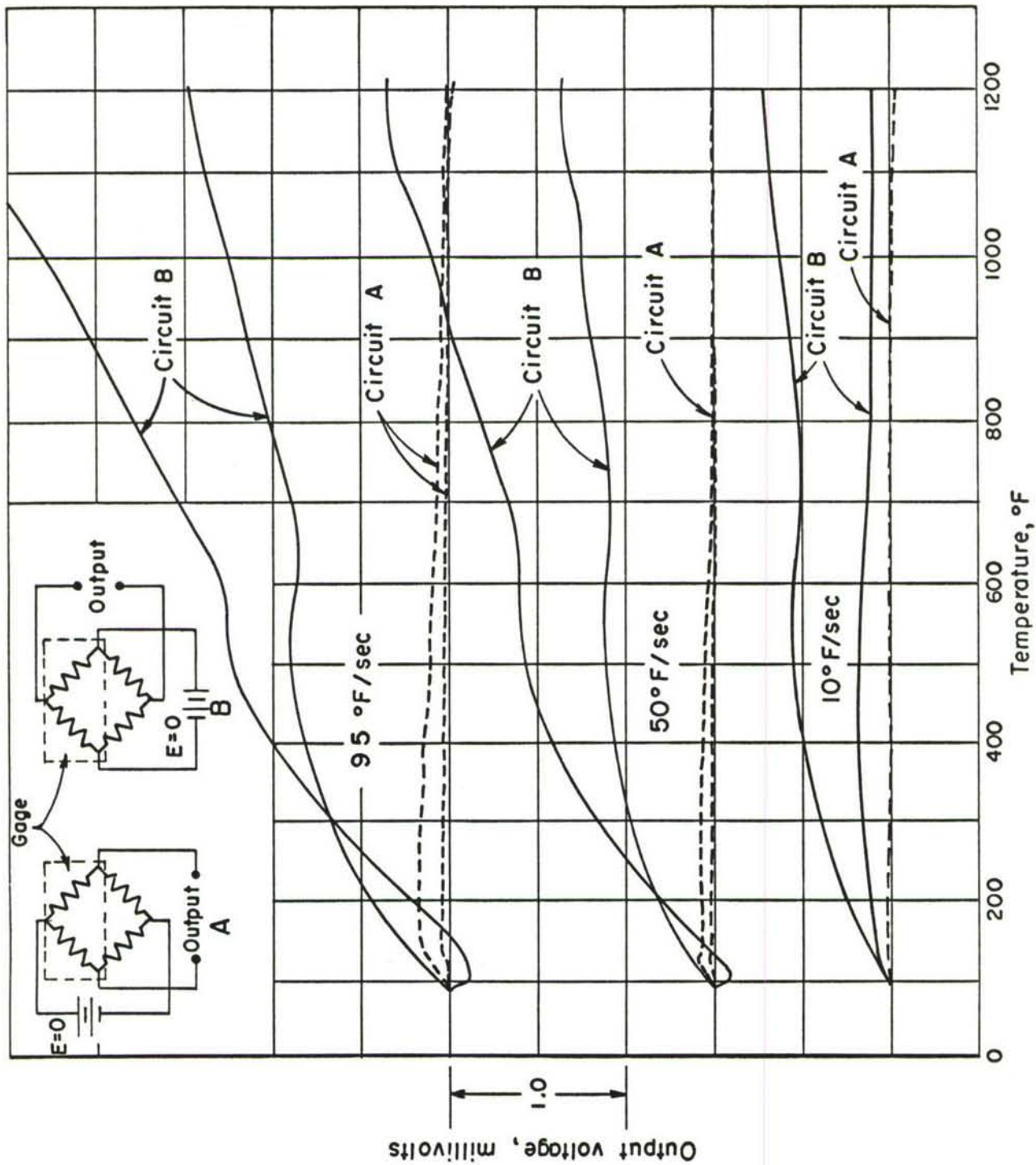


Fig. 21 Circuit output voltage due to heating with no input power

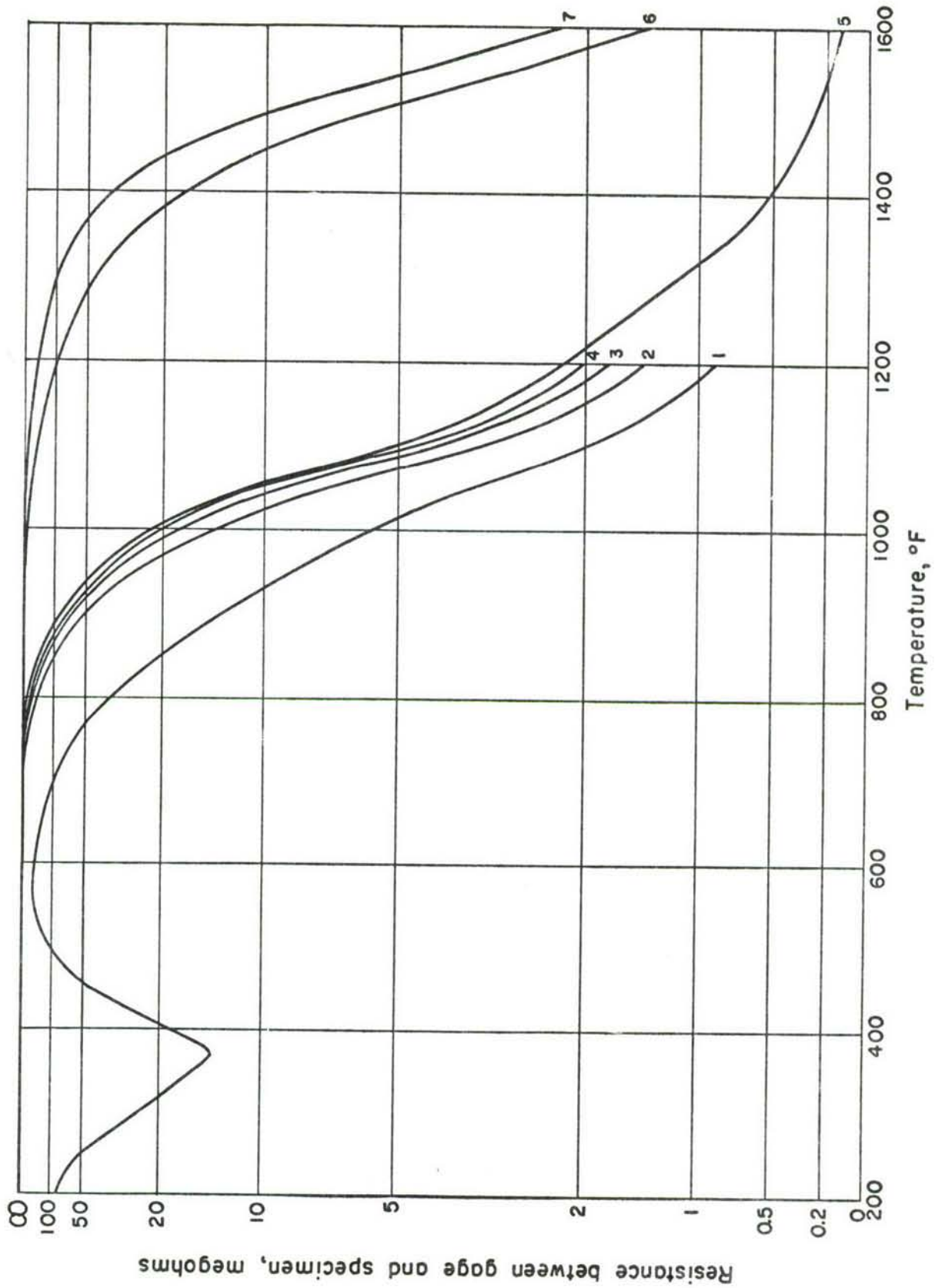


Fig. 22 Leakage resistance for Gage No. 13

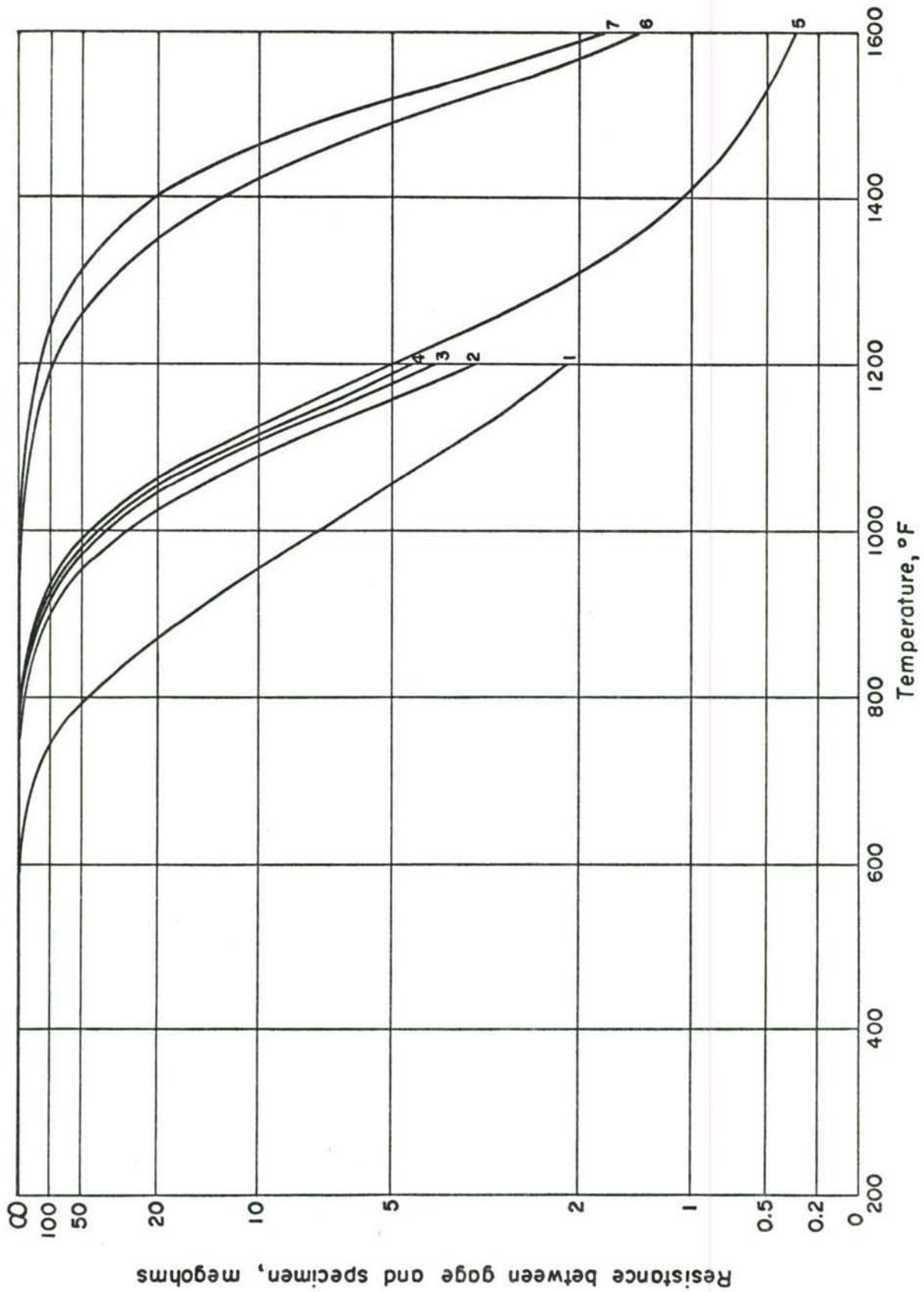


Fig. 23 Leakage resistance for Gage No. 14

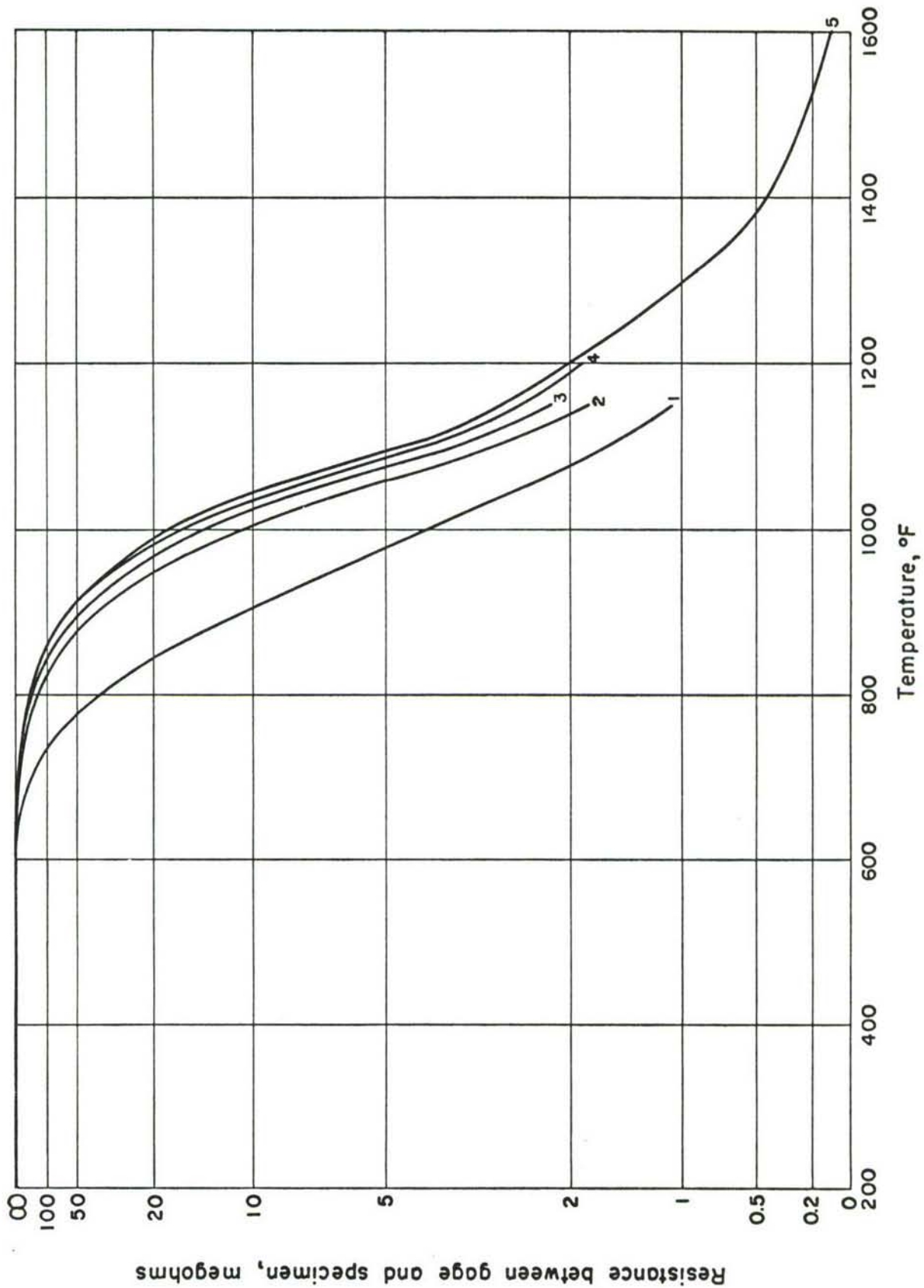


Fig. 24 Leakage resistance for Gage No. 15